Human hippocampal theta and high-gamma oscillations in spatial encoding and consolidation in a virtual Morris water maze task

Yi Pu

A thesis submitted in fulfilment of the requirements for the degree of

DOCTOR OF PHILOSOPHY

ARC Centre of Excellence in Cognition and its Disorders

Department of Cognitive Science

Faculty of Human Sciences

Macquarie University

Sydney, Australia

Table of contents

Statement of candidate

I, Yi Pu, certify that the content in this thesis has not previously been submitted for a higher degree to any other university or institution. This thesis is an original piece of research written by myself, and any assistance I have received in the preparation of this thesis has been appropriately acknowledged. All information sources that have contributed to the thesis have also been acknowledged throughout the thesis.

The research reported in thesis has received ethical approval by the Human Research Ethics Committee (project reference No.: 5201300054).

. . . . . .

Yi Pu

April, 2017

Acknowledgements

First and foremost, I would like to express my sincere gratitude to my supervisor Associate Professor Blake Johnson. Thank you for recruiting me into your lab three and half years ago, for the continuous and unwavering support of my Ph.D study and related research, for your enormous patience, for your academic foresight and tremendous knowledge. That you fully believe in my ability to overcome difficulties gives me an impetus to explore scientific uncertainties without fear of failure. You wisely guide me to achieve the goals which I originally thought I could never ever achieve and give me the freedom I need to move on during my journey. Your advice on both research and my life is priceless. You set a good example for me by being a researcher who never gets lazy and is willing to explore new territories and take on challenges.

I would like to thank Dr. Brian Cornwell for discussing research results with me over the phone. Thank you for listening to my opinions patiently and for encouraging me when I encountered difficulties. My sincere thanks also go to Professor Douglas Cheyne. Thank you for giving me tremendously valuable and detailed research suggestions, for teaching me beamforming analysis and connectivity analysis in person, for hosting my visit to your lab. Your calmness and wisdom in the face of problems and difficulties will influence the rest of my life.

I thank other researchers of our research centre for providing high-quality courses and research training to make our centre a stimulating and lovely research environment, from which students at all levels can benefit. Especially, I want to thank Associate Professor Anina Rich, Professor Amanda Barnier, Professor

Lyndsey Nickels for setting a fantastic example for female scientists. Your genuine passion for truths, open attitudes towards science, critical thinking, and the support for younger researchers have influenced me significantly. My thanks also go to Dr. Vladimir Litvak and Dr. Suresh Muthukumaraswamy for answering my questions and providing valuable suggestions through emails during my Ph.D studies. Thank you to Dr. Xiangzhen Kong, Dr. Jie Yang, Dr. Zhiguo Wang for your patience and kindness of discussing my experiments. I would also like to express my appreciation to Distinguished Professor Stephen Crain for your support during my funding application.

Thanks go to my current and previous lab members Rebecca Gelding, David Meng, Dr. Yanan Sun, Dr. Joann Tang for your help and support whenever I need. Thank you to my current and previous fellow Ph.D students: Tijl Grootswagers, Kelly Rombough, Sarah Pini, Dr. Andy Etchell. Dr. Manjunath Narra, Dr. Mili Mathew, Dr. Qandeel Hussain, Yu Li, Erika Contini, Ann Carrigan, Haiquan Huang, Huijing Chen. You are a source of friendship.

A special thanks to my family back in China. Thank you for your patience, support and unconditional love. Because of all of you, I always feel loved, supported, cared and not lonely overseas. Finally, to my dearest grandpa, words cannot express my infinite miss and love. Thank you for instilling in me good values from my young age, for nurturing and cultivating a love of learning within me and for encouraging me to bravely pursue my dreams and become the person I want to be. I miss you and wish you happy and healthy everyday in the heaven!

General summary

The formation of spatial memories has been proposed to proceed in two stages. In the initial stage, which occurs during active navigation in a new environment, hippocampal cell assemblies are activated to encode spatial information. The activation of encoding assemblies is accompanied by low frequency theta band neuronal oscillations. In the second stage, which occurs during rest or sleep, hippocampal assemblies activated during the encoding phase are reactivated to consolidate the newly formed but labile memory traces. These reactivations are accompanied by high frequency neuronal rhythms. In Buszaki's (1989) two-stage model of spatial learning, theta rhythms are proposed to provide a mechanism to bind sequential hippocampal place-cell assemblies over time; while the high-frequency oscillations are hypothesized to potentiate and consolidate the sequential activation of cell assemblies. These oscillatory mechanisms are well-established in animal models, but evidence in the human hippocampus is lacking. In the current thesis, I aimed to bridge this gap between animal and human models of spatial memory formation. I used non-invasive magnetoencephalography (MEG) recordings, and a virtual Morris water maze (vMWM) task to investigate whether human hippocampal low and high frequency oscillations play roles in different stages of spatial leaning.

In **Chapter One**, I briefly review research on the functions of hippocampal rhythms and put forward the research questions I aimed to address in the thesis. In **Chapter Two**, I review evidence and make the case that MEG is a suitable technique for addressing these questions. Based on this, in **Chapter Three**, using MEG I examined whether low frequency human hippocampal theta oscillations play a role in spatial encoding during virtual navigation. Consistent with previous work, the results showed left hippocampal theta power increase during goal-directed navigation, supporting the contention that MEG can reliably detect and localize human hippocampal signals. Further, my analyses showed that right hippocampal theta oscillations were modulated by environmental novelty and were correlated with navigation performance, providing strong support for the idea that theta plays an important role in environmental encoding during navigation. In **Chapter Four**, I analysed the same MEG dataset to examine high frequency gamma activity during the

inter-trial rest periods. The results confirmed significantly increased right hippocampal high-gamma during the inter-trial period in the new environment relative to the familiar one; and that gamma was positively correlated with theta power measured during navigation; and also with subsequent navigation performance in the familiar environment. In **Chapter Five**, I examined theta and high-gamma oscillations in a group of age-matched females, and compared these to the male data described in chapters three and four. Since there are clear and well-established gender differences in spatial behaviour, this study was designed to determine if these are reflected in the neurophysiological measurements. Consistent with the previous literature, the behavioural results showed clear gender differences. Males scored higher on a psychometric test of spatial ability, were faster in navigating the vMWM, and showed significant speed improvements in familiar versus new maze environments, while females did not improve. The MEG analyses confirmed corresponding gender differences in both the theta and gamma rhythms, strongly reinforcing the functional importance of these two rhythms in spatial learning. In the concluding **Chapter Six**, I summarize the results and discuss how they contribute to our understanding of the neurophysiological mechanisms of memory formation in the human brain. I conclude that MEG provides sensitive, reliable, and behaviourally-relevant measurements of human hippocampal function during spatial navigation. Consequently, MEG is a crucially important technique for bridging the gap between animal and human models of hippocampal function. Future developments in MEG sensor technology are likely to further enhance its sensitivity and utility in this regard.

Abbreviation list

CA: Cornu ammonis

CSF: Cerebrospinal fluid

DLE: Dipole localization error

EBB: Empirical Bayes beamformer

ECoG: Electrocorticography

EEG: Electroencephalography/ Electroencephalographic

HFOs: High frequency oscillations

ICA: Independent component analysis

iEEG: Intracranial electroencephalography/electroencephalographic

IPSPs: Inhibitory postsynaptic potentials

ITI: inter-trial-interval

LFP: Local field potential

LTP: Long-term potentiation

LTD: Long-term depression

MEG: Magenetoencephalography/Magnetoencephalographic

MFT: Magnetic field tomography

MNE: Minimum norm estimation

MTL: Medial temporal lobe

MRI: Magnetic resonance imaging

MS-DBB: Medial septum diagonal band of Broca

MSP: Multiple sparse priors

MSR: Magnetically shielded room

OPM: Optically pumped magnetometer

pHFOs: pathological high frequency oscillations

PSF: Point-spread functions

REM: Rapid eye movement

RMSE: Root mean square error

Sharp-wave ripple: SPW-R

SNR: Signal-to-noise ratio

SQUID: Superconducting quantum interference device

SSP: Signal-space projection

STS: Superior temporal sulcus

dSPM: Dynamic statistical parametric mapping

sLORETA: Standardized low-resolution electromagnetic tomography

SQUID: Superconducting quantum interference device

VEF: Visual evoked field

vMWM: virtual Morris water maze

Chapter one

Introduction: Rhythms of the hippocampus

The chapter will start with a brief discussion on the definition of brain rhythms and the reason why they are important for cognition and why they interest neuroscientists. Then two prominent hippocampal local field potential (LFP) rhythms, i.e., theta and ripple oscillations will be discussed. Findings from animal studies about the two oscillations will be briefly reviewed, followed by the findings from human research. Finally, the research questions I aim to address in this thesis will be put forward.

Brain rhythms

Brain rhythms (or oscillations, used interchangeably) refer to periodic neuronal activities in the central nervous system. Neuronal oscillations can be observed at the level of single neurons. For instance, a neuron can rhythmically generate action potentials (X. J. Wang, 2010). Neuronal oscillations can also be observed at a larger scale in LFP recordings within the brain or electroencephalographic (EEG) / magnetoencephalographic (MEG) recordings outside the brain. The LFP is the linear sum of the membrane potential in the extracellular space around neurons, and reflects the activity of a neuron population. It has been shown that individual neurons in isolation are not capable of operating complex cognitive processing (Quiroga, 2013). To do so, they need to form cell assemblies as a functional network through synchronous activity (the 'cell assembly hypothesis', put forward by Hebb (1949); Harris et al. (2003) tested this idea experimentally). Thus, the brain rhythms at the

level of the LFP are thought to be of critical importance to cognition (Colgin, 2016).

Rhythms of the hippocampus

The hippocampus is a brain region buried deep in the medial temporal lobe and is important for spatial navigation and memory (Buzsaki & Moser, 2013; O'Keefe & Nadel, 1978). It is one of the most intensively studied brain areas, partly because relative to other neocortical areas, it has a relatively simplified architecture, where principal neurons are neatly arranged in layers and the somatic and dendritic laminae are well defined (Andersen et al., 2006). Thus, it is relatively accessible to recordings of single neurons and the local field potential (LFP). In fact, the hippocampus is the structure in which some of the general principles of modern neuroscience (e.g., cross-frequency coupling) have been studied and established (Andersen et al., 2006). In addition, the hippocampus is vulnerable to pathological processes and pervasive mental disorders associated with Alzheimer's disease, epilepsy, schizophrenia, anxiety and stress (Matthew, 2006; Morris, 2006). Therefore, an understanding of hippocampal functions is a crucial step in the effort to provide treatments of these brain diseases and dysfunctions.

Rhythms are a prominent feature of hippocampal activity and different rhythms are observed during different behavioral states (Sirota & Buzsaki, 2005). Two distinctive behavioral states of animals are a "preparatory" state and a "consummatory"

state (see Buzsaki, 2015 for a review). Preparatory actions are related to active exploration and goal-directed behaviors, during which, a slow frequency theta band oscillation (4 – 12 Hz in rodents; in humans, the frequency range might be lower (Jacobs, 2014)) is the dominant LFP in the hippocampal formation (Buzsaki, 2002). The consummatory state includes awake immobility and sleep, and refers to the behavioral state in which an action such as explorative ambulation has been completed. During this behavioral state, a high frequency ripple oscillation (110 – 250 Hz in rodents; human version of ripple oscillations are slower, see Axmacher et al., 2008; Bragin et al., 1999) is the most dominant LFP (Buzsaki, 2015). A consensus is emerging on the functional importance of the two oscillations in memory, with theta rhythm being involved in memory encoding during navigation (Fig. 1) and ripple rhythm being associated with replay and memory consolidation during rest/sleep (Fig. 2). These two rhythms are thus proposed to constitute the neurophysiological mechanisms for a two-stage model of memory formation (Buzsaki, 1989, 2015), which posits that memory formation proceeds through two functionally distinct stages (i.e., encoding and consolidation stages) which occur during active navigation and rest/sleep phase respectively.[1]

[1] The rodent hippocampus also exhibits other frequency band oscillations, notably a 25 – 100 Hz rhythm. There is less agreement on the functional role of this rhythm (Colgin, 2016; Colgin & Moser, 2010). Therefore, this chapter mainly focuses on theta and ripple oscillations.

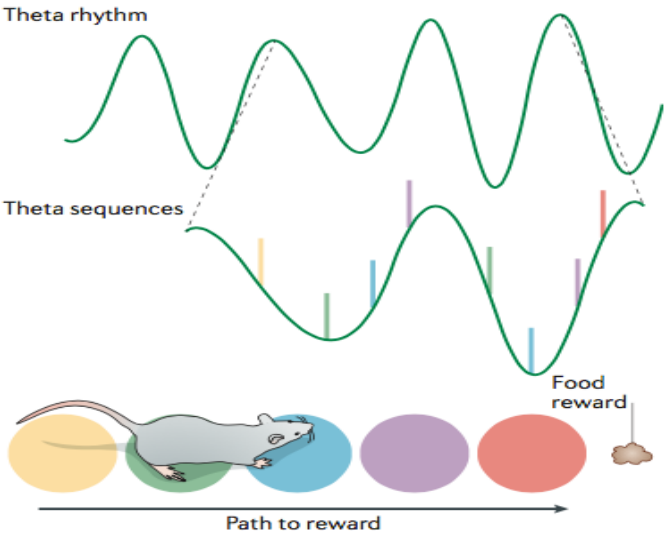

Figure 1. Theta sequences in the hippocampus during spatial memory encoding. Successive locations (depicted by colored ovals) in the trajectory are represented by temporally ordered spikes of different place cell[2] ensembles (depicted by short colour bars) in the hippocampus within individual theta cycles. For individual place cell ensembles (depicted by a short colour bar) representing a place field (depicted by the oval with the same colour as the short colour bar), spikes occur at progressively earlier theta phases across successive theta cycles as the rodent is approaching the place field. As a result of this, spikes at early and late theta phases represent earlier and later locations, respectively, in the trajectory. The low frequency theta oscillations are thought to provide a timing mechanism for place cell firing and thus are thought to be important for spatial encoding.

From Colgin (2016).

---

[2] A place cell is a type of pyramidal neuron within the hippocampus. It fires when a rodent enters a specific location in its environment. Different place cells were found to have different firing locations. These different firing locations are called the place fields of their corresponding place cells (please refer to O'Keefe, 1976).

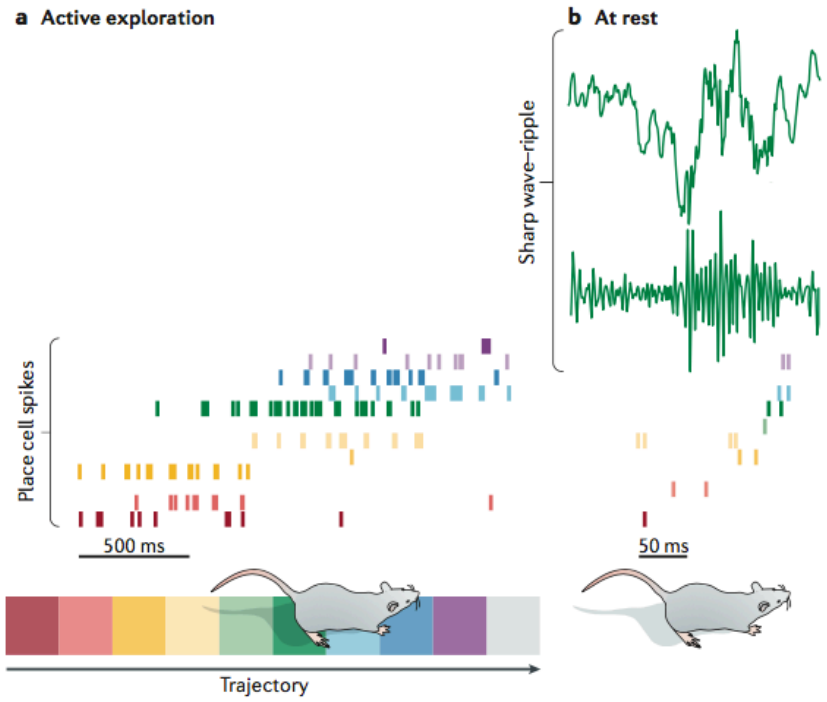

Figure 2. Replay during sharp-wave ripples when a rodent rests at the end of the linear track. a. spikes from successively activated place cells (depicted by short colour bars) as a rodent passes through the cells' place fields (depicted by squares in the corresponding colour) in a particular trajectory on a linear track. b. The top panel shows an example of a sharp wave–ripple event (raw recording) recorded during subsequent rest at the end of the linear track and a bandpass filtered (150–300 Hz, ripple oscillations) version of the sharp wave–ripple is shown immediately below the raw recording. Spikes from the place cell ensemble temporally activated during navigation are shown to reactivate during the sharp wave–ripple event. This replay mechanism is found to be related to memory consolidation. Thus, ripple oscillations are thought to be associated with consolidation.

From Colgin (2016).

The hippocampal theta rhythm in rodents

The theta rhythm (4 – 12 Hz in rats) is a low frequency oscillation. Besides the hippocampus, a theta rhythm can also be observed in some other cortical and subcortical areas, such as entorhinal cortex, cingulate gyrus, prefrontal cortex and amygdala (Leung & Borst, 1987; Mitchell & Ranck, 1980; Pare´ & Collins, 2000). Subcortical nuclei including the medial septum diagonal band of Broca (MS-DBB) and fornix are believed to be the pacemakers of theta oscillations (Aggleton et al., 1995; Green & Ardunini, 1959), because lesions of these structures abolish theta rhythms in the hippocampus.

A basic observation is that hippocampal theta power increases when rats are behaving, e.g., when free running, running on a track or on a running wheel or treadmill (Buzsaki et al., 1983; Fox et al., 1986; Skaggs et al., 1996; see Hasselmo, 2005 for a review). Thus, theta rhythm is believed to be closely related to behaviours described as "voluntary" movements (Vanderwolf, 1968) or preparatory and exploratory movements (Buzsaki, 2015). Studies have further found that both frequency and power of hippocampal theta, as well as the firing rate of place cells increase as a function of movement velocity (Hinman et al., 2011; Slawinska & Kasicki, 1998); hippocampal theta frequency and power are also sensitive to environmental novelty (Jeewajee et al., 2008; Lever et al., 2009; Penley et al., 2013; Wells et al., 2013). Since theta is associated with movements used to acquire sensory

information from external world, it has been proposed as a mechanism for coordinating multimodal sensory information for learning (see Colgin, 2016 for a review). Studies have shown that odor discrimination performance is poor if sniffing is slower than the theta range of about 6 – 9 Hz (Kepecs et al., 2007); and hippocampal theta oscillations are not phase-locked to whisking measured via the mystacial electromyogram if rats are simply whisking in air instead of actively acquiring tactile information (Berg et al., 2006). Please note that hippocampal theta rhythm is distinct from a so-called 'hippocampal respiration rhythm', which couples to nasal respiration and is caused by the olfactory bulb (Nguyen Chi et al., 2016). This mechanism may aid the information exchange between olfactory and memory system.

Evidence for the specific importance of hippocampal theta phase in spatial learning came from O'Keefe and Recce (1993). They found that as a rat was entering the field, place cell firing consistently began near the peak of theta waves, recorded at the CA1 pyramidal layer, but then shifted systematically to progressively earlier phases of the LFP theta rhythm as the rat traversed the place field. The phase angle of spiking was highly correlated with the rat's location but not with the velocity of the rat. The phenomenon, termed 'phase precession', has since been extensively replicated (e.g., Dragoi & Buzsaki, 2006; Foster & Wilson, 2007; Skaggs et al., 1996). Phase precession suggests that the hippocampal theta rhythm provides a temporal 'code' for encoding an animal's location. As a result, the sequential locations and their distances can be computed from the velocity-independent theta phase and the

velocity-dependent firing rates of place cell (Buzsaki, 2006). Thus, the temporal code of theta rhythm has been proposed to play an important role in formation of a cognitive map of an environment, allowing the association of individual locations within an environment (Hasselmo & Eichenbaum, 2005; Jensen & Lisman, 2000; Redish & Touretzky, 1998, see Hasselmo & Stern, 2014 for a review).

Phase coding is important because it also provides a mechanism for encoding new information and retrieving previously stored information without causing confusion (see Hasselmo, 2005 for a review). Physiological data (Brankack et al., 1993; Kamondi et al., 1998) have shown that when information was being encoded at one phase of local field theta rhythm, the dendrites were depolarized by input from entorhinal cortex, while there were only small spikes in the cell bodies in the pyramidal layer, and transmission from CA3 was weak (Wyble et al., 2000). This was hypothesized to create an optimal setting for encoding and preventing interference from retrieval (Hasselmo et al., 2002). At the opposite phase, cell bodies were depolarized by input from hippocampal CA3 region, when synaptic currents from entorhinal cortex were weak and dendrites were hyperpolarized, thereby allowing retrieval of a previously established pattern and preventing new encoding. The separation of theta phase for encoding and retrieval has been further supported by the evidence (Holscher et al., 1997; Hyman et al., 2003) that stimulation at a certain phase of theta rhythm causes long-term potentiation (LTP), an important mechanism for synaptic plasticity and a candidate mode for memory storage at the cellular-molecular

level (Buzsaki, 2002). Conversely, stimulation at the opposite phase causes long-term depression (LTD).

A causal relationship between hippocampal theta and learning and memory has been established by a series of studies. Silencing the theta rhythm by inactivation of its pacemaker (MS-DBB or fornix) impaires rat's performance and disrupted sequenced firing of place cell assemblies (Ennaceur et al., 1996; Givens & Olton, 1994; Y. Wang et al., 2015). However, stimulation of the fornix at a theta rhythm recovers both hippocampal theta rhythm and spatial navigation performance (McNaughton et al., 2006).

Since the theta rhythm also appears in other brain areas as mentioned above, theta-range synchrony has been proposed as a mechanism for brain-wide integration, which can drive plastic changes in short- and long-range synaptic connections to create integrated representations of experiences (Benchenane et al., 2010). Neuronal firing in brain areas such as cingulate cortex (Colom et al., 1988), amygdala (Pare & Gaudreau, 1996), entorhinal cortex (Frank et al., 2001), striatum (Berke et al., 2004) and prefrontal cortex (Hyman et al., 2011; Hyman et al., 2005) have been found to be phase-locked to hippocampal theta rhythms. Moreover, theta phase synchronization (coherence) has also been found between brain regions such as the hippocampus and the prefrontal cortex during learning, especially at choice points after task rule acquisition (Benchenane et al., 2010) during a working memory task (Jones & Wilson,

2005). The increased coherence has been proposed to reflect binding of cortico-hippocampal pathways into temporary functional units for information integration (Young & McNaughton, 2009).

The hippocampal ripple rhythm in rodents

The hippocampal ripple rhythm (140 – 200 Hz in rats, Csicsvari et al., 1999; 120 – 180 Hz in mice, Buzsaki et al., 2003) is a high frequency LFP oscillation generated in CA1 pyramidal layer and is often observed to be superimposed on an irregular large amplitude sharp-wave (Buzsaki et al., 1992; Buzsaki et al., 1983). The complex is termed "sharp-wave ripple (SPW-R)" and is one of the most robust examples of cross-frequency coupling in the brain (Buzsaki & Lopes da Silva, 2012). Although sharp waves and ripple rhythms are coupled, they are two separate neurophysiological events (Buzsaki, 2015; Colgin, 2016). Previous experiments support the view that sharp waves are generated in CA3 and propagated to CA1, while the ripple oscillations are generated locally in CA1 (Buzsaki et al., 1983; Sullivan et al., 2011). Some other brain areas also exhibit SPW-R-like events, such as olfactory cortex (Manabe et al., 2011; Narikiyo et al., 2014), and the amygdala (Ponomarenko, Korotkova, et al., 2003).

The SPW-R has often been observed when rats have little or no interaction with the environment, such as during awake immobility or sleep (Buzsaki & Lopes da

Silva, 2012). It has been hypothesized to be the neurophysiological mechanism underlying memory consolidation (Buzsaki, 1989; Buzsaki et al., 1996), partly because SPW-R meets many criteria for induction of long-term potentiation (LTP) (Buzsaki, 2015), a model of synaptic plasticity, which can potentiate the weak synaptic changes brought about by inputs from entorhinal cortex during exploration to make them stronger. The high frequency oscillation during SPW-R events also resembles the tetanic stimulation with high frequency electrical pulses, which are usually used to induce LFP. King et al. (1999) have demonstrated that the naturally occurring SPW-Rs could indeed induce LTP between CA3 and CA1 neurons. More convincing evidence of SPW-Rs in memory consolidation come from the studies which have shown that neuronal activation during SPW-Rs is biased by recent hippocampal network pattern in the preparatory theta states (i.e., hippocampal "replay", see Buzsaki, 2015; Carr et al., 2011 for reviews).

Buzsaki (1986) found that neurons which were most active during running would also activate strongly during SPW-R event in non-REM sleep after running, even though they were silent during SPW-R event in non-REM sleep before running. Place cells with overlapping place fields which showed high correlations during running also showed higher correlation during post-run sleep compared to pre-run sleep (Wilson & McNaughton, 1994); the temporal order of place cell firing during running was also preserved (Qin et al., 1997; Skaggs & McNaughton, 1996). Moreover, studies have found that the occurrences of SPW-Rs during non-REM (REM: rapid eye

movement) sleep after exploration were positively correlated with previous waking experience during exploration (Buzsaki, 1985; Ponomarenko, Korotkova, et al., 2003; Ponomarenko, Lin, et al., 2003). A similar replay phenomenon has also been observed in awake immobility after active navigation (Csicsvari et al., 2007; Foster & Wilson, 2006; Jackson et al., 2006), except that the order of place cell reactivation was the reverse of that during running. Further, Diba and Buzsaki (2007) have found that while at the end of the track after running, the order of place cell replay during awake SPW-R events was reverse to that of running, forward place cell firing occurred at the starting position of the track before running, indicating a role of forward replay in planning the upcoming trajectories. The difference between sleep replay and awake replay during SPW-R event may be due to the influence of sensory stimulation during awake immobility in contrast to the more isolated state of sleep (Buzsaki, 2015). A recent study (Gupta et al., 2010) has demonstrated that besides consolidating previous learning experience, replay during SPW-R event may also have a potential role in active construction of the cognitive map.

A causal relationship between SPW-R and memory consolidation has been established by silencing the hippocampal SPW-Rs. Studies (Ego-Stengel & Wilson, 2010; Girardeau et al., 2009) have found that interrupting the SPW-Rs by stimulation of the ventral hippocampal commissure during SPW-R event in post-learning sleep significantly impaired learning performance compared with controlled stimulation outside of SPW-R event during post-learning sleep. A recent study (van de Ven et al.,

2016) further elucidated the role of SPW-Rs in consolidation of recently learnt information, because interrupting SPW-Rs during post-learning sleep only impaired the newly formed memory but not the memory which had already been consolidated.

While the evidence reviewed above refers to activity within the hippocampus, researchers have also found SPW-R events can participate in a system consolidation process in which the encoded information in the hippocampus is transferred to neocortex for permanent storage (Diekelmann & Born, 2010) by cross-frequency oscillatory coupling (Sirota & Buzsaki, 2005). During slow wave sleep, the hippocampal ripples are phase-locked to around the troughs of the thalamocortical sleep spindles (7 – 14 Hz or 12 – 18 Hz, depending on the experiment), which together are modulated by the depolarized up-state of thalamocortical slow oscillations (0.5 – 1.5 Hz) (Molle et al., 2006; Siapas & Wilson, 1998; Sirota et al., 2003). This observation suggests that cross-frequency coupling between the hippocampus and neocortex may provide a temporally fine-tuned pathway for information transfer. However, the available physiological evidence about system level consolidation is limited to the sleep state. Future studies are required to investigate whether systems consolidation occurs during awake immobility.

The hippocampal theta rhythm in humans

Since the theta rhythm plays such an important role in navigation and memory in

rodents, there is considerable interest in whether there is a comparable rhythm in humans and if so, whether it possesses the same functional properties reported in rodents. The studies reviewed below mainly focus on findings from experiments using virtual navigation tasks (Lever et al., 2014), analogous to the tasks used in rodent studies.

Using intracranial electroencephalographic (iEEG) recordings, Kahana et al. (1999) reported for the first time that navigation-related theta rhythm (4 – 8 Hz) in several regions such as temporal lobe, and the frequency of theta rhythm occurrence was modulated by complexity of the virtual maze. Similar effects have been reported in later research (Caplan et al., 2001; Caplan et al., 2003). Later, using iEEG recordings with electrodes implanted in the hippocampus, Ekstrom et al. (2005) reported movement-related theta in the hippocampus during virtual spatial navigation. With the development of whole-head magnetoencephalography (MEG) and sophistication of source localization techniques, studies using MEG (Cornwell et al., 2008; de Araujo et al., 2002; Kaplan et al., 2012) have also reported hippocampal theta power increases after virtual navigation.

An iEEG study (Watrous, Lee, et al., 2013) has reported that the human hippocampal theta is more transient and in a lower frequency range (centered around 3 Hz) compared to the rat theta rhythm (centered around 8 Hz). However, a recent study (Bohbot et al., 2017) reported clear evidence of 7 – 9 Hz rhythmicity in raw

intra-hippocampus EEG traces during real as well as virtual movement in the human brain. Moreover, Watrous et al. (2011) have found that hippocampal theta power increased as movement speed increased and compared with viewing background, there was more theta power when viewing landmarks such as stores. An MEG study by Kaplan et al. (2012) has reported increased theta power change[3] in novel compared to familiar environments, implying that, as with rodents, hippocampal theta might play a role in encoding new environment. With iEEG recordings, Park et al. (2014) have reported that hippocampal theta was sensitive to environmental novelty, although this environmental effect was confounded by learning object locations within the environment.

The role of theta phase has been has been investigated in humans as well. Jacobs et al. (2007) found that during spatial navigation individual neurons in the hippocampus phase-locked to various phases theta and delta rhythm, but were only active at the trough of gamma oscillations (30 – 90 Hz). Later, Rutishauser et al. (2010) have reported that single neuron phase-locking to local theta rhythm during encoding was related to better memory formation, providing important evidence for phase coding hypothesis in human brain. Recently, in a working memory paradigm, Zhang and Jacobs (2015) have shown that human theta oscillations were traveling waves, i.e., theta phase shifted consistently in a posterior-anterior direction along the

[3] The study only reported the theta power change as a function of environmental novelty at the MEG sensor level.

longitudinal axis of the hippocampus. This result suggests that neurons at different locations of the hippocampus can experience different theta phases simultaneously; therefore, this might provide a neurophysiological basis for neurons to signal future and past events by activating at different phases (Dragoi & Buzsaki, 2006; Lubenov & Siapas, 2009).

Consistent with the rodent literature, human theta oscillations also seem to play a role in whole brain integration, supporting complex cognitive processing. In a virtual taxi game task, by using low frequency theta phase synchronization as a measure of network functional connectivity, Watrous, Tandon, et al. (2013) reported that successful memory retrieval corresponded to greater global connectivity among various brain regions, including medial temporal lobe (MTL), prefrontal cortex and parietal cortex, with MTL acting as the hub of those interactions. Kaplan et al. (2014) have found that after spatial learning, when cued with the object whose location the participant would navigate to in the subsequent retrieval phase, there was more theta phase coupling between the prefrontal cortex and the medial temporal lobe compared to baseline.

Deep brain stimulation has provided mixed results about the role of the hippocampal theta rhythm. Suthana et al. (2012) have found that stimulating entorhinal cortex while participants were learning locations of landmarks reset the phase of the hippocampal theta rhythm and resulted in better spatial performance

relative to no stimulation. However, direct stimulation of the hippocampus did not exert any significant effects. In an effort to replicate this study, Jacobs et al. (2016) have found that instead of improving memory performance, electrical stimulation of entorhinal cortex or hippocampus impaired memory performance significantly. Nevertheless, both sets of results implicate the human hippocampus in memory process.

Hippocampal ripple rhythm in humans

Compared to theta oscillations, human hippocampal LFP ripple oscillations are less studied (Bragin et al., 1999). One line of this work is to find out whether there is an equivalent of ripple oscillations in the healthy human brain, since medial temporal lobe epilepsy also generates high frequency neural activities. Studies have shown that there exists a human homologue of ripples, but the frequency range is lower, with frequencies in the range of 80 – 160 Hz (Bragin et al., 1999; Staba et al., 2004; Staba et al., 2002, see Bragin et al., 2010 for a review); pathological high frequency oscillations (pHFOs), in contrast, are in the range of 250 – 600 Hz. Other distinctions between normal ripples and pHFOs are that ripples reflect inhibitory postsynaptic potentials (IPSPs) on the soma of the pyramidal cells (Bragin et al., 1999), while pHFOs reflect synchronized firing of abnormally bursting neurons instead of inhibitory field potentials (Engel et al., 2009). Recently, Le Van Quyen et al. (2008) observed cellular correlates of human ripples, which were similar to that observed in

vivo in the rodents, with pyramidal cells firing preferentially at the highest amplitude of the ripple and interneurons discharging earlier than pyramidal cells.

Having established a human analogue of ripples, researchers began to explore their functional role, motivated by the model of rodent ripples participating in memory consolidation via a replay mechanism (Tambini et al., 2010). The first experiment examining the functional role of human ripple was conducted by Axmacher et al. (2008) in a verbal memory task. With intracranial depth electrodes implanted in the hippocampus and the rhinal cortex contralateral to the seizure onset zone, they have observed ripple oscillations (80 – 140 Hz) when the participants napped after learning a list of words. The occurrence of rhinal ripples was correlated with the number of successfully recalled words in the post-nap retrieval task. Using a similar correlational strategy, with MEG recordings and a virtual Morris water maze task, Cornwell et al. (2014) have found the power of bilateral hippocampal high frequency oscillations (80 – 140 Hz) during a 5-minute resting period after initial spatial learning correlated with rate of the initial learning but not with subsequent navigation performance. The results of the above experiments suggest that human ripples may play a role in memory consolidation, but they do not provide direct evidence of replay by showing the brain region used for encoding accompanied by theta oscillations is reactivated during awake immobility or sleep accompanied by high frequency oscillations. Moreover, in the two studies, no control condition was investigated, therefore it is possible that ripples are only a trait marker related to

general cognitive ability rather than a learning-specific phenomenon.

Researchers have also examined whether there is cross-frequency coupling between the hippocampus and other neocortical areas to transfer the information from the hippocampus to neocortex for long-term storage. Clemens et al. (2011) have shown that at the timescale of milliseconds, parahippocampal ripples were tightly phase-locked to the troughs of sleep spindles from the parietal lobe and parahippocampus. Staresina et al. (2015) have reported that hippocampal sleep spindles clustered hippocampal ripples in their troughs, which together were modulated by the up-state (around 160 degrees' phase angle) of hippocampal slow oscillations. These findings provide potential neurophysiological mechanisms of a temporally-structured frame for the transfer of memory trances. However, fewer studies have directly shown hierarchical phase-amplitude coupling after learning of a hippocampus-dependent task. With this aim, Molle et al. (2009) used scalp EEG recordings to investigate the influence of learning on sleep oscillations and sleep spindles in humans. They found that learning induced a discrete increase in amplitude during the depolarizing up-state (in an interval 500 – 800 ms following the negative peak and 450 – 200 ms before the negative peak) of the slow oscillation as compared to the non-learning condition. Spindle activity was clearly modulated by the slow oscillation phase and reduced during the down-state (30 – 110°) and enhanced during the up-state (220 – 320°). As compared with the non-learning control condition, after learning, spindle activity was enhanced at the transition into and during the up- states.

The researchers did not directly investigate human ripples in this experiment, since these are not readily accessible in EEG recordings.

Research questions to be addressed in the current thesis

The broad aim of this thesis is to investigate whether the two-stage model of spatial memory (Buzsaki, 1989, 2015), based on electrophysiological studies of the rodent hippocampus, can be translated to the human hippocampus. Navigating in a new environment is an essential activity in daily life. How to find a way in the new environment and to build an internal representation is crucial for human activities. Theories based on animal models of the hippocampus posit that memorizing new spatial information needs to undergo two stages, and that hippocampal theta and high frequency oscillations are the two dominant neuronal rhythms supporting cognitive processes during the two stages (Buzsaki, 1989, 2015). In the first stage, which often occurs during active navigation, new information is encoded accompanied by low frequency hippocampal theta oscillations. Memories are typically not imprinted immediately in the brain, but rather require repetition and reinforcement for consolidation (Skinner, 1938; Sutton & Barto, 1998). Thus, in the second stage, which happens when animals have finished exploration and are quietly resting or sleeping, the activated place cell assemblies during navigation will be reactivated accompanied by high frequency oscillations to strengthen the otherwise labile memory traces. In the current thesis, I aimed to investigate whether human hippocampal low frequency theta

and high frequency gamma oscillations[4] play similar roles in encoding and consolidation of new spatial information as reported in rodent studies.

Human hippocampal rhythms can be studied with invasive recordings in the hippocampus of the pre-surgery patients. However, opportunities for recordings from the brains of these patients are very limited. Due to the fact that the skull, scalp and cerebrospinal fluid (CSF) are almost transparent to magnetic fields, identifying and localizing hippocampal signals from the sensor signals non-invasively recorded by magnetoencephalography (MEG) provides a promising avenue to study human hippocampal rhythms by routine experimentation. However, it is still debated whether MEG can detect the signals from the human hippocampus, although a small but increasing body of evidence show that the MEG-recorded signals indexes neurophysiological mechanisms that are functionally comparable to those measured with invasive recordings in the hippocampus of humans (e.g., Bohbot et al., 2017; Ekstrom et al., 2005; Jacobs et al., 2016; Kahana et al., 1999) and animals (e.g., Buzsaki, 2002; Dragoi & Buzsaki, 2006; O'Keefe & Recce, 1993).

In the present thesis, I had the following objectives. **First,** I aimed to review

[4] Different researchers use different terminologies to refer to human analogue of ripple oscillations. Axmacher et al. (2008) termed 80 – 140 Hz as ripples, while Cornwell et al. (2014) termed the same frequency band as fast/high gamma. I used high-gamma oscillations/rhythms in the following chapters in this thesis to refer to 80 – 140 Hz frequency band in humans.

evidence and to make the case that MEG can reliably detect the signals from the human hippocampus. **Second,** I aimed to confirm that MEG can detect and localise hippocampal activities in healthy humans performing a virtual Morris water maze task, and to investigate the role of human hippocampal theta in environmental encoding and aimed to relate these oscillations to navigation performance. **Third,** I aimed to investigate whether hippocampal high frequency gamma oscillations during the inter-trial rest period play a role in memory consolidation, and aimed to investigate the relationship between hippocampal theta during navigation and high-gamma during inter-trial rest period and the relationship between high-gamma and navigation performance. **Fourth,** I aimed to examine whether the two rhythms would reflect the well-established behavioural differences between males and females in spatial navigation.

Organization of the thesis

The remainder of the thesis is organized as follows. **Chapter two** reviews evidence that MEG is capable of investigating neuronal oscillations from the human hippocampus. **Chapter three** replicates left hippocampal activation during goal-directed navigation in a vMWM task reported by a previous study and further investigates a new potential role of hippocampal theta rhythms in environment encoding during navigation. **Chapter four** examines the functional relevance of hippocampal high-gamma oscillations in replay of newly encoded environment during

inter-trial rest period. **Chapter five** compares theta and high-gamma rhythms of males and females during navigation and rest period to test whether the difference of the two hippocampal rhythms could reflect the behavioural differences of the two groups in environmental learning during navigation, thereby reinforcing the functional importance of the two rhythms. **Chapter six** concludes the thesis by summarizing the main results and their theoretical significance, and indicates some future directions for MEG research on human hippocampal function.

References

Aggleton, J. P., Neave, N., & Hunt, N. P. R. (1995). A comparison of the effects of anterior thalamic, mamillary body and fornix lesions on reinforced spatial alternation. *Behav Brain Res, 68*, 91-101.

Andersen, P., Morris, R., Amaral, D., Bliss, T., & O'Keefe, J. (2006). The hippocampal formation. In P. Andersen, R. Morris, D. Amaral, T. Bliss, & J. O'Keefe (Eds.), *The hippocampus book*: Oxford University Press.

Axmacher, N., Elger, C. E., & Fell, J. (2008). Ripples in the medial temporal lobe are relevant for human memory consolidation. *Brain, 131*(Pt 7), 1806-1817. doi:10.1093/brain/awn103

Benchenane, K., Peyrache, A., Khamassi, M., Tierney, P. L., Gioanni, Y., Battaglia, F. P., & Wiener, S. I. (2010). Coherent theta oscillations and reorganization of spike timing in the hippocampal- prefrontal network upon learning. *Neuron, 66*(6), 921-936. doi:10.1016/j.neuron.2010.05.013

Berg, R. W., Whitmer, D., & Kleinfeld, D. (2006). Exploratory whisking by rat is not phase locked to the hippocampal theta rhythm. *J Neurosci, 26*(24), 6518-6522. doi:10.1523/JNEUROSCI.0190-06.2006

Berke, J. D., Okatan, M., Skurski, J., & Eichenbaum, H. B. (2004). Oscillatory entrainment of striatal neurons in freely moving rats. *Neuron, 43*(6), 883-896. doi:10.1016/j.neuron.2004.08.035

Bohbot, V. D., Copara, M. S., Gotman, J., & Ekstrom, A. D. (2017). Low-frequency theta oscillations in the human hippocampus during real-world and virtual

navigation. *Nat Commun, 8*, 14415. doi:10.1038/ncomms14415

Bragin, A., Engel, J., Jr., & Staba, R. J. (2010). High-frequency oscillations in epileptic brain. *Curr Opin Neurol, 23*(2), 151-156. doi:10.1097/WCO.0b013e3283373ac8

Bragin, A., Jr., J. E., Wilson, C. L., Fried, I., & Buzsaki, G. (1999). High-frequency oscillations in human brain. *Hippocampus, 9*, 137-142.

Brankack, J., Stewart, M., & Fox, S. E. (1993). Current source density analysis of the hippocampal theta rhythm: associated sustained potentials and candidate synaptic generators. *Brain Res, 615*, 310-327.

Buzsaki, G. (1985). What does the "LTP model of memory" model? In G. E. Will, P. Schmitt, & J. C. Dalrymple-Alford (Eds.), *Brain plascitiy, learning and memory*. New York: Plenum Press.

Buzsaki, G. (1986). Hippocampal sharpWaves: their origin and significance. *Brain Res, 398*, 242-252.

Buzsaki, G. (1989). Two-stage model of memory trace formation: a role for "noisy" brain states *Neuroscience, 31*(3), 551-570.

Buzsaki, G. (2002). Theta oscillations in the hippocampus. *Neuron, 33*, 325-340.

Buzsaki, G. (2006). *Rhythms of the brain*. Oxford: Oxford University Press.

Buzsaki, G. (2015). Hippocampal sharp wave-ripple: A cognitive biomarker for episodic memory and planning. *Hippocampus, 25*(10), 1073-1188. doi:10.1002/hipo.22488

Buzsaki, G., Buhl, D. L., Harris, K. D., Csicsvari, J., Czeh, B., & Morozov, A. (2003).

Hippocampal network patterns of activity in the mouse. *Neuroscience, 116*, 201-211.

Buzsaki, G., Horvath, Z., Urioste, R., Hetke, J., & Wise, K. (1992). High-frequency network oscillation in the hippocampus. *Science, 256*, 1025-1027.

Buzsaki, G., Leung, L. W. S., & Vanderwolf, C. H. (1983). Cellular bases of hippocampal EEG in the behaving rat. *Brain Res Rev, 6*, 139-171.

Buzsaki, G., & Lopes da Silva, F. H. (2012). High frequency oscillations in the intact brain. *Prog Neurobiol, 98*(3), 241-249. doi:10.1016/j.pneurobio.2012.02.004

Buzsaki, G., & Moser, E. I. (2013). Memory, navigation and theta rhythm in the hippocampal-entorhinal system. *Nat Neurosci, 16*(2), 130-138. doi:10.1038/nn.3304

Buzsaki, G., Penttonen, M., Nadasdy, Z., & Bragin, A. (1996). Pattern and inhibition-dependent invasion of pyramidal cell dendrites by fast spikes in the hippocampus in vivo. *Proc Natl Acad Sci U S A, 93*, 9921-9925.

Caplan, J. B., Madsen, J. R., Raghavachari, S., & Kahana, M. J. (2001). Distinct patterns of brain oscillations underlie two basic parameters of human maze learning. *J Neurosci, 23*, 10897–10903.

Caplan, J. B., Madsen, J. R., Schulze-Bonhage, A., Aschenbrenner-Scheibe, R., Newman, E., & Kahana, M. J. (2003). Human theta oscillations related to sensorimotor integration and spatial learning. *J Neurosci, 23*(11), 4726 – 4736.

Carr, M. F., Jadhav, S. P., & Frank, L. M. (2011). Hippocampal replay in the awake state: a potential substrate for memory consolidation and retrieval. *Nat*

Neurosci, 14(2), 147-153. doi:10.1038/nn.2732

Clemens, Z., Molle, M., Eross, L., Jakus, R., Rasonyi, G., Halasz, P., & Born, J. (2011). Fine-tuned coupling between human parahippocampal ripples and sleep spindles. *Eur J Neurosci, 33*(3), 511-520. doi:10.1111/j.1460-9568.2010.07505.x

Colgin, L. L. (2016). Rhythms of the hippocampal network. *Nat Rev Neurosci, 17*(4), 239-249. doi:10.1038/nrn.2016.21

Colgin, L. L., & Moser, E. I. (2010). Gamma oscillations in the hippocampus. *Physiology (Bethesda), 25*(5), 319-329. doi:10.1152/physiol.00021.2010

Colom, L. V., Christie, B. R., & Bland, B. H. (1988). Cingulate cell discharge patterns related to hippocampal EEG and their modulation by muscarinic and nicotinic agents. *Brain Res, 460*, 329-338.

Cornwell, B. R., Johnson, L. L., Holroyd, T., Carver, F. W., & Grillon, C. (2008). Human hippocampal and parahippocampal theta during goal-directed spatial navigation predicts performance on a virtual Morris water maze. *J Neurosci, 28*(23), 5983-5990. doi:10.1523/JNEUROSCI.5001-07.2008

Cornwell, B. R., Overstreet, C., & Grillon, C. (2014). Spontaneous fast gamma activity in the septal hippocampal region correlates with spatial learning in humans. *Behav Brain Res, 261*, 258-264. doi:10.1016/j.bbr.2013.12.031

Csicsvari, J., Hirase, H., Czurko, A., Mamiya, A., & Buzsaki, G. (1999). Oscillatory coupling of hippocampal pyramidal cells and interneurons in the behaving rat. *J Neurosci, 19*(1), 274-287.

Csicsvari, J., O'Neill, J., Allen, K., & Senior, T. (2007). Place-selective firing contributes to the reverse-order reactivation of CA1 pyramidal cells during sharp waves in open-field exploration. *Eur J Neurosci, 26*(3), 704-716. doi:10.1111/j.1460-9568.2007.05684.x

de Araujo, D. B., Baffa, O., & Wakai, R. T. (2002). Theta oscillations and human navigation: A magnetoencephalography study. *J Cogn Neurosci, 14*(1), 70-78.

Diba, K., & Buzsaki, G. (2007). Forward and reverse hippocampal place-cell sequences during ripples. *Nat Neurosci, 10*(10), 1241-1242. doi:10.1038/nn1961

Diekelmann, S., & Born, J. (2010). The memory function of sleep. *Nat Rev Neurosci, 11*(2), 114-126. doi:10.1038/nrn2762

Dragoi, G., & Buzsaki, G. (2006). Temporal encoding of place sequences by hippocampal cell assemblies. *Neuron, 50*(1), 145-157. doi:10.1016/j.neuron.2006.02.023

Ego-Stengel, V., & Wilson, M. A. (2010). Disruption of ripple-associated hippocampal activity during rest impairs spatial learning in the rat. *Hippocampus, 20*(1), 1-10. doi:10.1002/hipo.20707

Ekstrom, A. D., Caplan, J. B., Ho, E., Shattuck, K., Fried, I., & Kahana, M. J. (2005). Human hippocampal theta activity during virtual navigation. *Hippocampus, 15*(7), 881-889. doi:10.1002/hipo.20109

Engel, J., Jr., Bragin, A., Staba, R., & Mody, I. (2009). High-frequency oscillations: what is normal and what is not? *Epilepsia, 50*(4), 598-604.

doi:10.1111/j.1528-1167.2008.01917.x

Ennaceur, A., Neave, N., & Aggleton, J. P. (1996). Neurotoxic lesions of the perirhinal cortex do not mimic the behavioural effects of fornix transection in the rat. *Behav Brain Res, 80*, 9-25.

Foster, D. J., & Wilson, M. A. (2006). Reverse replay of behavioural sequences in hippocampal place cells during the awake state. *Nature, 440*(7084), 680-683. doi:10.1038/nature04587

Foster, D. J., & Wilson, M. A. (2007). Hippocampal theta sequences. *Hippocampus, 17*(11), 1093-1099. doi:10.1002/hipo.20345

Fox, S. E., Wolfson, S., & Ranck, J. B. (1986). Hippocampal theta rhythm and the firing of neurons in walking and urethane anesthetized rats. *Exp Brain Res, 62*, 495-508.

Frank, L. M., Brown, E. N., & Wilson, M. A. (2001). A comparison of the firing properties of putative excitatory and inhibitory neurons from CA1 and the entorhinal cortex. *J Neurophysiol, 86*, 2029-2040.

Girardeau, G., Benchenane, K., Wiener, S. I., Buzsaki, G., & Zugaro, M. B. (2009). Selective suppression of hippocampal ripples impairs spatial memory. *Nat Neurosci, 12*(10), 1222-1223. doi:10.1038/nn.2384

Givens, B., & Olton, D. (1994). Local modulation of forebrain: effects working reference memory. *J Neurosci, 14*(5), 3578-3587.

Green, J. D., & Ardunini, A. A. (1959). Hippocampal electrical activity in arousal. *J Neurophysiol, 17*(6), 533-557.

Gupta, A. S., van der Meer, M. A., Touretzky, D. S., & Redish, A. D. (2010). Hippocampal replay is not a simple function of experience. *Neuron, 65*(5), 695-705. doi:10.1016/j.neuron.2010.01.034

Harris, D. K., Csicsvari, J., Hirase, H., Dragoi, G., & Buzsaki, G. (2003). Organization of cell assemblies in the hippocampus. *Nature, 424*(6948), 552-556. doi:10.1038/nature01765

Hasselmo, M. E. (2005). What is the function of hippocampal theta rhythm?--Linking behavioral data to phasic properties of field potential and unit recording data. *Hippocampus, 15*(7), 936-949. doi:10.1002/hipo.20116

Hasselmo, M. E., Cannon, R. C., & Koene, R. A. (2002). A simulation of parahippocampal and hippocampal structures guiding spatial navigation of a virtual rat in a virtual environment: a functional framework for theta theory. In M. P. Witter & F. G. Wiyterlood (Eds.), *The parahippocampal region: organization and role in cognitive functions* (pp. 136-161). Oxford: Oxford University Press.

Hasselmo, M. E., & Eichenbaum, H. (2005). Hippocampal mechanisms for the context-dependent retrieval of episodes. *Neural Netw, 18*(9), 1172-1190. doi:10.1016/j.neunet.2005.08.007

Hasselmo, M. E., & Stern, C. E. (2014). Theta rhythm and the encoding and retrieval of space and time. *Neuroimage, 85 Pt 2*, 656-666. doi:10.1016/j.neuroimage.2013.06.022

Hebb, D. O. (1949). *The organization of behavior: A neuropsychological theory*:

Wiley: New York.

Hinman, J. R., Penley, S. C., Long, L. L., Escabi, M. A., & Chrobak, J. J. (2011). Septotemporal variation in dynamics of theta: speed and habituation. *J Neurophysiol, 105*(6), 2675-2686. doi:10.1152/jn.00837.2010

Holscher, C., Anwyl, R., & Rowan, M. J. (1997). Stimulation on the positive phase of hippocampal theta rhythm induces long-term potentiation that can be depotentiated by stimulation on the negative phase in area CA1 In Vivo. *J Neurosci, 17*(16), 6470-6477.

Hyman, J. M., Hasselmo, M. E., & Seamans, J. K. (2011). What is the Functional Relevance of Prefrontal Cortex Entrainment to Hippocampal Theta Rhythms? *Front Neurosci, 5*, 24. doi:10.3389/fnins.2011.00024

Hyman, J. M., Wyble, B. P., Goyal, V., Rossi, C. A., & Hasselmo, M. E. (2003). Stimulation in hippocampal region CA1 in behaving rats yields long-term potentiation when delivered to the peak of theta and long-term depression when delivered to the trough. *J Neurosci, 17*, 11725-11731.

Hyman, J. M., Zilli, E. A., Paley, A. M., & Hasselmo, M. E. (2005). Medial prefrontal cortex cells show dynamic modulation with the hippocampal theta rhythm dependent on behavior. *Hippocampus, 15*(6), 739-749. doi:10.1002/hipo.20106

Jackson, J. C., Johnson, A., & Redish, A. D. (2006). Hippocampal sharp waves and reactivation during awake states depend on repeated sequential experience. *J Neurosci, 26*(48), 12415-12426. doi:10.1523/JNEUROSCI.4118-06.2006

Jacobs, J. (2014). Hippocampal theta oscillations are slower in humans than in rodents: implications for models of spatial navigation and memory. *Philos Trans R Soc Lond B Biol Sci, 369*(1635), 20130304. doi:10.1098/rstb.2013.0304

Jacobs, J., Kahana, M. J., Ekstrom, A. D., & Fried, I. (2007). Brain oscillations control timing of single-neuron activity in humans. *J Neurosci, 27*(14), 3839-3844. doi:10.1523/JNEUROSCI.4636-06.2007

Jacobs, J., Miller, J., Lee, S. A., Coffey, T., Watrous, A. J., Sperling, M. R., . . . Rizzuto, D. S. (2016). Direct Electrical Stimulation of the Human Entorhinal Region and Hippocampus Impairs Memory. *Neuron, 92*(5), 983-990. doi:10.1016/j.neuron.2016.10.062

Jeewajee, A., Lever, C., Burton, S., O'Keefe, J., & Burgess, N. (2008). Environmental novelty is signaled by reduction of the hippocampal theta frequency. *Hippocampus, 18*(4), 340-348. doi:10.1002/hipo.20394

Jensen, O., & Lisman, J. E. (2000). Position reconstruction from an ensemble of hippocampal place cells: contribution of theta phase coding. *J Neurophysiol, 83*, 2602-2609.

Jones, M. W., & Wilson, M. A. (2005). Theta rhythms coordinate hippocampal-prefrontal interactions in a spatial memory task. *PLoS Biol, 3*(12), e402. doi:10.1371/journal.pbio.0030402

Kahana, M. J., Sekuler, R., Caplan, J. B., Kirschen, M., & Madsen, J. R. (1999). Human theta oscillations exhibit task dependence during virtual maze navigation. *Nature, 399*(24), 781-784.

Kamondi, A., Acsady, L., Wang, X. J., & Buzsaki, G. (1998). Theta oscillations in somata and dendrites of hippocampal pyramidal cells In vivo: activity-dependent phase-precession of action potentials. *Hippocampus, 8*, 244-261.

Kaplan, R., Bush, D., Bonnefond, M., Bandettini, P. A., Barnes, G. R., Doeller, C. F., & Burgess, N. (2014). Medial prefrontal theta phase coupling during spatial memory retrieval. *Hippocampus, 24*(6), 656-665. doi:10.1002/hipo.22255

Kaplan, R., Doeller, C. F., Barnes, G. R., Litvak, V., Duzel, E., Bandettini, P. A., & Burgess, N. (2012). Movement-related theta rhythm in humans: coordinating self-directed hippocampal learning. *PLoS Biol, 10*(2), e1001267. doi:10.1371/journal.pbio.1001267

Kepecs, A., Uchida, N., & Mainen, Z. F. (2007). Rapid and precise control of sniffing during olfactory discrimination in rats. *J Neurophysiol, 98*(1), 205-213. doi:10.1152/jn.00071.2007

King, C., Henze, D. A., Leinekugel, X., & Buzsaki, G. (1999). Hebbian modification of a hippocampal population pattern in the rat. *J. Physiol., 521*(1), 159-167.

Le Van Quyen, M., Bragin, A., Staba, R., Crepon, B., Wilson, C. L., & Engel, J., Jr. (2008). Cell type-specific firing during ripple oscillations in the hippocampal formation of humans. *J Neurosci, 28*(24), 6104-6110. doi:10.1523/JNEUROSCI.0437-08.2008

Leung, L. W. S., & Borst, J. G. G. (1987). Electrical activity of the cingulate cortex. I. Generating mechanisms and relations to behavior. *Brain Res, 407*, 68-80.

Lever, C., Jeewajee, A., Burton, S., O'Keefe, J., & Burgess, N. (2009). Hippocampal theta frequency, novelty, and behavior. *Hippocampus, 19*(4), 409-410. doi:10.1002/hipo.20557

Lever, C., Kaplan, R., & Burgess, N. (2014). The function of oscillations in the hippocampal formation. In D. Derkikman & J. J. Knierim (Eds.), *Space, time and memory in the hippocampal formation* (pp. 303-350): Springer Vienna.

Lubenov, E. V., & Siapas, A. G. (2009). Hippocampal theta oscillations are travelling waves. *Nature, 459*(7246), 534-539. doi:10.1038/nature08010

Manabe, H., Kusumoto-Yoshida, I., Ota, M., & Mori, K. (2011). Olfactory cortex generates synchronized top-down inputs to the olfactory bulb during slow-wave sleep. *J Neurosci, 31*(22), 8123-8133. doi:10.1523/JNEUROSCI.6578-10.2011

Matthew, W. (2006). Hippocampus and human disease. In P. Andersen, R. Morris, D. Amaral, T. Bliss, & J. O'Keefe (Eds.), *The hippocampus book*. Oxford: Oxford University Press.

McNaughton, N., Ruan, M., & Woodnorth, M. A. (2006). Restoring theta-like rhythmicity in rats restores initial learning in the Morris water maze. *Hippocampus, 16*(12), 1102-1110. doi:10.1002/hipo.20235

Mitchell, S. J., & Ranck, J. B. (1980). Generation of theta rhythm in medial entorhinal cortex of freely moving rats. *189, 49-66*(189), 49-66.

Molle, M., Eschenko, O., Gais, S., Sara, S. J., & Born, J. (2009). The influence of learning on sleep slow oscillations and associated spindles and ripples in

humans and rats. *Eur J Neurosci, 29*(5), 1071-1081. doi:10.1111/j.1460-9568.2009.06654.x

Molle, M., Yeshenko, O., Marshall, L., Sara, S. J., & Born, J. (2006). Hippocampal sharp wave-ripples linked to slow oscillations in rat slow-wave sleep. *J Neurophysiol, 96*(1), 62-70. doi:10.1152/jn.00014.2006

Morris, R. (2006). Stress and the hippocampus. In P. Andersen, R. Morris, D. Amaral, T. Bliss, & J. O'Keefe (Eds.), *The hippocampus book*. Oxford: Oxford University Press.

Narikiyo, K., Manabe, H., & Mori, K. (2014). Sharp wave-associated synchronized inputs from the piriform cortex activate olfactory tubercle neurons during slow-wave sleep. *J Neurophysiol, 111*(1), 72-81. doi:10.1152/jn.00535.2013

Nguyen Chi, V., Muller, C., Wolfenstetter, T., Yanovsky, Y., Draguhn, A., Tort, A. B., & Brankack, J. (2016). Hippocampal Respiration-Driven Rhythm Distinct from Theta Oscillations in Awake Mice. *J Neurosci, 36*(1), 162-177. doi:10.1523/JNEUROSCI.2848-15.2016

O'Keefe, J., & Nadel, L. (1978). The hippocampus as a cognitive map. *Hippocampus, 9*, 352-364.

O'Keefe, J., & Recce, M. L. (1993). Phase relationship between hippocampal place units and the EEG theta rhythm. *Hippocampus, 3*(3), 317-330.

O'Keefe, J. (1976). Place units in the hippocampus of the freely moving rat. *Exp Neurol, 51*, 78-109.

Pare´, D., & Collins, D. R. (2000). Neuronal correlates of fear in the lateral amygdala:

multiple extracellular recordings in conscious cats. *J Neurosci, 20*(7), 2701-2710.

Pare, D., & Gaudreau, H. (1996). Projection cells and interneurons of the lateral and basolateral amygdala: distinct firing patterns and differential relation to theta and delta rhythms in conscious cats. *J Neurosci, 16*(10), 3334-3350.

Park, J., Lee, H., Kim, T., Park, G. Y., Lee, E. M., Baek, S., . . . Kang, J. K. (2014). Role of low- and high-frequency oscillations in the human hippocampus for encoding environmental novelty during a spatial navigation task. *Hippocampus, 24*(11), 1341-1352. doi:10.1002/hipo.22315

Penley, S. C., Hinman, J. R., Long, L. L., Markus, E. J., Escabi, M. A., & Chrobak, J. J. (2013). Novel space alters theta and gamma synchrony across the longitudinal axis of the hippocampus. *Front Syst Neurosci, 7*, 20. doi:10.3389/fnsys.2013.00020

Ponomarenko, A. A., Korotkova, T. M., & Haas, H. L. (2003). High frequency (200 Hz) oscillations and firing patterns in the basolateral amygdala and dorsal endopiriform nucleus of the behaving rat. *Behavioural Brain Research, 141*(2), 123-129. doi:10.1016/s0166-4328(02)00327-3

Ponomarenko, A. A., Lin, J. S., Selbach, O., & Haas, H. L. (2003). Temporal pattern of hippocampal high-frequency oscillations during sleep after stimulant-evoked waking. *Neuroscience, 121*(3), 759-769. doi:10.1016/s0306-4522(03)00524-4

Qin, Y. L., McNaughton, B. L., Skaggs, W. E., & Barnes, C. A. (1997). Memory

reprocessing in corticocortical and hippocampocortical neuronal ensembles. *Philos Trans R Soc Lond B Biol Sci, 352*, 1525-1533.

Quiroga, Q. R. (2013). Gnostic cells in the 21st century. *Acta Neurobiol Exp, 73*, 463-471.

Redish, A. D., & Touretzky, D. S. (1998). The role of the hippocampus in solving the Morris water maze. *Neural Comput, 10*, 73-111.

Rutishauser, U., Ross, I. B., Mamelak, A. N., & Schuman, E. M. (2010). Human memory strength is predicted by theta-frequency phase-locking of single neurons. *Nature, 464*(7290), 903-907. doi:10.1038/nature08860

Siapas, A. G., & Wilson, M. A. (1998). Coordinated interactions between hippocampal ripples and cortical spindles during slow-wave sleep. *Neuron, 21*.

Sirota, A., & Buzsaki, G. (2005). Interaction between neocortical and hippocampal networks via slow oscillations. *Thalamus Relat Syst, 3*(4), 245-259.

Sirota, A., Csicsvari, J., Buhl, D. L., & Buzsaki, G. (2003). Communication between neocortex and hippocampus during sleep in rodents. *Proc Natl Acad Sci U S A, 100*(4), 2065-2069.

Skaggs, W. E., & McNaughton, B. L. (1996). Replay of neuronal firing sequences in rat hippocampus during sleep following spatial experience. *Science, 271*, 1870-1873.

Skaggs, W. E., McNaughton, B. L., Wilson, M. A., & Barnes, C. A. (1996). Theta phase precession in hippocampal neuronal populations and the compression of temporal sequences. *Hippocampus, 6*, 149-172.

Skinner, B. F. (1938). *The behavior of organisms*. New York: Applenton-Century-Crofts.

Slawinska, U., & Kasicki, S. (1998). The frequency of rat's hippocampal theta rhythm is related to the speed of locomotion. *Brain Res, 1998*(796), 327-331.

Staba, R. J., Wilson, C. L., Bragin, A., Jhung, D., Fried, I., & Engel, J., Jr. (2004). High-frequency oscillations recorded in human medial temporal lobe during sleep. *Ann Neurol, 56*(1), 108-115. doi:10.1002/ana.20164

Staba, R. J., Wilson, C. L., Fried, I., & Engel, J., Jr. (2002). Single neuron burst firing in the human hippocampus during sleep. *Hippocampus, 12*(6), 724-734. doi:10.1002/hipo.10026

Staresina, B. P., Bergmann, T. O., Bonnefond, M., van der Meij, R., Jensen, O., Deuker, L., . . . Fell, J. (2015). Hierarchical nesting of slow oscillations, spindles and ripples in the human hippocampus during sleep. *Nat Neurosci, 18*(11), 1679-1686. doi:10.1038/nn.4119

Sullivan, D., Csicsvari, J., Mizuseki, K., Montgomery, S., Diba, K., & Buzsaki, G. (2011). Relationships between hippocampal sharp waves, ripples, and fast gamma oscillation: influence of dentate and entorhinal cortical activity. *J Neurosci, 31*(23), 8605-8616. doi:10.1523/JNEUROSCI.0294-11.2011

Suthana, N., Haneef, Z., Stern, J., Mukamel, R., Behnke, E., Knowlton, B., & Fried, I. (2012). Memory enhancement and deep-brain stimulation of the entorhinal area. *N Engl J Med, 366*(6), 502-510. doi:10.1056/NEJMoa1107212

Sutton, R., & Barto, A. (1998). *Reinforcement learning* Cambridge: MIT Press.

Tambini, A., Ketz, N., & Davachi, L. (2010). Enhanced brain correlations during rest are related to memory for recent experiences. *Neuron, 65*(2), 280-290. doi:10.1016/j.neuron.2010.01.001

van de Ven, G. M., Trouche, S., McNamara, C. G., Allen, K., & Dupret, D. (2016). Hippocampal Offline Reactivation Consolidates Recently Formed Cell Assembly Patterns during Sharp Wave-Ripples. *Neuron, 92*(5), 968-974. doi:10.1016/j.neuron.2016.10.020

Vanderwolf, C. H. (1968). Hippocampal electrical activity and voluntary movement in the rat *Electroencephalogr Clin Neurophysiol, 26*, 407-418.

Wang, X. J. (2010). Neurophysiological and computational principles of cortical rhythms in cognition. *Physiol Rev, 90*(3), 1195-1268. doi:10.1152/physrev.00035.2008

Wang, Y., Romani, S., Lustig, B., Leonardo, A., & Pastalkova, E. (2015). Theta sequences are essential for internally generated hippocampal firing fields. *Nat Neurosci, 18*(2), 282-288. doi:10.1038/nn.3904

Watrous, A. J., Fried, I., & Ekstrom, A. D. (2011). Behavioral correlates of human hippocampal delta and theta oscillations during navigation. *J Neurophysiol, 105*(4), 1747-1755. doi:10.1152/jn.00921.2010

Watrous, A. J., Lee, D. J., Izadi, A., Gurkoff, G. G., Shahlaie, K., & Ekstrom, A. D. (2013). A comparative study of human and rat hippocampal low-frequency oscillations during spatial navigation. *Hippocampus, 23*(8), 656-661. doi:10.1002/hipo.22124

Watrous, A. J., Tandon, N., Conner, C. R., Pieters, T., & Ekstrom, A. D. (2013). Frequency-specific network connectivity increases underlie accurate spatiotemporal memory retrieval. *Nat Neurosci, 16*(3), 349-356. doi:10.1038/nn.3315

Wells, C. E., Amos, D. P., Jeewajee, A., Douchamps, V., Rodgers, J., O'Keefe, J., . . . Lever, C. (2013). Novelty and anxiolytic drugs dissociate two components of hippocampal theta in behaving rats. *J Neurosci, 33*(20), 8650-8667. doi:10.1523/JNEUROSCI.5040-12.2013

Wilson, M. A., & McNaughton, B. L. (1994). Reactivation of hippocampal ensemble memories during sleep. *Science, 265*, 676-678

.

Wyble, B. P., Linster, C., & Hasselmo, M. E. (2000). Size of CA1-evoked synaptic potentials Is related to theta rhythm phase in rat hippocampus. *J Neurophysiol, 83*, 2138-2144.

Young, C. K., & McNaughton, N. (2009). Coupling of theta oscillations between anterior and posterior midline cortex and with the hippocampus in freely behaving rats. *Cereb Cortex, 19*(1), 24-40. doi:10.1093/cercor/bhn055

Zhang, H., & Jacobs, J. (2015). Traveling Theta Waves in the Human Hippocampus. *J Neurosci, 35*(36), 12477-12487. doi:10.1523/JNEUROSCI.5102-14.2015

Chapter two

Non-invasive detection of hippocampal signals using magnetoencephalography: A systematic review

Abstract

Hippocampal rhythms are believed to support crucial cognitive processes including memory, navigation and language. Due to the location of the hippocampus deep in the brain, studying hippocampal rhythms using non-invasive magnetoencephalography (MEG) recordings has generally been assumed to be difficult or impossible. However, with the advent of whole-head MEG systems and development of advanced source localization techniques, simulation and empirical studies have provided good evidence that human hippocampal signals can be sensed by MEG and reliably reconstructed by source localization algorithms. This paper systematically reviews the simulation and empirical evidence and indicates the current state-of-the-art of the capacities and limitations of MEG "deep source imaging" of the human hippocampus.

Keywords: Magnetoencephalography (MEG), hippocampus, deep source imaging

Introduction

The hippocampus is an important brain region for various cognitive processes, including spatial navigation (Buzsaki & Moser, 2013; O'Keefe & Nadel, 1978), memory (Horner & Doeller, 2017), and language comprehension (Piai et al., 2016). Neuronal oscillations are believed to be important mechanisms for these processes (Colgin, 2016) and it is thus of great importance to understand the functions of hippocampal rhythms. At the present time, there are several different methods available to investigate the function of the human hippocampus. fMRI is frequently used in experimental studies of hippocampal function in healthy humans; however due to its temporal resolution (on the order of seconds, Buckner & Logan, 2001), rapid rhythmic neuronal activities cannot be resolved with this technique. The scalp electroencephalogram (EEG) provides high temporal resolution on a timescale of milliseconds. However, source reconstruction of the EEG is complicated by the fact that electrical signals are vulnerable to distortions by skull, skin and cerebrospinal fluid (CSF) (Cohen, 2017; Lopes da Silva, 2010). Intracranial EEG (iEEG) provides both excellent spatial and temporal resolution, but it depends on very limited opportunities to obtain recordings from surgical patients.

Compared to scalp EEG, magnetoencephalography (MEG) has an advantage in identifying brain currents giving rise to the signals (Hari et al., 2000) recorded from MEG sensors outside the brain, because the skull, skin and CSF are almost

transparent to magnetic fields. This advantage allows MEG to contribute to comprehending and exploiting both regional and large-scale neural dynamics by clarifying the nature of spontaneous and event-related brain activities and by the elucidation of the mechanisms underlying inter-regional connectivity (Baillet, 2017). Due to its non-invasive nature, MEG may provide an avenue to study the function of neuronal dynamics of the human hippocampus by routine experimentation. Accordingly, it would play an important role in connecting the human data with animal and computational models of electrophysiology in health and disease (Baillet, 2017). However, whether MEG can reliably detect hippocampal signals has been a topic of debate, due to the following considerations. First, magnetic signals decay rapidly with distance, so signals from the hippocampus are thus assumed to be strongly attenuated relative to signals from the neocortex (Hillebrand & Barnes, 2002; Moses et al., 2011). Second, some widely used source localization techniques such as minimum norm estimation are strongly biased towards the neocortical surface and away from deep brain regions (Attal & Schwartz, 2013). Third, some studies (Mikuni et al., 1997; Oishi et al., 2002) have reported variable and limited ability of MEG to detect interictal spiking in the hippocampus of epileptic patients observable with intracranial electrodes or electrocorticography (ECoG) grids. Fourth, the folded nature of the hippocampal morphology may lead to signal cancelation (Mikuni et al., 1997).

However, with the advent of whole-brain MEG systems and increasing sophistication of source localization algorithms, a number of laboratories have

reported detection of hippocampal signals with MEG (e.g., Backus et al., 2016; Cornwell et al., 2008; Moses et al., 2009). A series of simulation studies (e.g., Attal & Schwartz, 2013; Meyer et al., 2017; Stephen et al., 2005) have been carried out to systematically investigate the feasibility of and limits on MEG measurements of hippocampal activity with known ground truth about the whether the source is the hippocampus or not. The present review aims to integrate and synthesize the findings of the major simulation and empirical studies of MEG measurements of hippocampal activity. The reviews begin with a brief introduction of the anatomy and cellular architecture of the hippocampus, followed by a brief introduction to MEG. Simulation studies and empirical studies are then reviewed.

Anatomy of the hippocampus

The hippocampus is one of several related brain regions that together constitute a functional system called the hippocampal formation (Amaral & Lavenex, 2006). The constituent areas include the dentate gyrus, hippocampus proper, subicular complex (subiculum, presubiculum, and parasubiculum), and entorhinal cortex (Insausti, 1993). The hippocampus proper has three subfields: CA1, CA2 and CA3 (CA is short for *cornu ammonis*; "Ammon's horn", referring to the ram-headed god Amun of Egyptian mythology). Some researchers further subdivide CA3 into CA3 and CA4 regions. The basic morphology of the mammalian hippocampus proper is an elongated, curved and rod-like structure (Insausti, 1993) (Fig. 1A). The hippocampus proper consists of one

layer of principal neurons (e.g., pyramidal neurons) (Forster et al., 2006), which are neatly arranged in parallel with the dendrites aligned perpendicularly to the surface of the hippocampus proper (Fig. 1B). Due to the geometric configuration of pyramidal neurons with the dendrites facing one direction and the soma another, the electrical fields from such cells can extend over long distances and can induce substantial ionic flow in the extracelluar medium (Lorente de No, 1947). In principle, then, the synchronized activation of this type of cells could produce signals measurable at a distance by MEG and EEG (Murakami & Okada, 2006).

A

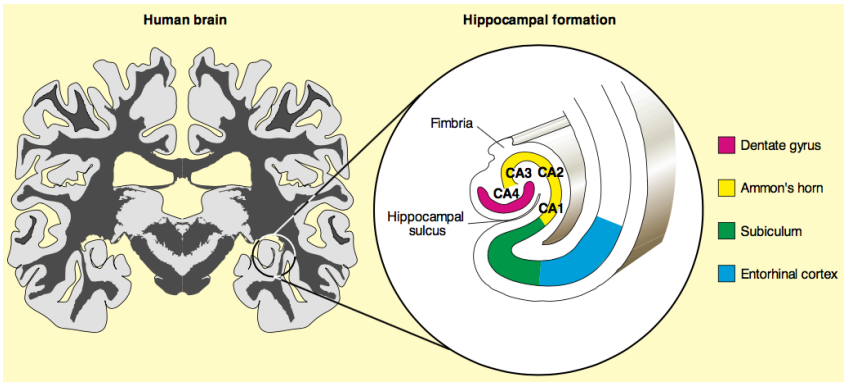

B

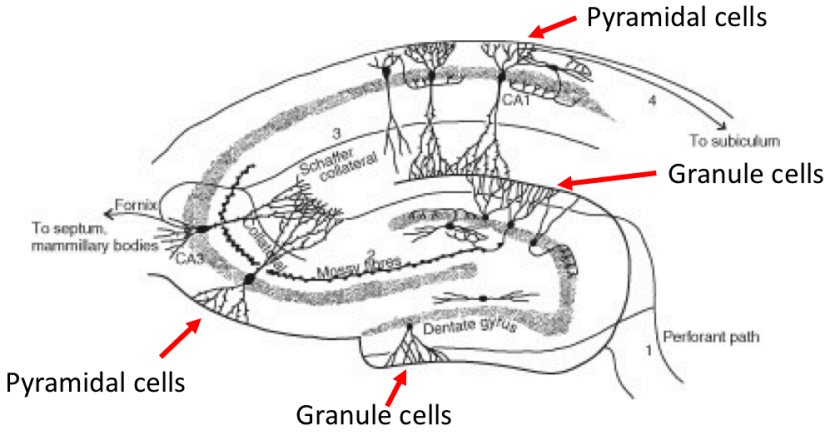

Figure 1. Anatomical and cellular architecture of the hippocampus. **A.** Subfields of the hippocampal formation. **B.** Principal neurons in the hippocampal proper (CA regions) and the dentate gyrus.

Figure 1A is reproduced from Parkin (1996). Figure 1B was reproduced from Rolls (2010).

MEG

MEG is a technique for measurement of human brain function via detection and interpretation of magnetic fields emanated from the brain with millisecond temporal

resolution (Hämäläinen et al., 1993; Ioannides, 2006). Compared with Earth's magnetic field and urban magnetic noise, the magnetic field magnitude of the brain is about a factor of 1 million to 1 billion smaller (Vrba & Robinson, 2001). To detect such small magnetic fields, highly sensitive magnetic detectors are needed in conjunction with noise reduction techniques. Current technology is based on the superconducting quantum interference device (SQUID) coupled with flux transformers bathed in cryogen, and contained within a magnetically shielded room (MSR) to increase the overall magnetic field sensitivity[1] (Fagaly, 2006). The flux transformer pickup coils can have various configurations and different commercial MEG companies employ different types. There are three main types of coil configurations: magnetometers with a single loop of wire, axial gradiometers and planar gradiometers with two or more magnetometers combined with opposite orientation and with a certain distance between coils (called baselines) (Fig. 2). Different coil configurations have different performances in terms of noise reduction and sensitivity to depth below the scalp (Fig. 3). In general, axial magnetometers with a baseline of 3 – 8 cm give optimum signal-to-noise ratios (SNRs) compared to magnetometers (the baseline of magnetometers can be regarded as infinite) and planar gradiometers (the baseline of planar gradiometers is about 1.4 – 1.6 cm) and the order of the sensitivity to signals in depth is magnetometers, axial gradiometers and planar gradiometers (Lopes da Silva, 2010).

[1] New sensing technology is emerging and maturing, such as non-cryogenic HyQUID detectors and optically pumped magnetometers, see Baillet (2017).

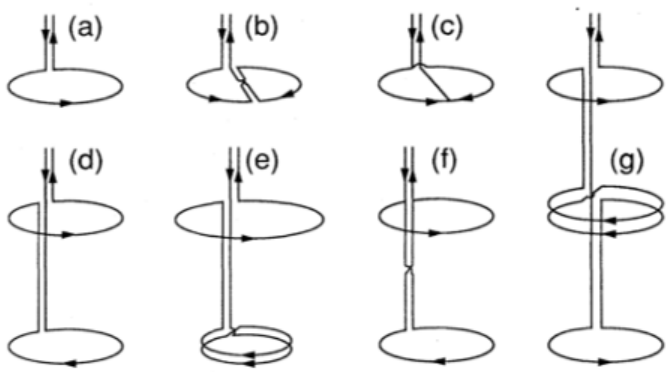

Figure 2. Flux transformer pick up coils. (a) magnetometer; (b) first-order series planar gradiometer (c) first-order parallel planar gradiometer (d) first-order symmetric series axial gradiometer (e) first-order asymmetric series axial gradiometer; (f) first-order symmetric parallel axial gradiometer (g) second-order series axial gradiometer.

Figure 2 is reproduced from Hämäläinen et al. (1993).

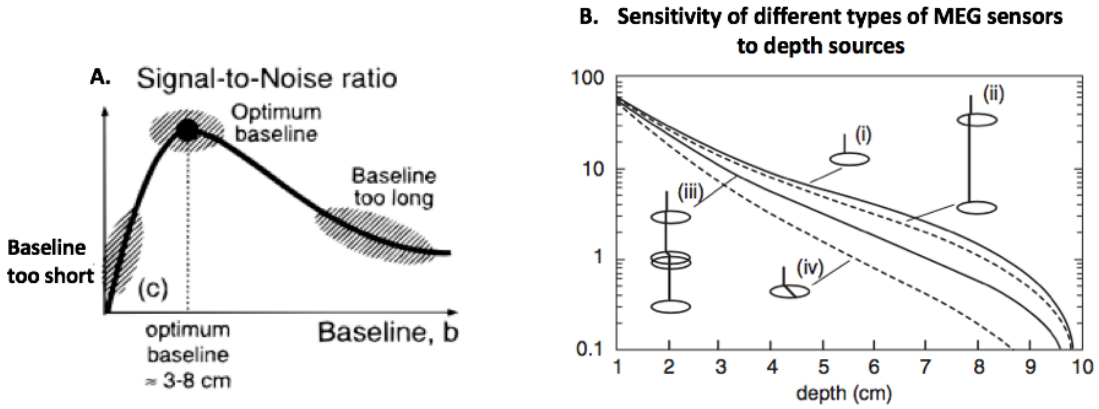

Figure 3. A. Signal-to-noise ratio (y-axis with arbitrary units) of MEG sensors as a function of the length of the baseline of the flux transformer pick up coils (x-axis). **B.** Sensitivity of different types of flux transformer pick up coils (y-axis with arbitrary units) as a function of

depth under the scalp (x-axis). The hippocampus is about 5 cm beneath the scalp.

Figure 3A is reproduced from Vrba and Robinson (2001). Figure 3B is reproduced from Lopes da Silva (2010).

From the measured data on the scalp, we typically wish to infer the spatiotemporal dynamics of neural activities at the source level, a process referred to as source localization. This is an ill-posed problem, because given a certain topography at the sensor level, there are an infinite number of configurations at the source level that could produce the measured magnetic fields (Baillet, 2017). However, by adding prior information and constraints, such as the anatomy from magnetic resonance imaging (MRI), and head geometry, the problem can be solved with source localization algorithms (Gorodnitsky et al., 1995; Im et al., 2005; Ioannides et al., 1990; Mattout et al., 2006; Wolters et al., 2006). To estimate sources from MEG scalp signals, the general procedure is to solve the forward and inverse problems sequentially (Attal et al., 2012; Hämäläinen et al., 1993). The forward solution computes the gain matrix composed of the contribution of each brain source to the external sensors, and with the head geometry modelled using realistic (e.g., Fuchs et al., 1998; Nolte, 2003) or spherical head models (e.g., Sarvas, 1987). Therefore, it answers the question of 'what would activity at the scalp look like, given activation of dipole sources in the brain' (Cohen, 2014). The inverse solution then computes the current sources from the topographical pattern of activity seen in the data by considering the topographical patterns generated by forward solutions.

MEG inverse solutions can be roughly categorized into two classes: equivalent current dipole fitting and distributed-source imaging methods (Hämäläinen & Hari, 2002). Distributed-source imaging methods can be subdivided into nonadaptive distributed-source imaging methods, including minimum norm estimation (MNE) and its variants such as low-resolution electromagnetic tomography (LORETA); and adaptive distributed-source imaging methods, such as beamforming (Cohen, 2014). As previously mentioned, it has been conventionally assumed that MEG is insensitive to signals from deep sources in the brain (Moses et al., 2011), because neuromagnetic signals decay strongly as a function of distance and some source localization algorithms have a strong bias towards the neocortex.

MEG and the hippocampus: Simulation studies

Simulation studies (Table 1) have been directed to two broad questions. First, can hippocampal activation be reliably detected by MEG sensors and if so, can this activity be dissociated from other signals and noise? Second, can hippocampal activation be localized by source localization algorithms, especially in the presence of concurrent sources in the cerebral cortex?

Studies	Summary
Chupin et al. (2002)	This study evaluated the relative contributions of hippocampal and neocortical regions to MEG sensor signals.
Stephen et al., (2005)	This study investigated whether MEG was able to differentiate between hippocampal activity and neocortical activity and between hippocampal activity and parahippocampal activity.
Attal et al., 2007 **A**ttal & Schwartz, 2013 **A**ttal et al, 2012 (a review)	In these studies, simulations were performed to determine the detectability of the activation from deep sources including the hippocampus by MEG sensors; the performances of different depth- weighted minimum norm inverse operators in deep source localization were compared.
Quraan et al., 2011 **M**ills et al., 2012	The study investigated the ability of beamforming technique to localize the hippocampal signals with different strengths in presence of different strengths of neocortical activation.
Meyer et al., 2017	Using Bayesian model comparison, this study investigated which model (one containing cortical surface and one containing both cortical surface and the hippocampus) provided a more likely explanation of the dataset with simulated hippocampal activity. The performances of different inverse operators were compared as well.

Table 1. MEG simulation studies of the human hippocampus

An early study (Chupin et al., 2002) was carried out to evaluate the relative contribution of hippocampal and neocortical regions to MEG sensor signals from a forward problem point of view. This work simulated the activation of hippocampal and neocortical patches one after the other based on different current dipole moment densities estimated in those regions from animal models (Murakami & Okada, 2006;

Okada et al., 1996). The MEG gain matrices (MEG fields) relating to the hippocampus and neocortical areas were computed in a spherical head model in accordance with a CTF whole-head 151-channel system configuration (with first-order axial gradiometers). Results showed that average cortical activation increased linearly as a function of patch size, whereas hippocampal fields reached a plateau (saturation) for patches greater than about 2 cm^2. This might be due to the geometry of the hippocampus, causing partial cancellation of the signal when large areas of the hippocampus are activated. The cortical magnetic fields were larger than the hippocampal fields, but the hippocampal fields (a mean of about 100 fT) were significantly larger than intrinsic MEG device noise level (10 fT at 10 Hz) and averaged brain background activity (a few tens of fT). These results show that although the hippocampus is farther away from the sensors relative to the neocortex, physiologically reasonable activations can result in magnetic fields large enough to be detected by MEG sensors. It may be that the higher current densities in the hippocampus relative to the neocortex compensate for the greater distance away from MEG sensors (Attal et al., 2007).

Stephen et al. (2005) explored whether MEG is able to differentiate between activity in different subfields of the hippocampus and superficial neocortex and between activity in the hippocampus and the parahippocampus, when activated sequentially and concurrently. The simulated signals were embedded in real background brain activities recorded using a 122-channel Elekta system (with planar

gradiometers) from five epileptic patients in the resting state. They found that at the sensor level, the addition of real background brain activity to the simulated activity could significantly change the waveform of the simulated activity relative to that modelled without background activity. To determine the discriminability of the simulated sources at the sensor level, root mean square error (RMSE) values were computed (derived from RMSE = $||1-C_{sim}||$; with '|| ||' being the Euclidean form; C_{sim} defined as the correlation value at each channel between the simulated waveform with background activities and that without background activities; the auto-correlation at each channel of the noise-free waveform = 1). They hypothesized that if two sources can be differentiated, for instance CA1 and parahippocampus, the RMSE of CA1 with versus without background activity should be significantly smaller than RMSE of parahippocampus with background activity versus CA1 without background activity. If a significant difference was found, they tested whether a double dissociation was achieved. For instance, whether RMSE of parahippocampus with background activity versus without was also significantly less than RMSE of CA1 with background activity vs. parahippocampus without background activity. If a double dissociation did not occur, it suggested weak differentiability but with significant differences in the waveform patterns.

The results showed that activation of the hippocampus with one subfield or all subfields could be differentiated from activation from superficial neocortex and doubly dissociated. Parahippocampal activation could be differentiated from

hippocampal activation when the two regions were simulated sequentially. Simultaneous activation of parahippocampus and hippocampus could also be differentiated from single hippocampal or parahippocampal activation in isolation, but no double dissociation was achieved in either case. At the source space, dipole fitting was used for source location. To avoid biasing the results with known source locations, and to ensure the global minimum was reached, searches with random starting parameters were carried out across the whole brain. Results demonstrated that hippocampal sources and superficial cortical sources could both be located and differentiated, with 73% of all sources within a 10 mm error range and the mean amplitude-peak time difference between modeled peak and the simulated peak being 1.1 ms. When all the subfields of the hippocampus and dentate gyrus were simulated simultaneously, there was partial cancellation. However, hippocampal sources could only be differentiated from parahippocampal sources when the two regions activated sequentially and could not be resolved when activation overlapped in time.

Attal and colleagues (Attal et al., 2007; Attal et al., 2012; Attal & Schwartz, 2013) performed simulation studies based on realistic anatomical and electrophysiological models to explore the detectability of MEG for deep sources, such as the hippocampus, the amygdala, and thalamus, and to compare the performance of different depth weighted minimum norm inverse operators (one depth weighted MNE and two noise-normalized depth weighted MNE algorithms). As in Chupin et al. (2002), to mimic the activations of different areas, different values of

current dipole moment density in different regions of interest were based on animal models to calculate the simulated MEG fields on a 151-channel sensor array (axial gradiometers) for each region of interest. Simulation of activation from each region of interest in seven participants was performed for patch sizes ranging from 1 – 5 cm^2 for surface patches and 1 – 5 cm^3 for volume patches sequentially or concurrently. As expected, the simulated MEG fields for subcortical areas were ten times lower than that for neocortex, but were strong enough to overlap parts of the distribution of the MEG field of neocortex, especially for the hippocampus and the amygdala. Then, the simulated fields were added to individual resting state MEG data, which were then inverted with a forward spherical head model and three inverse operators (depth weighted MNE (wMNE), dynamic statistical parametric mapping (dSPM) and standardized low-resolution electromagnetic tomography (sLORETA)), to localize the sources. DLE_g (the Euclidian distance of a solution's gravity center from the reconstructed source location to the true location) and DLE_m (the Euclidian distance of a solution's maximum from the reconstructed source location to the true location) were used to assess the ability of the three operators.

With a single subcortical activation, DLE_g showed better results using wMNE than the two noise-normalized depth-weighted MEG inverse operators (dSPM and sLORETA) with errors less than 8 mm in the majority of the hippocampus and the amygdala. Conversely, the better DLE_m was obtained by dSPM and sLORETA, but the spatial patterns for the two inverse operators were not the same. sLORETA had a

lower DLE_g in the deeper central regions, such as the thalamus, whereas dSPM had a very good estimation over the hippocampus but strong errors in the thalamus. For concurrent activation of two sources, one in the hippocampus and one in the visual cortex, when the two activations had little overlap (25%), hippocampal generators were well estimated by the three inverse operators, but only dSPM maintained the local maximum in the hippocampus. With increasing overlap of the activation of the two areas, the performance of all of the methods decreased. wMNE had good detection of hippocampal activation when the overlap was up to 50%, whereas sLORETA and sSPM had good estimation of hippocampal activation even when the two sources were simultaneously activated, but created a local maximum in the thalamus (a deep ghost source).

The researchers further computed point-spread functions (PSF) to quantify the distortion of the source reconstruction by the inverse operators, namely, the spread of hippocampal sources to other cortical and subcortical areas. The resulting PSF maps of hippocampal sources showed that highest values were localized in the medial (parahippocampus and entorhinal cortex) and lateral temporal lobe. Compared to wMNE PSF map, sLORETA PSF map of hippocampal sources showed a significant decrease in PSF value in the neocortex but still significant values in the parahippocampal areas; however, the deeper regions in the thalamus and the nearest amygdala part showed a PSF value increase. dSPM PSF map of hippocampal sources showed small values in the neocortex and other subcortical structures. To quantify the

distortion that is induced from other source locations, cross-talk functions (CTF) were computed. The three inverse operators returned very similar CTF maps, and the strongest values of the CTF maps were located in the lateral temporal lobe, especially in the superior temporal sulcus (STS), which suggests the activity of STS is most likely to influence the reconstructed hippocampal sources.

Beamforming source localization methods are increasing in popularity, due to an intrinsic ability to attenuate signals from outside the region of interest (Mills et al., 2012). Quraan and colleagues (Quraan et al., 2011) have simulated the ability of beamformers to localize hippocampal activation. In one set of simulations, activations placed in the anterior part of bilateral hippocampi with respect to each of 15 participants' hippocampi were added to uncorrelated random Gaussian noise at typical levels in an MEG system. Each source was simulated in the tangential orientation as a 50 ms segment of a 10 Hz sinusoid with a physiologically realistic range of amplitudes ranging from 10 – 40 nAm, Group average results showed that beamforming was able to localize the hippocampus at all simulated strengths. At 40 nAm, the average localization error was 7.5 mm and went up to 10 mm at 10 nAm. Only a small systematic bias was found for the x, y, z coordinate errors ($X_{error}=X_{reconstructed}-X_{simulated}$).

To represent the real case scenario, in the second set of simulations, the simulated hippocampal activation was added to real visual evoked fields (VEFs)

acquired with a 151-channel CTF system (axial gradiometers), but temporally displaced from the visual activation. When the simulation strength was greater than or equal to 30 nAm, the simulated field was visible on the sensor level global field power (GFP) plot; but disappeared when the simulation strength was at or below 20 nAm. However, beamforming was able to localize the hippocampal activation at all simulated source strengths and the localization varied by a maximum of 7 mm among the four group averages of different activation strengths. However, lower simulated hippocampal activation resulted in less focal localizations. At 10 nAm, artifactual peaks appeared outside the hippocampus. The researchers also tested the influence of other factors such as trial number and participant number on localization accuracy. Overall, more trials and participants resulted in more accurate source localization. Analyses which aimed to investigate whether there was any systematic localization bias in the presence of low brain noise were performed as in the first simulation. A localization bias was found in the lateral direction toward the MEG sensors. Thus, noise can introduce systematic bias to reconstructed hippocampal sources.

In the third set of simulations, the simulated source was added to temporally overlapping visual evoked fields (VEFs). At strengths of 40 nAm, hippocampal activation was detected as the strongest activation across the whole brain, but at 30 nAm, the visual source was stronger (although the hippocampal activation was still visible). At 20 and 10 nAm, the hippocampal signal was no longer visible due to leakage from the visual sources. To remove leakage from the visual source, condition

subtraction was used. That is, the source localization image of the experimental condition was subtracted from that of the control condition which evoked similar basic sensory responses but not the same degree of hippocampal activation. Using this subtraction method, hippocampal activation was clearly detected even at 10 nAm. However, at the individual participant level, in the presence of both low and high brain noise, hippocampal activation could be detected in only 2 or 3 out of 15 participants even with condition subtraction.

In a follow-up study, Mills et al. (2012) compared the accuracy of localizing hippocampal activation using different subtraction methods: post-localization subtraction (used in Quraan et al., 2011), and pre-localization subtraction. Pre-localization was done by first subtracting the sensor data of the two conditions and beamforming was performed on the difference sensor data to localize the source. In situations of hippocampal activation embedded in either low or high brain noise, pre-localization outperformed post-localization subtraction method in terms of source localization accuracy and the ability to detect weak hippocampal activation. Applying the pre-localization method to empirical data acquired with a 151-channel CTF system while participants were performing a transverse patterning task (shown to activate the hippocampus using other imaging modalities; e.g., Driscoll, 2003; Meltzer et al., 2008) at the individual level, hippocampal activation could be detected in up to six out of fourteen participants, compared to only two participants using post-localization subtraction. These researchers noted that the main drawback of

sensor data subtraction is that it is susceptible to changes in head position which would limit the localization accuracy. Thus, for the ideal situation, the experimental and control conditions should be interleaved in one experimental run so that the head movement and MEG-MRI co-registration error is the same.

Recently, Meyer et al. (2017) used Bayesian model comparison to examine MEG sensitivity to hippocampal activity. A single dipole perpendicular to the surface of the hippocampal curvature or cortical surface was simulated in either the hippocampus or the cortical areas with a 300 ms segment of a sinusoidal waveform of 20 Hz and a dipole moment of 20 nAm. Gaussian white noise was added to simulated MEG fields. Then the researchers inverted the data using two different realistic forward models, one which included both the cortical surface and the hippocampus and one which only included cortical surface and with three inverse operators, namely, minimum norm estimation (MNE), empirical Bayes beamformer (EBB) and multiple sparse priors (MSP). Free energy (Friston et al., 2006) was used as an index to quantify the model evidence of a given forward model with a given inverse operator. Free energy rewards the model that fits the data appropriately and penalizes models that are overly-complex. The researchers hypothesized if the simulation was in the hippocampus, the combined model with cortical areas and the hippocampus would outperform the model with only cortical areas (and would return a higher free energy value), because if using the cortical model, one needed a more complex combination of cortical sources to fit the data equally well. Results showed for all the three inverse

operators, the combined model had a higher free energy value than the cortical model, but only the free energy value obtained from EBB and MSP inverse operators reached significance.

The source images echoed these results. When the correct model was used, the source maps of EBB and MSP were accurate and focal. When the wrong model was used, the source maps of EBB and MSP showed an increase in spatial spread and decrease in accuracy of the peak location. MNE returned the most diffuse source map with the peak outside the hippocampus, but the general pattern was similar across the three inverse operators. An alternative measure — dipole localization error (DLE) – was concordant with the results using free energy values and the cortical model gave higher DLE values than the combined model.

The researchers further simulated a medial cortical area, only 2.14 mm from the hippocampus, to see whether the model comparison would return false positive results. The two models did not return significantly different results. These researchers also tested the influence of signal-to-noise ratio (SNR) and MEG-MRI co-registration error on the model comparison. It was shown that poor SNR was less harmful to the ability to differentiate models than co-registration error. When the co-registration error was greater than 3 mm, the model comparison could not return accurate results.

Interim summary

Based on the results of simulation studies reviewed above, we can begin to answer the questions posed in the previous section. Magnetic fields emanating from the hippocampus can be detected by MEG sensors (by both planar gradiometers and axial gradiometers). Cancellation occurs when hippocampal subfields and dentate gyrus were activated together but is only partial. Whether the hippocampal magnetic fields are visible or not on the global field power plot depends on the strengths of background brain 'noise', including whether there are strong magnetic fields from cortex (e.g., visual area). However, whether the signal is visible at the sensor level or not, source localization algorithms can localize hippocampal sources at the group level. SNR at the sensor level does not reflect the ability to localize weak hippocampal sources (Meyer et al., 2017), in line with results from other quantitative fields that small signals embedded in high noise backgrounds can be detected at high confidence levels (Quraan et al., 2011). A variety of source localization algorithms such as dipole fitting, depth-weighted MNE, and beamforming can be used to localize hippocampal sources. Condition subtraction can increase the ability to detect hippocampal activation, especially for beamforming. At the individual level, MEG-MRI co-registration errors strongly influence localization accuracy. If these co-registration errors are not systematic across participants, and the head movement is reasonably low (less than 5mm in any direction), group averaging can alleviate the influence of co-registration errors and increase accuracy of localization of the

hippocampal sources.

MEG and the hippocampus: Empirical studies

Hippocampal sources have now been reported by a number of MEG studies (Table 2). The empirical studies (unlike simulation studies) do not have a known ground truth. Therefore, common reports of hippocampal activation from MEG studies and other techniques/methods (e.g., iEEG, fMRI, lesion studies and animal studies) using the same/similar paradigm provide validation that hippocampal activation can indeed be detected by MEG. These experimental paradigms used to elicit hippocampal activation in MEG studies include memory encoding (e.g., Crespo-Garcia et al., 2016), retrieval (e.g., Guderian & Duzel, 2005) and integration (e.g., Backus et al., 2016), spatial navigation (e.g., Cornwell et al., 2008), violation detection (e.g., Garrido et al., 2015), and transverse patterning (e.g., Moses et al., 2009).

As described in chapter one, hippocampal low frequency theta oscillations during virtual navigation are of considerable interest because of the linkages to classic studies in rodents (e.g., Buzsaki et al., 1983; Fox et al., 1986; O'Keefe & Recce, 1993) showing that when animals are actively exploring the environment, there is a striking increase in theta power in the hippocampus. Theta oscillations are believed to provide a timing mechanism for place cell firing (Colgin, 2016; O'Keefe & Recce, 1993) and

are thought to play an important role in learning (Burgess & O'Keefe, 2011; Buzsaki & Moser, 2013; Lever et al., 2014). Subsequently, iEEG studies (e.g., Bohbot et al., 2017; Ekstrom et al., 2005; Jacobs et al., 2009; Vass et al., 2016; Watrous et al., 2013) have reported a comparable low frequency theta power increase in the human hippocampus during virtual, real or mental navigation.

Using a whole-head MEG system with 275 first-order axial gradiometers, Cornwell et al. (2008) recorded neuromagnetic responses of the brain of normal healthy participants while they were performing a virtual version of Morris water maze task (Morris, 1984), which has been used extensively to elicit the hippocampal theta oscillations in rodent studies (e.g., Olvera-Cortes et al., 2012; Olvera-Cortes et al., 2004). In the virtual water maze task, participants are required to find a hidden platform fixed in a goal location in hidden platform condition and to randomly swim in a control condition. Beamforming was used to localize hippocampal theta signals. It was found that hippocampal theta power in the hidden platform condition was significantly stronger than that in the random swimming condition, in agreement with what has been found by human iEEG studies and animal studies in a similar behavioural context. Recently, Meyer et al. (2016) recorded participants' brain responses using a whole-head MEG system with 275 axial gradiometers during a spatial navigation task which has been shown to activate the hippocampus. They tested how well the sensor level signals could be predicted by the lead fields computed based on two different generative forward models respectively: one that

had MRI-derived correct anatomy and one that contained MRI-derived anatomy but with rotated hippocampi. They found that the lead field computed from the model with rotated hippocampi explained significantly less MEG sensor data than that computed from the correct model.

Comparison of source reconstructed images of patients with the hippocampus removed with that of normal controls in a hippocampus-dependent task offers a way to evaluate the validity of using MEG to detect hippocampal signals in empirical experiments. In an auditory oddball paradigm (a deviant sound embedded in a series of standard sounds) shown with iEEG (Halgren et al., 1980) to activate the hippocampus, Ioannides et al. (1995) and Okada et al. (1983) successfully localized hippocampal activity using MEG recordings. In addition, Ioannides et al. (1995) compared the source localization image of the patient with hippocampus and amygdala removed with normal participants. They found no activation in the hippocampus and amygdala complex in the MEG source image of the patient, while clear hippocampal activities were seen in normal participants responding to the deviant sound. These findings support that contention that MEG can reliably detect hippocampal signals, and argue against the possibility that the reconstructed hippocampal signals are artefactual.

Simultaneous iEEG and MEG recordings also support the idea that MEG can measure hippocampal activity. In an intensive reading task, with the depth electrodes

placed in the hippocampus of four patients with epilepsy, Dalal et al. (2013) simultaneously recorded MEG and iEEG data. Results showed that depth EEG in the theta frequency range (4 – 8 Hz) from the hippocampus was strongly correlated at zero lag with MEG sensor signals over the temporal lobe. In another study, with a whole-head MEG system with 248 magnetometers, MEG signals were acquired while participants were performing an associative memory task, Crespo-Garcia et al. (2016) found that the power of low frequency (2 – 3 Hz) oscillations in the mid-posterior hippocampi reconstructed by beamforming was significantly larger than that in the pre-trial interval, and the increased hippocampal power was negatively correlated with subsequent memory accuracy, indicating that local suppression of low-frequency activity is essential for more efficient processing of detailed information. These results were corroborated by results from simultaneously recorded iEEG data. Note that the direction of correlation with behavioral performance is opposite to what has been found for higher frequency 4 – 8 Hz in other studies (e.g., Cornwell et al., 2008; Kaplan et al., 2012), suggesting that there might be different subsequent memory effects for lower and higher low frequency oscillations.

Findings from parallel MEG/fMRI provide further validation for using MEG to detect hippocampal signals. Although fMRI signals are blood oxygen level-dependent (BOLD) signals related to neuronal activities (Ogawa et al., 1990) and MEG directly measures the magnetic fields induced by neuronal activities, the origin of at least some of the signals of the two imaging modalities are likely to originate from

comparable underlying physiological processes (i.e., post-synaptic current flow; Hall et al., 2014). Moreover, a number of studies (e.g., Brookes et al., 2005; Muthukumaraswamy & Singh, 2008; Singh et al., 2002) have shown a close spatial relationship between MEG-derived signals such as oscillatory power in multiple frequency bands with BOLD. Further, it was found that the use of fMRI based priors to solve the MEG inverse problem would return higher model evidence in a Bayesian framework for fMRI constrained MEG source reconstruction (Henson et al., 2010). All these lines of evidence support the contention that fMRI and MEG have some spatial concordance (Hall et al., 2014). On this logic, using parallel fMRI and MEG recordings during a virtual spatial navigation task, Kaplan et al. (2012) reported fMRI observed increased hippocampal activation during movement initiation periods versus stationary periods. Constructing the time series of this location from MEG sensor data using beamforming revealed that there was a theta power increase during movement initiation periods, supporting the idea that hippocampal theta supports volitional navigation.

In a study of functional connectivity in the resting state (Cousijn et al., 2015), independent component analysis (ICA) was used to identify networks in resting state fMRI data and MEG theta band activity reconstructed by beamforming. ICA of MEG theta band activity and fMRI data identified similar left and right lateralized hippocampal networks. Moreover, the spatial patterns of regions coactivated with the hippocampal network for fMRI and MEG was found to be highly correlated ($r = 0.54$).

Further analyses showed that intrahippocampal theta obtained from MEG was negatively correlated with hippocampal-prefrontal cortex coactivation obtained from fMRI, in agreement with the idea that hippocampal theta plays an important role in hippocampal-prefrontal integration (Benchenane et al., 2010). While the exact relationship between MEG and fMRI signals is a complicated topic (Hall et al., 2014) and beyond the scope of this paper, the point here is hippocampal activities reported by both fMRI and MEG argue strongly that hippocampal activities can be detected by MEG.

Article	**Task**	**MEG system**	**Forward model**	**Inverse model**
Backus et al., 2016	**M**emory integration	Whole-head system with 275 axial gradiometers	Single shell head model	Beamforming
Breier et al. (1998) **B**reier et al. (1999)	**M**emory recognition **A**uditory verbal and non-verbal Memory	148 magnetometers	Spherical head model	Dipole fitting
Campo et al. (2012) **C**ampo et al. (2005)	**W**orking memory	148 magnetometers	Spherical head model	Multiple sparse priors (MSP)
Cornwell et al. (2012) **C**ornwell et al. (2008) **C**ornwell et al. (2014) **C**ornwell et al. (2010)	**S**patial navigation	275 axial gradiometers	Spherical head model	Beamforming
Cousijn et al. (2015)	**R**esting state	102 magnetometers and 204 planar gradiometers	Spherical head model	Beamformer and Independent component analysis (ICA)

Crespo-Garcia et al. (2016)	**I**tem-place encoding	148 magnetometers	Realistic anatomical and electrophysiological model	Beamforming
Engels et al. (2016)	**R**esting state	102 magnetometers and 204 planar gradiometers	Spherical head model	Beamforming
Fuentemilla et al., 2014	**A**utobiographical and Semantic retrieval	275 axial gradiometers	Single shell head model	Beamforming
Guderian et al. (2009) **G**uderian and Duzel (2005)	**M**emory encoding **M**emory retrieval	148 magnetometers	Not reported	Minimum-norm current–density reconstruction
Hamada et al. (2004)	**O**ddball task	80 axial gradiometers	Spherical head model	Dipole fitting
Hanlon et al. (2003) **H**anlon et al. (2005) **H**anlon et al. (2011)	**T**ransverse patterning	122 planar gradiometers; 275 axial gradiometers	Spherical head model; Not reported in the paper of 2011	Dipole fitting; standardized Low Resolution Electromagnetic Tomography (sLORETA)
Hopf et al. (2013)	**T**ransverse patterning	151 axial gradiometers	Not reported	Beamforming
Ioannides et al. (1995)	**O**ddball task	7 second-order gradiometers	Spherical head model	Magnetic field tomography (MFT)
Kirsch et al. (2003)	**E**yebink conditioning	122 planar gradiometers	Not reported	Dipole fitting
Kaplan et al. (2012)	**S**patial navigation	275 axial gradiometers	Single shell model head model	Beamforming
Leirer et al. (2010)	**T**ransverse patterning	148 magnetometers	Spherical head model	Dipole fitting
Garrido et al. (2015)	**S**equence violation	275 axial gradiometers	Single shell model head model	Beamforming

Martin et al. (2007)	**T**ransverse patterning **O**ddball task	102 magnetometers and 204 planar gradiometers	Spherical head model	Dipole fitting
Moses et al. (2009)	**T**ransverse patterning	151 axial gradiometers	Not reported	Beamforming
Nishitani et al. (1998) **N**ishitani et al. (1999) **N**ishitani (2003)	**O**ddball task **E**motional picture discrimination	122 planar gradiometers	Spherical head model	Dipole fitting
Papanicolaou et al. (2002)	**M**emory retrieval	148 magnetometers	Spherical head model	Dipole fitting
Poch et al. (2011)	**D**elayed match-to-sample task	275 axial gradiometers	Single-shell head model	Beamforming
Riggs et al. (2009)	**S**cene recognition	151 axial gradiometers	Not reported	Beamforming
Taylor et al. (2012) **T**aylor et al. (2011)	**W**orking memory **F**ace recognition	151 axial gradiometers	Spherical head model	Beamforming
Tesche et al. (1996) **T**esche (1997) **T**esche and Karhu (1999) **T**esche and Karhu (2000)	**O**ddball task **M**ental calculation and picture viewing **S**ensorimotor integration **W**orking memory	122 planar gradiometers	Single compartment boundary element conductor model	Signal-space projection (SSP)
Zouridakis et al. (1998)	**W**ord recognition	148 magnetometers	Spherical head model	Dipole fitting

Table 2. Empirical MEG studies of the human hippocampus.

Conclusions

Taken together, the evidence reviewed above strongly supports the contention that MEG can reliably detect signals from the hippocampus. We can draw on three converging lines of evidence:

(1) Physiological considerations. The principle neurons in the hippocampus are neatly aligned with the dendrites facing one direction and the soma another (Lorente de No, 1947), such that the signals produced by synchronization of those neurons can be detected by MEG (Murakami & Okada, 2006); the current dipole moment density in the hippocampus is several times larger than that in the neocortex, such that it can generate signals strong enough to be sensed by MEG sensors (Attal et al., 2007); although the geometry of the hippocampal formation is folded, signal cancellation is partial and occurs only when all hippocampal subfields and dentate gyrus are activate simultaneously (Stephen et al., 2005);

(2) Simulation studies. Simulation studies show that hippocampal signals can be sensed by MEG sensors even with quite different pickup coil configurations, such as axial versus planar gradiometers. Various source localization algorithms can be used to reconstruct hippocampal sources from MEG data, as long as the algorithm can suppress the strong signals from other brain regions including the neocortex. In this sense, beamforming does a good job of suppressing the signal outside the region of interest without compromising the signal from the region of interest. Compared to source image reconstructed by MNE, the source image reconstructed by beamforming is more focal and the peak better localized to the hippocampus (Meyer et al., 2017) and compared to dipole fitting or

MSP, no priors about activation locations need to be specified for beamforming. Although this review mainly focused on evaluating detecting hippocampal signals with MEG in cognitive experiments, another good piece of evidence in favor of beamforming came from a recent study (Hillebrand et al., 2016) which used MEG and iEEG to detect the interictal spike discharges in epileptic patients. It was found that the time series of the virtual sensor in the hippocampi reconstructed by beamforming accurately matched the spike discharges identified in recordings from depth electrodes placed in hippocampi. A consideration, as shown in Quraan et al. (2011), is that beamforming cannot completely suppress strong signals from the neocortex, but condition subtraction can alleviate the leakage. Thus, researchers need to consider appropriate control condition during experimental design, as well as other factors such as the number of trials to increase the length of the covariance matrix (Brookes et al., 2008).

(3) Empirical studies. A range of empirical studies have successfully shown that MEG can reliably detect and localize the hippocampal signals in various experimental paradigms which have already been shown hippocampal activation using other modalities and methods. Simultaneous iEEG and MEG recordings, and parallel MEG and fMRI studies both provide good evidence that MEG is capable of detecting hippocampal

signals. A lack of hippocampal signals from MEG data for the patient with removed hippocampus and amygdala complex supports the conclusion that hippocampal signals reconstructed in normal participants are not artefactual (Ioannides et al., 1995). It is to be noted that at this stage, in empirical studies hippocampal detection by MEG still heavily rely on group averages. As shown in Meyer et al. (2017), co-registration error is important for accurate hippocampal source reconstruction. Group averaging can alleviate this problem if the co-registration error is not systematic across participants.

References

Amaral, D., & Lavenex, P. (2006). Hippocampal neuroanatomy. In P. Andersen, R. Morris, D. Amaral, T. Bliss, & J. O'Keefe (Eds.), *The hippocampus book*: Oxford University Press.

Attal, Y., Bhattacharjee, M., Yelnik, J., Cottereau, B., Lefevre, J., Okada, Y., . . . Baillet, S. (2007). Modeling and Detecting Deep Brain Activity with MEG & EEG. *Conf Proc IEEE Eng Med Biol Soc*, 4937-4940.

Attal, Y., Maess, B., Friederici, A., & David, O. (2012). Head models and dynamic causal modeling of subcortical activity using magnetoencephalographic/electroencephalographic data. *Rev Neurosci, 23*(1), 85-95. doi:10.1515/rns.2011.056

Attal, Y., & Schwartz, D. (2013). Assessment of subcortical source localization using deep brain activity imaging model with minimum norm operators: a MEG study. *PLoS One, 8*(3), e59856. doi:10.1371/journal.pone.0059856

Backus, A. R., Schoffelen, J. M., Szebenyi, S., Hanslmayr, S., & Doeller, C. F. (2016). Hippocampal-Prefrontal Theta Oscillations Support Memory Integration. *Curr Biol, 26*(4), 450-457. doi:10.1016/j.cub.2015.12.048

Baillet, S. (2017). Magnetoencephalography for brain electrophysiology and imaging. *Nat Neurosci, 20*(3), 327-339. doi:10.1038/nn.4504

Benchenane, K., Peyrache, A., Khamassi, M., Tierney, P. L., Gioanni, Y., Battaglia, F. P., & Wiener, S. I. (2010). Coherent theta oscillations and reorganization of spike timing in the hippocampal- prefrontal network upon learning. *Neuron,*

66(6), 921-936. doi:10.1016/j.neuron.2010.05.013

Bohbot, V. D., Copara, M. S., Gotman, J., & Ekstrom, A. D. (2017). Low-frequency theta oscillations in the human hippocampus during real-world and virtual navigation. *Nat Commun, 8*, 14415. doi:10.1038/ncomms14415

Breier, J. I., Simos, P. G., Zouridakis, G., & Papanicolaou, A. C. (1998). Relative timing of neuronal activity in distinct temporal lobe areas during a recognition memory task for words. *J Clin Exp Neuropsychol, 20*(6), 782-790. doi:10.1076/jcen.20.6.782.1116

Breier, J. I., Simos, P. G., Zouridakis, G., & Papanicolaou, A. C. (1999). Lateralization of cerebral activation in auditory verbal and non-verbal memory tasks using magnetoencephalography. *Brain Topogr, 12*, 89-97.

Brookes, M. J., Gibson, A. M., Hall, S. D., Furlong, P. L., Barnes, G. R., Hillebrand, A., . . . Morris, P. G. (2005). GLM-beamformer method demonstrates stationary field, alpha ERD and gamma ERS co-localisation with fMRI BOLD response in visual cortex. *Neuroimage, 26*(1), 302-308. doi:10.1016/j.neuroimage.2005.01.050

Brookes, M. J., Vrba, J., Robinson, S. E., Stevenson, C. M., Peters, A. M., Barnes, G. R., . . . Morris, P. G. (2008). Optimising experimental design for MEG beamformer imaging. *Neuroimage, 39*(4), 1788-1802. doi:10.1016/j.neuroimage.2007.09.050

Buckner, R. L., & Logan, J. M. (2001). Functional Neuroimaging Methods: PET and fMRI. In R. Cabeza & A. Kinstone (Eds.), *Handbook of Functional*

Neuroimaging of Cognition. Cambridge, MA: The MIT Press.

Burgess, N., & O'Keefe, J. (2011). Models of place and grid cell firing and theta rhythmicity. *Curr Opin Neurobiol, 21*(5), 734-744. doi:10.1016/j.conb.2011.07.002

Buzsaki, G., Leung, L. W. S., & Vanderwolf, C. H. (1983). Cellular bases of hippocampal EEG in the behaving rat. *Brain Res Rev, 6*, 139-171.

Buzsaki, G., & Moser, E. I. (2013). Memory, navigation and theta rhythm in the hippocampal-entorhinal system. *Nat Neurosci, 16*(2), 130-138. doi:10.1038/nn.3304

Campo, P., Garrido, M. I., Moran, R. J., Maestu, F., Garcia-Morales, I., Gil-Nagel, A., . . . Friston, K. J. (2012). Remote effects of hippocampal sclerosis on effective connectivity during working memory encoding: a case of connectional diaschisis? *Cereb Cortex, 22*(6), 1225-1236. doi:10.1093/cercor/bhr201

Campo, P., Maestu, F., Capilla, A., Fernandez, S., Fernandez, A., & Ortiz, T. (2005). Activity in human medial temporal lobe associated with encoding process in spatial working memory revealed by magnetoencephalography. *Eur J Neurosci, 21*(6), 1741-1748. doi:10.1111/j.1460-9568.2005.03943.x

Chupin, M., Baillet, S., Okada, Y. C., Hasboun, D., & Garnero, L. (2002). *On the detection of hippocampus activity with MEG*. Paper presented at the 13th International Conference on Biomagnetism, Germany.

Cohen, M. X. (2014). *Analyzing neural time series data*: MIT press.

Cohen, M. X. (2017). Where Does EEG Come From and What Does It Mean? *Trends Neurosci*. doi:10.1016/j.tins.2017.02.004

Colgin, L. L. (2016). Rhythms of the hippocampal network. *Nat Rev Neurosci, 17*(4), 239-249. doi:10.1038/nrn.2016.21

Cornwell, B. R., Arkin, N., Overstreet, C., Carver, F. W., & Grillon, C. (2012). Distinct contributions of human hippocampal theta to spatial cognition and anxiety. *Hippocampus, 22*(9), 1848-1859. doi:10.1002/hipo.22019

Cornwell, B. R., Johnson, L. L., Holroyd, T., Carver, F. W., & Grillon, C. (2008). Human hippocampal and parahippocampal theta during goal-directed spatial navigation predicts performance on a virtual Morris water maze. *J Neurosci, 28*(23), 5983-5990. doi:10.1523/JNEUROSCI.5001-07.2008

Cornwell, B. R., Overstreet, C., & Grillon, C. (2014). Spontaneous fast gamma activity in the septal hippocampal region correlates with spatial learning in humans. *Behav Brain Res, 261*, 258-264. doi:10.1016/j.bbr.2013.12.031

Cornwell, B. R., Salvadore, G., Colon-Rosario, V., Latov, D. R., Holroyd, T., Carver, F. W., . . . Grillon, C. (2010). Abnormal hippocampal functioning and impaired spatial navigation in depressed individuals: evidence from whole-head magnetoencephalography. *Am J Psychiatry, 167*(7), 836-844. doi:10.1176/appi.ajp.2009.09050614

Cousijn, H., Tunbridge, E. M., Rolinski, M., Wallis, G., Colclough, G. L., Woolrich, M. W., . . . Harrison, P. J. (2015). Modulation of hippocampal theta and hippocampal-prefrontal cortex function by a schizophrenia risk gene. *Hum*

Brain Mapp, 36(6), 2387-2395. doi:10.1002/hbm.22778

Crespo-Garcia, M., Zeiller, M., Leupold, C., Kreiselmeyer, G., Rampp, S., Hamer, H. M., & Dalal, S. S. (2016). Slow-theta power decreases during item-place encoding predict spatial accuracy of subsequent context recall. *Neuroimage, 142*, 533-543. doi:10.1016/j.neuroimage.2016.08.021

Dalal, S., Jerbi, K., Bertrand, O., Adam, C., Ducorps, A., Schwarts, D., . . . Lachaux, J. (2013). Simultaneous MEG-intracranial EEG: New insights into the ability of MEG to capture oscillatory modulations in the neocortex and the hippocampus. *Epilepsy Behav, 28*, 310-311. doi:10.1016/j.yebeh.2013.03.012

Driscoll, I. (2003). The Aging Hippocampus: Cognitive, Biochemical and Structural Findings. *Cerebral Cortex, 13*(12), 1344-1351. doi:10.1093/cercor/bhg081

Ekstrom, A. D., Caplan, J. B., Ho, E., Shattuck, K., Fried, I., & Kahana, M. J. (2005). Human hippocampal theta activity during virtual navigation. *Hippocampus, 15*(7), 881-889. doi:10.1002/hipo.20109

Engels, M. M., Hillebrand, A., van der Flier, W. M., Stam, C. J., Scheltens, P., & van Straaten, E. C. (2016). Slowing of Hippocampal Activity Correlates with Cognitive Decline in Early Onset Alzheimer's Disease. An MEG Study with Virtual Electrodes. *Front Hum Neurosci, 10*, 238. doi:10.3389/fnhum.2016.00238

Fagaly, R. L. (2006). Superconducting quantum interference device instruments and applications. *Review of Scientific Instruments, 77*(10), 101101-101145. doi:10.1063/1.2354545

Forster, E., Zhao, S., & Frotscher, M. (2006). Laminating the hippocampus. *Nat Rev Neurosci, 7*(4), 259-267. doi:10.1038/nrn1882

Fox, S. E., Wolfson, S., & Ranck, J. B. (1986). Hippocampal theta rhythm and the firing of neurons in walking and urethane anesthetized rats. *Exp Brain Res, 62*, 495-508.

Friston, K., Kilner, J., & Harrison, L. (2006). A free energy principle for the brain. *J Physiol Paris, 100*(1-3), 70-87. doi:10.1016/j.jphysparis.2006.10.001

Fuchs, M., Drenckhahn, R., Wischmann, H. A., & Wagner, M. (1998). An improved boundary element method for realistic volume-conductor modeling. *IEEE Trans Biomed Eng, 45*(8), 980-997.

Fuentemilla, L., Barnes, G. R., Duzel, E., & Levine, B. (2014). Theta oscillations orchestrate medial temporal lobe and neocortex in remembering autobiographical memories. *Neuroimage, 85 Pt 2*, 730-737. doi:10.1016/j.neuroimage.2013.08.029

Garrido, M. I., Barnes, G. R., Kumaran, D., Maguire, E. A., & Dolan, R. J. (2015). Ventromedial prefrontal cortex drives hippocampal theta oscillations induced by mismatch computations. *Neuroimage, 120*, 362-370. doi:10.1016/j.neuroimage.2015.07.016

Gorodnitsky, I. F., George, J. S., & Rao, B. D. (1995). Neuromagnetic source imaging with FOCUSS: a recursive weighted minimum norm algorithm. *Electroencephalogr Clin Neurophysiol, 95*, 231-251.

Guderian, S., & Duzel, E. (2005). Induced theta oscillations mediate large-scale

synchrony with mediotemporal areas during recollection in humans. *Hippocampus, 15*(7), 901-912. doi:10.1002/hipo.20125

Guderian, S., Schott, B. H., Richardson-Klavehn, A., & Duzel, E. (2009). Medial temporal theta state before an event predicts episodic encoding success in humans. *Proc Natl Acad Sci U S A, 106*(13), 5365-5370. doi:10.1073/pnas.0900289106

Halgren, E., Squires, N. K., Wilson, C. L., Rohrbaugh, J. W., Babb, T. B., & Crandall, P. H. (1980). Endogenous potentials generated in the human hippocampal formation and amygdala by infrequent events. *Science, 14*, 803-805.

Hall, E. L., Robson, S. E., Morris, P. G., & Brookes, M. J. (2014). The relationship between MEG and fMRI. *Neuroimage, 102 Pt 1*, 80-91. doi:10.1016/j.neuroimage.2013.11.005

Hamada, Y., Sugino, K., Kado, H., & Suzuki, R. (2004). Magnetic fields in the human hippocampal area evoked by a somatosensory oddball task. *Hippocampus, 14*(4), 426-433. doi:10.1002/hipo.10196

Hämäläinen, M., & Hari, R. (2002). Magnetoencephalographic (MEG) characterization of dynamic brain activation. In A. Toga & J. Mazziotta (Eds.), *Brain mapping: The methods* (2nd Edition ed., pp. 877): Academic Press

Hämäläinen, M., Hari, R., IImoniemi, R. J., Knuutila, J., & Lounasmaa, O. V. (1993). Magnetoencephalography theory, instrumentation, and applications to noninvasive studies of the working human brain. *Rev Mod Phys, 65*(2), 413-497. doi:10.1103/revmodphys.65.413

Hanlon, F. M., Houck, J. M., Pyeatt, C. J., Lundy, S. L., Euler, M. J., Weisend, M. P., . . . Tesche, C. D. (2011). Bilateral hippocampal dysfunction in schizophrenia. *Neuroimage, 58*(4), 1158-1168. doi:10.1016/j.neuroimage.2011.06.091

Hanlon, F. M., Weisend, M. P., Huang, M., Lee, R. R., Moses, S. N., Paulson, K. M., . . . Canive, J. M. (2003). A non-invasive method for observing hippocampal function. *Neuroreport, 14*(15), 1957-1960. doi:10.1097/01.wnr.0000092788.85539.7a

Hanlon, F. M., Weisend, M. P., Yeo, R. A., Huang, M., Lee, R. R., Thoma, R. J., . . . Canive, J. M. (2005). A specific test of hippocampal deficit in schizophrenia. *Behav Neurosci, 119*(4), 863-875. doi:10.1037/0735-7044.119.4.863

Hari, R., Levanen, S., & Raij, T. (2000). Timing of human cortical functions during cognition: role of MEG. *Trends Cogn Sci, 4*(12), 455-462.

Henson, R. N., Flandin, G., Friston, K. J., & Mattout, J. (2010). A parametric empirical Bayesian framework for fMRI-constrained MEG/EEG source reconstruction. *Hum Brain Mapp, 31*(10), 1512-1531. doi:10.1002/hbm.20956

Hillebrand, A., & Barnes, C. A. (2002). A quantitative assement of the sensitivity of whole-head MEG to activity in the adult human cortex. *Neuroimage, 16*, 638-650. doi:10.1006/nimg.2002.1102

Hillebrand, A., Nissen, I. A., Ris-Hilgersom, I., Sijsma, N. C., Ronner, H. E., van Dijk, B. W., & Stam, C. J. (2016). Detecting epileptiform activity from deeper brain regions in spatially filtered MEG data. *Clin Neurophysiol, 127*(8),

2766-2769. doi:10.1016/j.clinph.2016.05.272

Hopf, L., Quraan, M. A., Cheung, M. J., Taylor, M. J., Ryan, J. D., & Moses, S. N. (2013). Hippocampal lateralization and memory in children and adults. *J Int Neuropsychol Soc, 19*(10), 1042-1052. doi:10.1017/S1355617713000751

Horner, A., & Doeller, C. F. (2017). Plasticity of hippocampal memories in humans. *Curr Opin Neurobiol, 43*, 102-109. doi:10.1016/j.conb.2017.02.004

Im, C. H., Jung, H. K., & Fujimaki, N. (2005). Anatomically constrained dipole adjustment (ANACONDA) for accurate MEG/EEG focal source localizations. *Phys Med Biol, 50*(20), 4931-4953. doi:10.1088/0031-9155/50/20/012

Insausti, R. (1993). Comparative anatomy of the entorhinal cortex and hippocampus in mammals. *Hippocampus, 3*, 19-26.

Ioannides, A. A. (2006). Magnetoencephalography as a research tool in neuroscience: state of the art. *Neuroscientist, 12*(6), 524-544. doi:10.1177/1073858406293696

Ioannides, A. A., Bolton, J. P. R., & Clarke, C. J. S. (1990). Continuous probabilistic solutions to the biomagnetic inverse problem. *Inverse Probl, 6*, 523-542.

Ioannides, A. A., Liu, M. J., Liu, L. C., Bamidis, P. D., Hellstrand, E., & Stephan, K. M. (1995). Magnetic field tomography of cortical and deep processes: examples of "real-time mapping" of averaged and single trial MEG signals. *Int J Psychophysiol, 20*, 161-175.

Jacobs, J., Lorolev, I. O., Caplan, J. B., Ekstrom, A., Litt, B., Baltuch, G., . . . Kahana, M. J. (2009). Right-lateralized brain oscillations in human spatial navigation. *J*

Cogn Neurosci, 22(5), 824-836. doi:10.1162/jocn.2009.21240

Kaplan, R., Doeller, C. F., Barnes, G. R., Litvak, V., Duzel, E., Bandettini, P. A., & Burgess, N. (2012). Movement-related theta rhythm in humans: coordinating self-directed hippocampal learning. *PLoS Biol, 10*(2), e1001267. doi:10.1371/journal.pbio.1001267

Kirsch, P., Achenbach, C., Kirsch, M., Heinzmann, M., Schienle, A., & Vaitl, D. (2003). Cerebellar and hippocampal activation during eyeblink conditioning depends on the experimental paradigm: A MEG study. *Neural Plast, 10*(4), 291-301.

Leirer, V. M., Wienbruch, C., Paul-Jordanov, I., Kolassa, S., Elbert, T., & Kolassa, I. (2010). Hippocampal activity during the transverse patterning task declines with cognitive competence but not with age. *Neuroscience, 11*, 113-122.

Lever, C., Kaplan, R., & Burgess, N. (2014). The function of oscillations in the hippocampal formation. In D. Derkikman & J. J. Knierim (Eds.), *Space, time and memory in the hippocampal formation* (pp. 303-350): Springer Vienna.

Lopes da Silva, F. H. (2010). Electrophysiological basis of MEG signals. In P. C. Hansen, M. L. Kringellbach, & R. Salmelin (Eds.), *MEG: An introduction to methods*: Oxford University Press.

Lorente de No, R. (1947). Action potential of the motoneurons in the hypoglossus nucleus. *J Cell Comp Physiol, 29*, 207-287.

Martin, T., McDaniel, M. A., Guynn, M. J., Houck, J. M., Woodruff, C. C., Bish, J. P., . . . Tesche, C. D. (2007). Brain regions and their dynamics in prospective

memory retrieval: a MEG study. *Int J Psychophysiol, 64*(3), 247-258. doi:10.1016/j.ijpsycho.2006.09.010

Mattout, J., Phillips, C., Penny, W. D., Rugg, M. D., & Friston, K. J. (2006). MEG source localization under multiple constraints: an extended Bayesian framework. *Neuroimage, 30*(3), 753-767. doi:10.1016/j.neuroimage.2005.10.037

Meltzer, J. A., Negishi, M., & Constable, R. T. (2008). Biphasic hemodynamic responses influence deactivation and may mask activation in block-design fMRI paradigms. *Hum Brain Mapp, 29*(4), 385-399. doi:10.1002/hbm.20391

Meyer, S. S., Bush, D., Bisby, J. A., Horner, A. J., Burgess, N., & Barnes, G. R. (2016). *It really is the hippocampus*. Paper presented at the The 20th International condrerence on biomagnetism, Seoul.

Meyer, S. S., Rossiter, H., Brookes, M. J., Woolrich, M. W., Bestmann, S., & Barnes, G. R. (2017). Using generative models to make probabilistic statements about hippocampal engagement in MEG. *Neuroimage*. doi:10.1016/j.neuroimage.2017.01.029

Mikuni, N., Nagamine, T., Ikeda, A., Terada, K., Taki, W., Kimura, J., . . . Shibasaki, H. (1997). Simultaneous Recording of Epileptiform Discharges by MEG and Subdural Electrodes in Temporal Lobe Epilepsy. *Neuroimage, 5*, 298-306.

Mills, T., Lalancette, M., Moses, S. N., Taylor, M. J., & Quraan, M. A. (2012). Techniques for detection and localization of weak hippocampal and medial frontal sources using beamformers in MEG. *Brain Topogr, 25*(3), 248-263.

doi:10.1007/s10548-012-0217-2

Morris, R. (1984). Development of a water-maze procedure for studying spatial learning in the rat. *J Neurosci Methods, 11*, 47-60.

Moses, S. N., Hanlon, F. M., & Ryan, J. D. (2011). Dynamic imaging of deep brain structures with MEG: Contributions to understanding human memory. In E. W. Pang (Ed.), *Magnetoencephalography*: InTech.

Moses, S. N., Ryan, J. D., Bardouille, T., Kovacevic, N., Hanlon, F. M., & McIntosh, A. R. (2009). Semantic information alters neural activation during transverse patterning performance. *Neuroimage, 46*(3), 863-873. doi:10.1016/j.neuroimage.2009.02.042

Murakami, S., & Okada, Y. (2006). Contributions of principal neocortical neurons to magnetoencephalography and electroencephalography signals. *J Physiol, 575*(Pt 3), 925-936. doi:10.1113/jphysiol.2006.105379

Muthukumaraswamy, S. D., & Singh, K. D. (2008). Spatiotemporal frequency tuning of BOLD and gamma band MEG responses compared in primary visual cortex. *Neuroimage, 40*(4), 1552-1560. doi:10.1016/j.neuroimage.2008.01.052

Nishitani, N. (2003). Dynamics of cognitive processing in the human hippocampus by neuromagnetic and neurochemical assessments. *Neuroimage, 20*(1), 561-571. doi:10.1016/s1053-8119(03)00280-5

Nishitani, N., Ikeda, A., Nagamine, T., Honda, M., Mikuni, N., Taki, W., . . . Shibasaki, H. (1999). The role of the hippocampus in auditory processing studied by event-related electric potentials and magnetic fields in epilepsy

patients before and after temporal lobectomy. *Brain, 122*, 687-707.

Nishitani, N., Nagamine, T., Fujiwara, N., Yazawa, S., & Shibasaki, H. (1998). Cortical-hippocampal auditory processing identiaed by magnetoencephalography. *J Cogn Neurosci, 10*(2), 231-247.

Nolte, G. (2003). The magnetic lead field theorem in the quasi-static approximation and its use for magnetoencephalography forward calculation in realistic volume conductors. *Phys Med Biol, 48*, 3637-3652.

O'Keefe, J., & Nadel, L. (1978). The hippocampus as a cognitive map. *Hippocampus, 9*, 352-364.

O'Keefe, J., & Recce, M. L. (1993). Phase relationship between hippocampal place units and the EEG theta rhythm. *Hippocampus, 3*(3), 317-330.

Ogawa, S., Lee, T. M., Kay, A. R., & Tank, D. W. (1990). Brain magnetic resonance imaging with contrast dependent on bloodoxygenation. *Proc Natl Acad Sci U S A, 87*, 9868-9872.

Oishi, M., Otsubo, H., Kameyama, S., Morota, N., Masuda, H. K., M., & Tanaka, R. (2002). Epileptic spikes: Magnetoencephalography versus simultaneous electrocorticography. *Epilepsia, 43*(11), 1390-1395.

OKada, Y., Kaufman, L., & Williamson, S. (1983). The hippocampal formation as a source of the slow endogenous potentials. *Electroencephalogr Clin Neurophysiol, 55*, 417-426.

Okada, Y., Papuashvili, N., & Xu, C. (1996). *Maximum current dipole moment density as an important physiological constraint in MEG inverse solutions.*

Paper presented at the International Conferance of Biomagnetism.

Olvera-Cortes, M. E., Garcia-Alcantar, I., Gutierrez-Guzman, B., Hernandez-Perez, J. J., Lopez-Vazquez, M. A., & Cervantes, M. (2012). Differential learning-related changes in theta activity during place learning in young and old rats. *Behav Brain Res, 226*(2), 555-562. doi:10.1016/j.bbr.2011.10.019

Olvera-Cortes, M. E., Guevara, M. A., & Gonzalez-Burgos, I. (2004). Increase of the hippocampal theta activity in the Morris water maze reflects learning rather than motor activity. *Brain Res Bull, 62*(5), 379-384. doi:10.1016/j.brainresbull.2003.10.003

Papanicolaou, A. C., Simos, P. G., Castillo, E. M., Breier, J. I., Katz, J. S., & Wright, A. A. (2002). The hippocampus and memory of verbal and pictorial material. *Learn Mem, 9*(3), 99-104. doi:10.1101/lm.44302

Parkin, A. J. (1996). Human memory: The hippocampus is the key. *Curr Biol, 6*(12), 1583–1585.

Piai, V., Anderson, K. L., Lin, J. J., Dewar, C., Parvizi, J., Dronkers, N. F., & Knight, R. T. (2016). Direct brain recordings reveal hippocampal rhythm underpinnings of language processing. *Proc Natl Acad Sci U S A, 113*(40), 11366-11371. doi:10.1073/pnas.1603312113

Poch, C., Fuentemilla, L., Barnes, G. R., & Duzel, E. (2011). Hippocampal theta-phase modulation of replay correlates with configural-relational short-term memory performance. *J Neurosci, 31*(19), 7038-7042. doi:10.1523/JNEUROSCI.6305-10.2011

Quraan, M. A., Moses, S. N., Hung, Y., Mills, T., & Taylor, M. J. (2011). Detection and localization of hippocampal activity using beamformers with MEG: a detailed investigation using simulations and empirical data. *Hum Brain Mapp, 32*(5), 812-827. doi:10.1002/hbm.21068

Riggs, L., Moses, S. N., Bardouille, T., Herdman, A. T., Ross, B., & Ryan, J. D. (2009). A complementary analytic approach to examining medial temporal lobe sources using magnetoencephalography. *Neuroimage, 45*(2), 627-642. doi:10.1016/j.neuroimage.2008.11.018

Rolls, E. T. (2010). Attractor networks. *Wiley Interdiscip Rev Cogn Sci, 1*(1), 119-134. doi:10.1002/wcs.1

Sarvas, J. (1987). Basic mathematical and electromagnetic concepts of the biomagnetic inverse problem. *Phys Med Biol, 32*(1), 11-22.

Singh, K. D., Barnes, G. R., Hillebrand, A., Forde, E. M., & Williams, A. L. (2002). Task-related changes in cortical synchronization are spatially coincident with the hemodynamic response. *Neuroimage, 16*(1), 103-114. doi:10.1006/nimg.2001.1050

Stephen, J. M., Ranken, D. M., Aine, C. J., Weisend, M. P., & Shih, J. J. (2005). Differentiability of simulated MEG hippocampal, medial temporal and neocortical temporal epileptic spike activity. *J Clin Neurophysiol, 22*, 388-401. doi:10.1097/01.WNP.0000172141.26081.78

Taylor, M. J., Donner, E. J., & Pang, E. W. (2012). fMRI and MEG in the study of typical and atypical cognitive development. *Neurophysiol Clin, 42*(1-2), 19-25.

doi:10.1016/j.neucli.2011.08.002

Taylor, M. J., Mills, T., & Pang, E. W. (2011). The development of face recognition; hippocampal and frontal lobe contributions determined with MEG. *Brain Topogr, 24*(3-4), 261-270. doi:10.1007/s10548-011-0192-z

Tesche, C. D. (1997). Non-invasive detection of ongoing neuronal population activity in normal human hippocampus. *Brain Res, 749*, 53-60.

Tesche, C. D., & Karhu, J. (1999). Interactive processing of sensory input and motor output in the human hippocampus. *J Cogn Neurosci, 11*(4), 424-436.

Tesche, C. D., & Karhu, J. (2000). Theta oscillations index human hippocampal activation during a working memory task. *Proc Natl Acad Sci U S A, 97*(2), 919-924.

Tesche, C. D., Karhu, J., & Tissari, S. O. (1996). Non-invasive detection of neuronal population activity in human hippocampus. *Cogn Brain Res, 4*, 39-47.

Vass, L. K., Copara, M. S., Seyal, M., Shahlaie, K., Farias, S. T., Shen, P. Y., & Ekstrom, A. D. (2016). Oscillations Go the Distance: Low-Frequency Human Hippocampal Oscillations Code Spatial Distance in the Absence of Sensory Cues during Teleportation. *Neuron, 89*(6), 1180-1186. doi:10.1016/j.neuron.2016.01.045

Vrba, J., & Robinson, S. E. (2001). Signal processing in magnetoencephalography. *Methods, 25*(2), 249-271. doi:10.1006/meth.2001.1238

Watrous, A. J., Lee, D. J., Izadi, A., Gurkoff, G. G., Shahlaie, K., & Ekstrom, A. D. (2013). A comparative study of human and rat hippocampal low-frequency

oscillations during spatial navigation. *Hippocampus, 23*(8), 656-661. doi:10.1002/hipo.22124

Wolters, C. H., Anwander, A., Tricoche, X., Weinstein, D., Koch, M. A., & MacLeod, R. S. (2006). Influence of tissue conductivity anisotropy on EEG/MEG field and return current computation in a realistic head model: a simulation and visualization study using high-resolution finite element modeling. *Neuroimage, 30*(3), 813-826. doi:10.1016/j.neuroimage.2005.10.014

Zouridakis, G., Simos, P. G., Breier, J. I., & Papanicolaou, A. C. (1998). Functional hemispheric asymmetry assessment in a visual languagetask using MEG. *Brain Topogr, 11*(1), 57-65.

Chapter three

The functional role of human right hippocampal/parahippocampal theta rhythm in environmental encoding during virtual spatial navigation

This chapter has been published as

Pu, Y., Cornwell, B.R., Cheyne, D., & Johnson, B.W. (2017). The functional role of human right hippocampal/parahippocampal theta rhythm in environmental encoding during virtual spatial navigation. *Human Brain Mapping*, 38(3), 1347–1361. doi:10.1002/hbm.23458

Abstract

Low frequency theta band oscillations (4 – 8 Hz) are thought to provide a timing mechanism for hippocampal place cell firing and to mediate the formation of spatial memory. In rodents, hippocampal theta has been shown to play an important role in encoding a new environment during spatial navigation, but a similar functional role of hippocampal theta in humans has not been firmly established. To investigate this question, we recorded healthy participants' brain responses with a 160-channel whole-head MEG system as they performed two training sets of a virtual Morris water maze task. Environment layouts (except for platform locations) of the two sets were kept constant to measure theta activity during spatial learning in new and familiar environments. In line with previous findings, left hippocampal/parahippocampal theta showed more activation navigating to a hidden platform relative to random swimming. Consistent with our hypothesis, right hippocampal/parahippocampal theta was stronger during the first training set compared to the second one. Notably, theta in this region during the first training set correlated with spatial navigation performance across individuals in both training sets. These results strongly argue for the functional importance of right hippocampal theta in initial encoding of configural properties of an environment during spatial navigation. Our findings provide important evidence that right hippocampal/parahippocampal theta activity is associated with environmental encoding in the human brain.

Keywords

Virtual reality, hippocampus, magnetoencephalography, spatial navigation, theta rhythm

Introduction

The hippocampal formation (HF) represents an environment via the firing of 'place cells' (O'Keefe & Nadel, 1978; Muller, 1996) and 'grid cells'[1] (Moser et al., 2008, 2015; Jacobs et al., 2013). The HF is also thought to play a critical role in encoding new information into memory, via neurophysiological processes modulated by a slow sinusoidal rhythm—theta oscillations. The theta rhythm is a prominent mode of hippocampal activity and has been extensively characterized in studies of spatial navigation and memory with invasive electrophysiological recordings in animals (e.g., O'Keefe and Nadel, 1978; Wang et al., 2015; Zhang et al., 2016; Agarwal et al., 2016). In rodents, hippocampal theta oscillations have been shown to play an important role in encoding a new environment during spatial navigation (Jeewajee, et al., 2008; Penley et al., 2013). In humans, previous fMRI studies (e.g. Wolbers & Buchel, 2005; Doeller et al., 2008) have linked activation of the hippocampus to environmental novelty processing and learning, but the electrophysiological mechanisms are yet to be fully understood (e.g. Park et al., 2014; Rutishauser et al., 2010; Suthana et al., 2012; Staudigl & Hanslmayr, 2013). In this study, we investigated whether and how human hippocampal theta rhythm contributes to environment encoding.

[1] There is no consensus concerning what brain regions are encompassed by the term 'hippocampal formation'. Some researchers include entorhinal cortex while some don't.

Theta rhythms (~4 – 8 Hz) associated with spatial navigation have been observed with intracranial EEG (iEEG) in epileptic patients (e.g. Caplan et al., 2001, 2003; Ekstrom et al., 2005; Vass et al., 2016), but the invasive nature of these methods has meant there have been limited opportunities to systematically explore cognitive correlates of human hippocampal theta oscillations. Non-invasive magnetoencephalography (MEG) source imaging provides a window for examining the function of neuronal signals from deep brain structures, such as the hippocampus (e.g. Tesche and Karhu, 2000; Cornwell et. al., 2008a, 2010, 2012; Riggs et al, 2009; Attal & Schwartz 2013; Guitart-Masip el al., 2013; Fuentemilla et al., 2010, 2014; Cousijn et al., 2015; Backus et al., 2016), the amygdala (e.g. Hung et al., 2010; Cornwell et al., 2008b) and the thalamus (Attal & Schwartz, 2013) in both healthy and patient populations. Perhaps most compelling is work (Dalal et al., 2013) showing that MEG-reconstructed hippocampal activity highly correlates (i.e., zero phase delay) with simultaneous depth recordings of hippocampal electrical activity, allowing unprecedented validation of MEG deep source reconstruction. Using MEG deep source imaging techniques, Cornwell et al. (2008a) found greater theta activity in the left anterior hippocampus and parahippocampus during goal-directed navigation relative to aimless movements in a virtual reality environment. In another recent MEG experiment, Kaplan et al. (2012) reported that hippocampal theta power increased during the self-initiation of virtual movement, and that hippocampal theta oscillations during a pre-retrieval planning phase predicted subsequent memory performance. Such experiments indicate that MEG source imaging can play a crucial role in

bridging the gap between animal models and human research to determine what aspects of hippocampal function are common across species and what aspects are unique to the human brain.

In this study, we extended this work using MEG to address an important theoretical question, i.e., whether and how the human hippocampal theta rhythm contributes to environmental encoding, as has been reported in rodents (e.g. Jeewajee et al., 2008; Penley et al., 2013). We recorded healthy male participants' brain responses during navigation of a virtual Morris water maze, a computer-simulated task modeled after one extensively used for testing hippocampal-dependent spatial navigation in rodents (Morris, 1984). The experimental design was adapted from that of Cornwell et al. (2008a), in which there were two conditions (hidden platform condition vs. random swimming condition). We expanded this design with an additional training set with the environmental layout constant across training sets to allow us to determine whether hippocampal theta rhythms are sensitive to environmental encoding as reported in animal literature (please refer to Fig. 1 for the overview of the experimental design). In the hidden platform condition, the environment consisted of a virtual pool with four visual cues (objects with abstract patterns) attached to the surrounding walls. In the random swimming condition, the virtual pool was the same as that in the hidden platform condition, except that there were no visual cues attached to the walls. The motivation for removing visual cues was to investigate whether hippocampal theta oscillations had a general role in

environmental encoding; and if so, it should be modulated by novelty of both a cue-rich environment as in the hidden platform condition and environment without cues as in the control condition. In the hidden platform condition, participants needed to find the hidden platform as quickly as possible, while in the random swimming condition, the task was swimming aimlessly non-stop. To avoid the possibility that the contrast between the first and second training set was confounded with learning of a specific location, we changed the hidden platform location in the second training set. This paradigm offered a way to replicate findings of Cornwell et al. (2008a) with a different whole-head magnetometer (a KIT MEG system in the present experiment vs. a CTF MEG system in Cornwell et al., 2008a), while investigating a new potential cognitive function of right hippocampal theta oscillations.

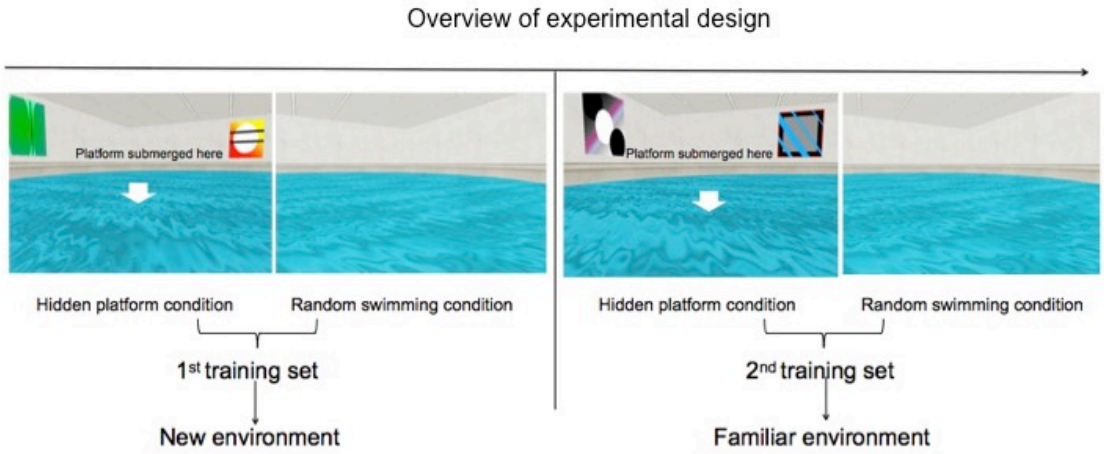

Figure 1. Overview of experimental design. There were two training sets in this task, each of which contained 20 hidden platform trials and 20 random swimming trials. Within each training set, the two conditions were alternatively presented (4 trials of hidden platform condition, 4 trials of random swimming condition, 4 trials of hidden platform condition, …). Hidden platform location differed between the two sets and was counterbalanced across

participants. Environment layouts in each condition were kept constant so that the first training set was in a new environment and the second one was in a familiar environment. Participants were instructed to find the hidden platform as quickly as possible in the hidden platform condition and to swim non-stop in the random swimming condition.

I made three predictions. First, left hippocampal theta activity should be greater in the hidden platform condition relative to the random swimming condition, as reported in Cornwell et al. (2008a), since the left hippocampus is thought to be a binding 'device' (e.g. Mitchell et al., 2000; Kessels et al., 2004). Second, right hippocampal theta activity should be greater in the new vs. familiar environment contrast in both conditions, as previous studies has shown that right hippocampal activation is associated with processing of a new configuration vs. a familiar one (Duzel et al., 2003) and with environmental novelty detection (Doeller et al., 2008). Third, right hippocampal theta activity during encoding in the first training set should be significantly associated with behavioral performance in both training sets, because if right hippocampal theta is for environmental encoding, and since good formation of configural knowledge of an environment (i.e., formation of a cognitive map of the space) would facilitate participant to choose an efficient path to move to any place in that particular environment (Wolbers & Hegarty, 2010), we should expect the magnitude of environment encoding-related right hippocampal theta correlated with navigation performance in both training sets where the environment was the same.

Methods

Participants. Eighteen right-handed healthy male participants (mean age = 29 years; range = 18-39 years) participated in the present experiment and were included in the final data analyses. Two additional participants were excluded from the final data analyses due to excessive head movement during the MEG recording session. All participants had normal or corrected-to-normal vision. Inclusion criteria were: (1) no past or current psychiatric disorders; (2) no current use of psychoactive medications by self-report. Participants were also screened for dental work, metallic implants, a cardiac pacemaker, metal rods, and other magnetic material permanently fixed to their body. All procedures were approved by the Human Research Ethics Committee of Macquarie University.

Virtual Morris water maze. This task was adapted from Cornwell et al. (2008a) (Fig. 1). PsychoPy software (Peirce, 2007; 2008) was used to present a first-person perspective viewpoint of two virtual circular pools filled with opaque water. The two pools had the same size and geometry, with the diameter of the pools being 80 virtual units. One pool contained four visual cues fixed to the walls of the square room surrounding the pool, and the other had no visual cues. The pool with visual cues contained a hidden platform and the participants' task was to navigate to the hidden platform as quickly as possible. If the hidden platform was not found within 25s, it became visible and participants were instructed to swim to it to finish the trial. If the

pool with no cue objects (random swimming condition) was presented, the task was to swim aimlessly non-stop for 15s. Environment layouts in each condition were the same for both training sets. Images were projected (InFocus Model IN5108; InFocus, Portland) onto a screen at a viewing distance of about 1 m.

Trial structure. There were two training sets in the experiment, each containing 40 trials (20 hidden platform trials, 20 aimless swimming control trials). Four trials were grouped as a block to be presented, so that in each training set, there were 5 blocks of hidden platform condition and 5 blocks of random swimming condition. Blocks of the two conditions were alternately presented (i.e., block 1 of hidden platform condition preceded block 1 of random swimming condition, followed by block 2 of hidden platform condition, which came before block 2 of random swimming condition,…, followed by block 5 of hidden platform condition, which went before block 5 of random swimming condition). Within each training set, the position of the hidden platform across blocks was fixed, but different between the two training sets and was counterbalanced across participants to avoid learning effect of a specific location between training sets. Environment layout was the same in the two training sets in each condition. During the inter-trial interval of 4.5 - 5.5s duration (randomly jittered) participants viewed a blank gray screen. There was a 3-minute break between the two training sets.

Task. Participants used a button box with three fingers (index, middle, ring fingers)

of their right hand to move forward or to turn left or right in the pools. Movement speed in this task was constant. They used the visual environment of the pool (wall cues or no cues) to determine whether they needed to search for a hidden platform or swim randomly. They were instructed to try their best to find the hidden platform as quickly as possible in the hidden platform condition. Thus, in the hidden platform, they would learn the hidden platform location trial by trial and would gradually take an optimal path to reach it. They were also told to look at the projected screen at all times and to swim non-stop until the trial finished. Participants began each trial facing the wall of the pool at one of three starting points (three starting points from the four positions in North, South, East, and West in pseudo-random order). Participants did not start from the quadrant of the hidden platform location and were observed throughout the experiment on a computer monitor outside the shielded room. Participants were monitored to ensure that they did not stop swimming for more than 1s at a time, and were attending to the visual display at all times. Path lengths to reach the platform from starting position were recorded for each trial. Before the start of the second training set, participants were told that the hidden platform was in a new position.

Data acquisition. Before MEG recordings, fiducial positions, marker coil positions and head shape were measured with a pen digitizer (Polhemus Fastrack, Colchester, VT). Neuromagnetic data were measured using a whole-head MEG system (Model PQ1160R-N2, KIT, Kanazawa, Japan) in a magnetically shielded room (Fujihara Co.

Ltd., Tokyo, Japan) with participants in a supine position. The MEG system consisted of 160 coaxial first-order gradiometers with a 50 mm baseline (Kado et al., 1999). Continuous MEG data were acquired during each training set at a sampling rate of 1000 Hz. Head positions were obtained from five head marker coils attached to an elasticized cap placed on each participant's head, and were measured before and after each recording. Maximum head movement tolerance was 4 mm in any direction.

High resolution T1-weighted anatomical brain images were acquired on a 3T Siemens Magnetom Verio scanner with a 12-channel head coil at Macquarie University Hospital. Those anatomical images were obtained using 3D GR\IR scanning sequence with the following parameters: repetition time, 2000 ms; echo time, 3.94 ms; flip angle, 9 degrees; slice thickness, 0.93 mm; field of view, 240 mm; image dimensions, 512 × 512 × 208.

Data analyses. Data analyses included two steps: (1) localization of brain activity using the synthetic aperture magnetometry (SAM) beamformer implemented in the BrainWave Matlab toolbox (Version 3.0; http://cheynelab.utoronto.ca/brainwave) and (2) group analyses of volumetric beamformer images using Analysis of Functional NeuroImages (AFNI; Cox, 1996; http://afni.nimh.nih.gov).

Source analysis. SAM (Robinson & Vrba, 1999) was used to estimate source activity in the theta frequency band (4 – 8 Hz). SAM estimates source signals at each brain voxel while suppressing signals from other locations by calculating optimum spatial

filters or beamformer weights at the location of interest using the signal covariance matrix from the sensor array (Hillebrand et. al., 2005).

In the current experiment, raw MEG data were epoched into 5 s windows including a 1s pretrial baseline period and 4 s following the onset of each trial (4 s was the fastest time from the starting point to the hidden platform, among all trials and participants). Magnetic fields were modeled with a single sphere head model derived from each participant's structural MRI to fit the inner skull surface of each participant's MRI (Sarvas, 1987). Covariance matrices were calculated from unaveraged 1 s active time windows locked to trial onset and 1 s pretrial baseline windows for each condition separately within a training set after applying a 4 – 8 Hz bandpass filter. Total covariance window length was 40 s for each condition (20 trials x 2 s). The source space was sampled into a three-dimensional grid of 4 mm^3 voxels with an equivalent current dipole source at each location.

Since beamformer weights increase with depth, and the sensor level noise remains constant throughout the volume, the raw source power at each voxel of the brain must be normalized (Cheyne et al., 2007). In our analyses, beamformer outputs were normalized by the dual-state imaging method (Hillebrand et al., 2005), which is a standard way of beamformer analyses. In this method, normalization is carried out using real brain noise, a so-called control state and the state being normalized is called the active state, so that the resulting brain volumes represent the voxel-wise relative power difference between the two states. In the current study, we used pseudo-F SAM

images to represent the percentage change of the brain signal between the two states (active state and control state). In the case of event-related synchronization, the pseudo-F value is derived from the formula A/C -1, in which A is the source power in the active state (in our study, active state was post trial onset window) and C is the source power in the control state (in our study, the control state was pre-trial window). For event-related desychronization, the formula is 1-1/(A/C)=1-C/A. Therefore, the pseudo-F SAM volumes for each participant contain a power ratio value in each voxel across the whole brain. The term 'pseudo-F' is used is because the ratio of source power of active state over control state resembles the F-ratio. But the estimates of variance in the calculation are based on sensor noise level instead of between-state (active and control states) variability. Thus, it does not conform to the true F distribution.

In the current study, the 1s active windows were advanced in 250 ms increments (one lower bound theta cycle) with 75% overlap up to the 4 s (e.g. 0 – 1 s, 0.25 – 1.25 s, 0.5 – 1.5 s, etc.), which was the fastest time from the starting point to the hidden platform among all trials and participants. The sliding window method (as opposed to simply analyzing the average power change of the entire post trial onset window of 4 s) increases the detectability of theta power changes, given their transient nature (< 500 ms in some cases; Arai, et al., 2014; Wyble, 2004; Kaplan et al., 2012; Sakimoto et al. 2013; Foster et al., 2013). This analysis produced pseudo-F SAM volumetric images to represent the percentage change of the theta power between the active

window and baseline window (i.e. pseudo-F values) for each condition.

Group statistics. Individual SAM images were normalized to a Talairach brain template in AFNI to allow for group analysis in a standardized space. Normalized SAM images of 4 – 8 Hz theta power (pseudo-F values) were analyzed with 2 (conditions: hidden platform condition vs. random swimming condition) × 2 (training sets: first vs. second) repeated measures ANOVAs. We chose three time windows of interest (1 – 2 s, 1.25 – 2.25 s, 1.5 – 2.5 s) based on the reported latencies of increased theta power in the study of Cornwell et al. (2008a). Additional time windows (0 – 1 s, 0.25 – 1.25 s, ..., 0.75 – 1.75 s, 1.75 – 2.75 s, ... , 2.75 – 3.75 s) were explored in post-hoc analyses.

Given our a priori hypothesis that the hippocampus and parahippocampal cortices would generate theta oscillations during spatial navigation and environmental learning (Cornwell et. al., 2008a; Park et al., 2014), a small-volume correction was performed over a mask containing both left and right hippocampi and parahippocampal cortices based on an automated Talairach atlas in AFNI. A cluster alpha of 0.05 was set as the threshold for statistical significance. A cluster size criterion was determined by Monte Carlo simulations conducted in the AFNI program 3dClustSim, an adaption of the program AlphaSim. This correction method has been employed by previous MEG beamformer studies (e.g. Mueller et al., 2012, 2013; Keil et al., 2012, 2015; Meltzer et al., 2013). Briefly, this correction method determines a

minimum cluster size (i.e. minimum number of continuous voxels) given a certain threshold that is required for significance (for a full description, refer to http://afni.nimh.nih.gov/pub/dist/doc/program_help/3dClustSim.html). In the present study, for our a priori comparison in the three time windows of interest, Monte Carlo simulations were iterated 10,000 times, with the voxel threshold being set at $p < 0.01$ and adjusted alpha threshold set at 0.05/3=0.017 (to correct for multiple comparisons across three time windows of interest). This requires a minimum of 21 continuous voxels in bilateral hippocampi and parahippocampi to be significant. For post-hoc comparisons, the voxel threshold was set at $p < 0.01$ and the adjusted alpha threshold at 0.05/9=0.006 (another six time windows except the primary three time windows of interest), requiring at least 30 continuous voxels to achieve significance.

Time frequency representations (TFRs). TFRs were constructed from source waveforms at the peak location of goal oriented navigation related left hippocampus and environmental encoding related right hippocampus determined by the ANOVA results on the pseudo-F images to show right hippocampal theta power change relative to the baseline window across the 4 s post trial onset window. This was accomplished using a five-cycle Morlet wavelet transformation (Tallon-Baudry et al., 1997) of single trial source activity over a frequency range of 3 – 50 Hz in 1 Hz steps using the formula:

$$w(t, f_0) = A \exp(-t^2/2\sigma_t^2) \exp(2i\pi f_0 t),$$

Wavelets were normalized so that the total energy was 1, with the normalization

factor A being equal to: $(\sigma_t\sqrt{\pi})^{-1/2}$.

To be specific, we reconstructed the activity of the peak voxel we specified, with beamformer covariance matrices being computed from -1 – 4 s (the whole epoch). A convolution of the complex wavelet with the beamformed MEG signal of each trial was derived and then averaged across all the trials. The magnitude of this convolution was converted to percentage change in power relative to the pre-trial baseline (Isabella et al., 2015). We did not show TF plots of the peak voxel of goal-oriented navigation related left hippocampus, because Cornwell et al. (2008a) has shown the evolution of goal-oriented navigation related theta power change across time.

Post-hoc analyses. To confirm the robustness of our results, we did a cross validation analysis. Participants were randomly split into two subsamples and separate 2 (conditions: hidden platform vs. random swimming) × 2 (training sets: first vs. second) within subject ANOVAs were performed with the beamformer volumetric images for each subsample for each time window. Moreover, in light of evidence that human hippocampal theta may extend below 4 Hz (Jacobs, 2014), we carried out secondary beamformer analyses using a 1 – 4 Hz bandpass filter to determine whether slower oscillatory power showed a similar pattern across conditions. We also performed an analysis encompassing a broad frequency range of 1 – 8 Hz. All other analytic steps were the same as above for these alternative frequency windows.

Correlation analysis. For those regions showing significant effects of environmental encoding in the group-level contrasts, individual cluster means of theta power (4 – 8 Hz, pseudo-F values) in the hidden platform condition in the first training set were extracted and correlated respectively with individual spatial navigation performance indexed by average path length in the hidden platform condition in each training set, using Pearson correlation implemented in IBM SPSS software (version 22) to test our third hypothesis.

Post-hoc correlation analyses. To explore whether in the familiar environment, right hippocampal theta correlated with navigation performance, we extracted cluster means of theta power (pseudo-F values) in the hidden platform condition in the second training set and correlated respectively with individual average path length in the hidden platform condition in each training set. The previous work (Cornwell et al., 2008a) found no significant association between theta elicited by goal-oriented spatial navigation related left anterior hippocampus and behavioural performance (Cornwell et al., 2008). To confirm this, we also extracted individual cluster means of theta power (pseudo-F values) in the hidden platform condition in each training set from the anterior hippocampal/parahippocampal region showing significant activation in the hidden platform vs. random swimming condition contrast, and computed correlations with average path length in the corresponding training set.

Finally, we performed a voxel-wise correlation between the theta power in both

training sets and the average path length in training set one and two respectively across the whole brain to investigate whether the correlation was lateralized to right hippocampus/parahippocampus, and whether the correlation was only restricted to the first training set in the initial stage of learning. The threshold was set at $p < 0.005$ (uncorrected).

Results

Spatial navigation performance. Path length from the starting point to the hidden platform location was measured as an index of spatial navigation performance. One-way repeated measures ANOVA showed that path lengths were significantly different across five blocks (four trials per block) in each training set: $F(4, 68) = 12.601$, $p < 0.001$, $\eta 2 = 0.825$ (run one); $F(4, 68) = 10.949$, $p < 0.001$, $\eta 2 = 0.784$ (run two). The decrease in path length over training (Fig. 2A) demonstrates a clear spatial learning effect, consistent with previous studies using the virtual Morris water maze task (e.g. Cornwell et al., 2008a, 2010). Collapsed across blocks, average path length was significantly shorter in the second training set (run two) than the first (run one) ($t (17) = 2.329$, $p = 0.032$, Cohen's $d = 0.29$) (Fig. 2B). Figure 3 shows some sample path trajectories in hidden platform condition and random swimming condition at the early and late spatial learning.

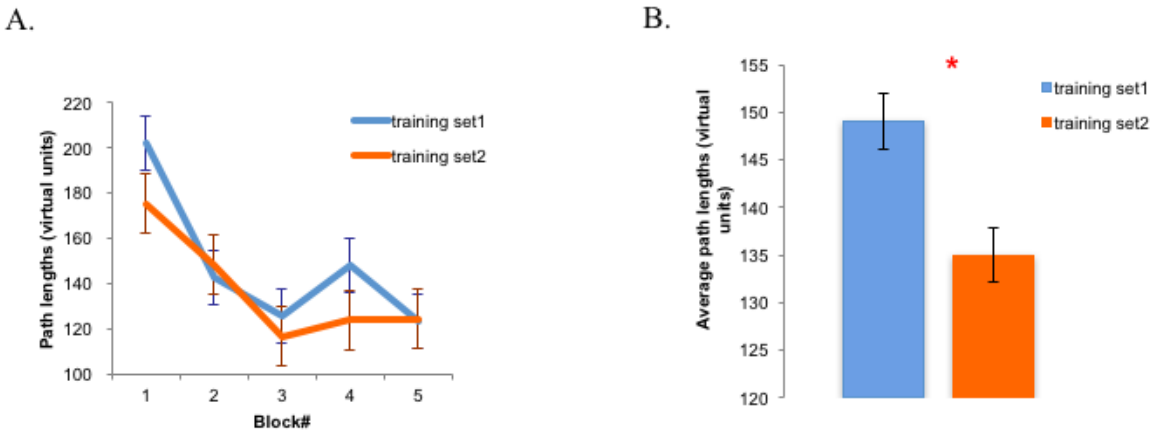

Figure 2. A. Average path length from the starting point to the hidden platform across 5 blocks (4 trials per block) in training set one and two. B. Average path length in the two training sets.

The diameter of the virtual pool was 80 virtual units.

Error bar represents standard errors. * represents $p < 0.05$.

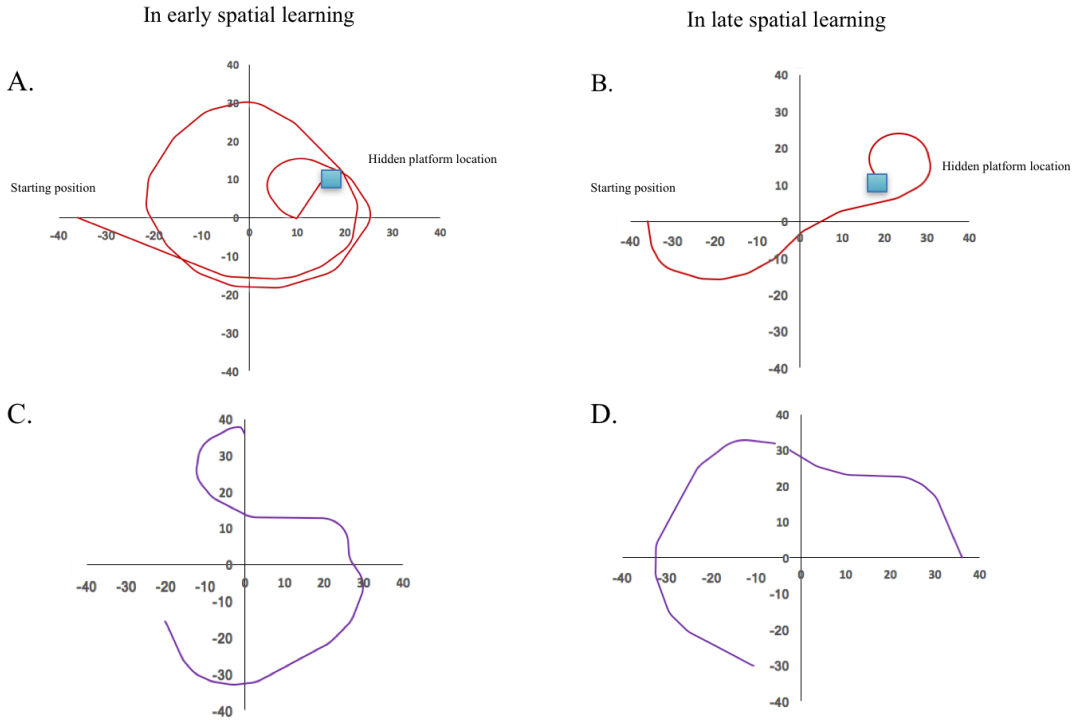

Figure 3. Sample path trajectories of one participant in one trial in the beginning and end of spatial training respectively in hidden platform condition (upper panel A & B) and in random

swimming condition (lower panel C & D).

Theta rhythm associated with environmental encoding. A 2 (conditions: hidden platform condition vs. random swimming condition) × 2 (training sets: first vs. second) repeated measures ANOVA was performed for theta power at the source level in each of our time windows of interest.

In two of our main time windows of interest (1 – 2 s, 1.25 – 2.25 s), we found main effects of condition in the anterior hippocampus and parahippocampus (**1 - 2 s:** $F = 8.4$, $p < 0.05$, small volume corrected across time, 43 voxels, $\eta 2 = 0.506$, peak voxel at left parahippocampus x = -26 y = -13 z = -20; **1.25 – 2.25 s**: $F = 8.4$, $p < 0.05$, small volume corrected across time, 29 voxels, $\eta 2 = 0.392$, peak voxel at left parahippocampus x= -22 y= -17 z = -24 (Fig. 3A & 3B). In the time window of 1.5 – 2.5s, we also found activation in the anterior left hippocampus (peak voxel at left hippocampus x = -30, y = -13, Z = -16), but it could not survive multiple comparison correction across time. These results are highly consistent with the findings by Cornwell et al. (2008a), showing that anterior left hippocampal/parahippocampal theta was stronger during navigation to the hidden platform relative to swimming aimlessly in the virtual pool. There was a slight difference in the timing between the present study and Cornwell et al. (2008a), where the peak difference of the similar comparison was during 1 – 2s and 1.5 – 2.5s.

No main effect of condition was found in other regions of the hippocampus or parahippocampus.

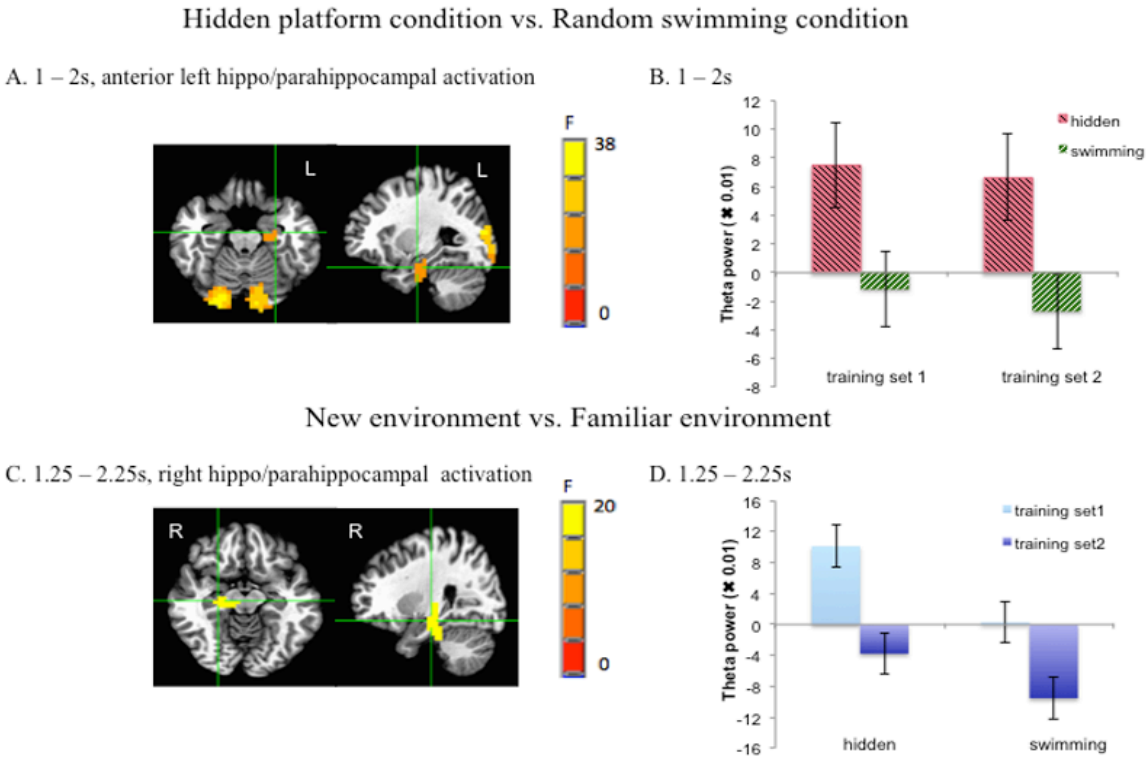

Figure 3. A. The whole brain images of main effect of condition in the time window of 1 – 2s as an example. The local maximum was in left parahippocampal gyrus (Talairach coordinates x=-26 y=-13 z=-20) (small volume corrected). **B.** Cluster mean of theta power (i.e. pseudo-F values: the percentage change of theta power in the active window relative to the baseline window) of anterior left hippocampus/parahippocampus showing main effect of condition in each condition and each training set in the time window of 1 – 2 s. **C.** The whole brain images of main effect of training set in the time window of 1.25 – 2.25s. The local maximum was in the right hippocampus (Talairach coordinates x=18 y=-21 z=-8) (small volume corrected). **D.** Cluster mean of theta power (i.e. pseudo-F values: theta power percentage change relative

to the baseline) of right hippocampal/parahippocampal activation region showing main effect of training set in each condition and each training set in the time window of 1.25 – 2.25 s.

We also found that in the 1.25 – 2.25 s time window, there was a main effect of training set with the peak in the right hippocampus ($F = 8.4$, $p < 0.05$, small volume corrected across time, 31 voxels, $\eta 2 = 0.453$, peak voxel at right hippocampus: x = 18 y = -21 z = -8) (Fig. 3C & 3D). This suggests that right hippocampal theta power decreased as participants became familiar with the structure of the environment, in line with previous work showing that hippocampal activation was most prominent during the initial learning phase and decayed after performance had approached ceiling level (Wolbers & Buchel, 2005). Time frequency plots also confirmed that during 1 – 2.25s, there was a transient increase in the hidden platform codnition vs. random swimming condition (Fig. 4) and during 1.25 – 2.25 s, there was a transient decrease in the second training set (Fig. 5). This transience is in line with the idea that theta power change is transient (e.g. Kaplan et al., 2012). No other parts of the hippocampus/parahippocampus were found to show a significant main effect of training set. Moreover, no left hemispheric effects were observed even at lower p thresholds ($p = 0.05$ uncorrected).

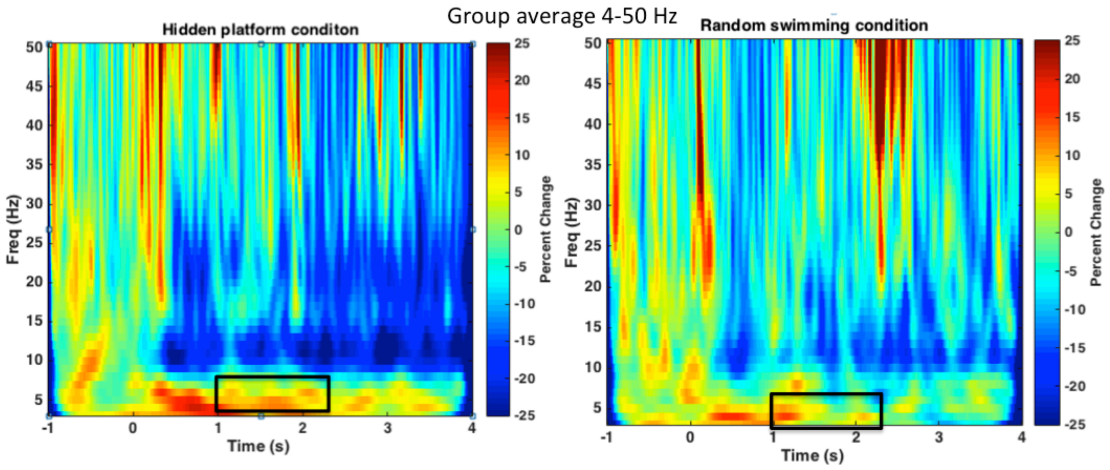

Figure 4. Time frequency plots (4 – 50 Hz) of the peak voxel of goal-orientated navigation related left hippocampus. This is replication of Cornwell et al. (2008). Left and right panel represent time frequency plots of the group average of left hippocampus in the hidden platform condition and random swimming condition respectively. The black rectangular shows the time window showing a decrease of theta band in the familiar environment relative to the new one revealed by SAM beamformer analysis (1 – 2s, 1.25 – 2.25s, 4 – 8 Hz).

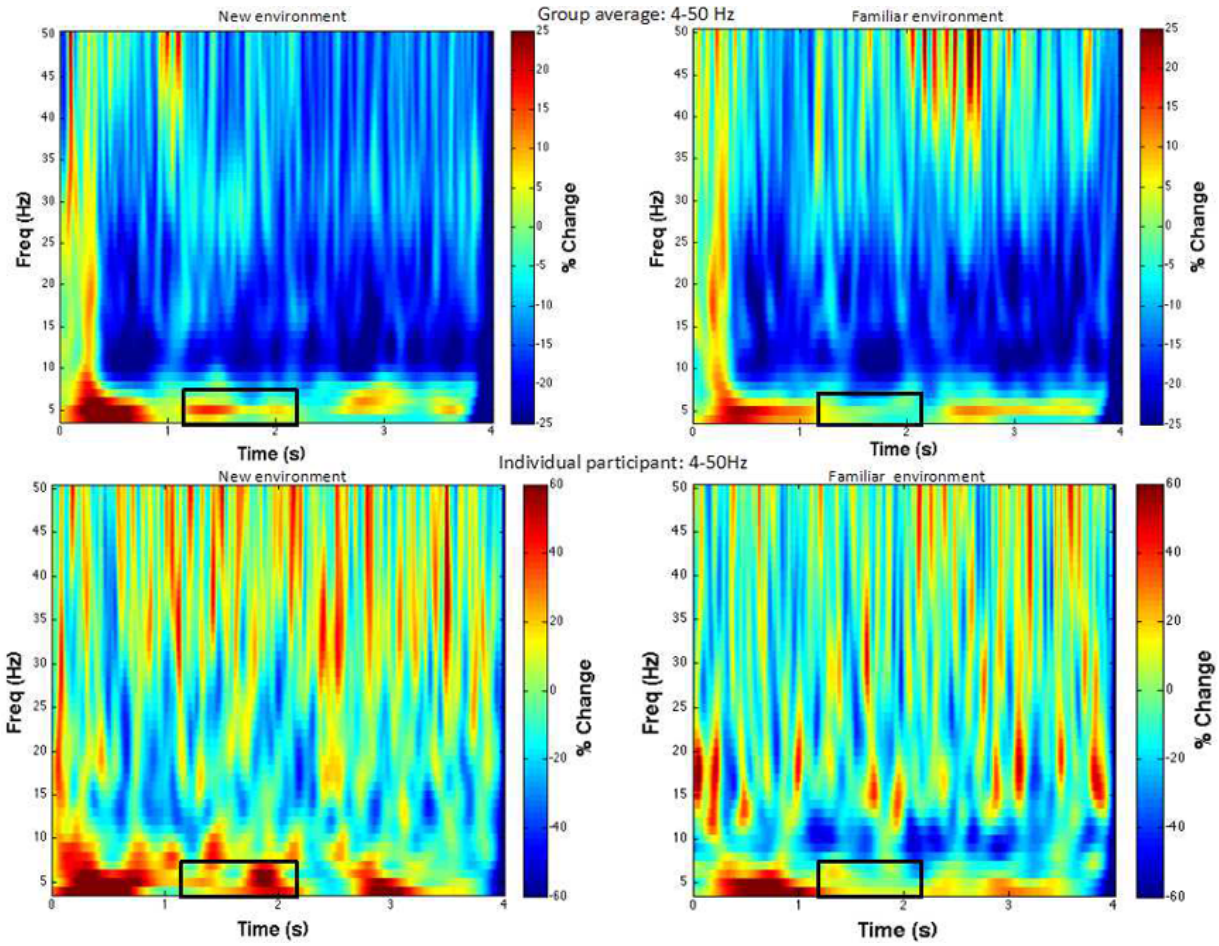

Figure 5. Time frequency plots (4 – 50 Hz) of the peak voxel of the environmental encoding related right hippocampus. **The upper panel** presents time frequency plots of the group average in the first (new environment) and the second (familiar environment) training set. **The lower panel** presents time frequency plots of one individual participant in the first (new environment) and the second (familiar environment) training set. The black rectangular shows the time window showing a decrease of theta band in the familiar environment relative to the new one revealed by SAM beamformer analysis (1.25 – 2.25s, 4 – 8 Hz).

No significant interactions between condition and training set were found. Exploratory post-hoc tests of other time windows apart from the primary windows of

interest (1 – 2 s, 1.25 – 2.25 s, 1.5 – 2.5 s) showed no statistically significant results.

For other activated brain regions, we only presented those in the new vs. familiar environment contrast, because the hidden platform vs. random swimming contrast was our replication result, and Cornwell et al. (2008a) has already reported those, which were similar to those in the present study. For new vs. familiar environment contrast, when the original voxel threshold was $p < 0.005$ (uncorrected), there were right hippocampus, left middle cingulate gyrus (peak voxel: x = -2, y = -25, z = 44). When the voxel threshold was set at $p < 0.001$ (uncorrected), only right hippocampus survived.

Split half analyses (cross validation) of the data are shown in Fig. 6. The results were similar in both subsamples and also similar to the results of the overall analysis reported above. The local maxima of main effect of condition were in the anterior left hippocampus/parahippocampus ($p < 0.05$, small volume corrected). The local maximum of the main effect of training set was in the right hippocampus ($p < 0.05$, small volume corrected). These results confirm the robustness of our main results.

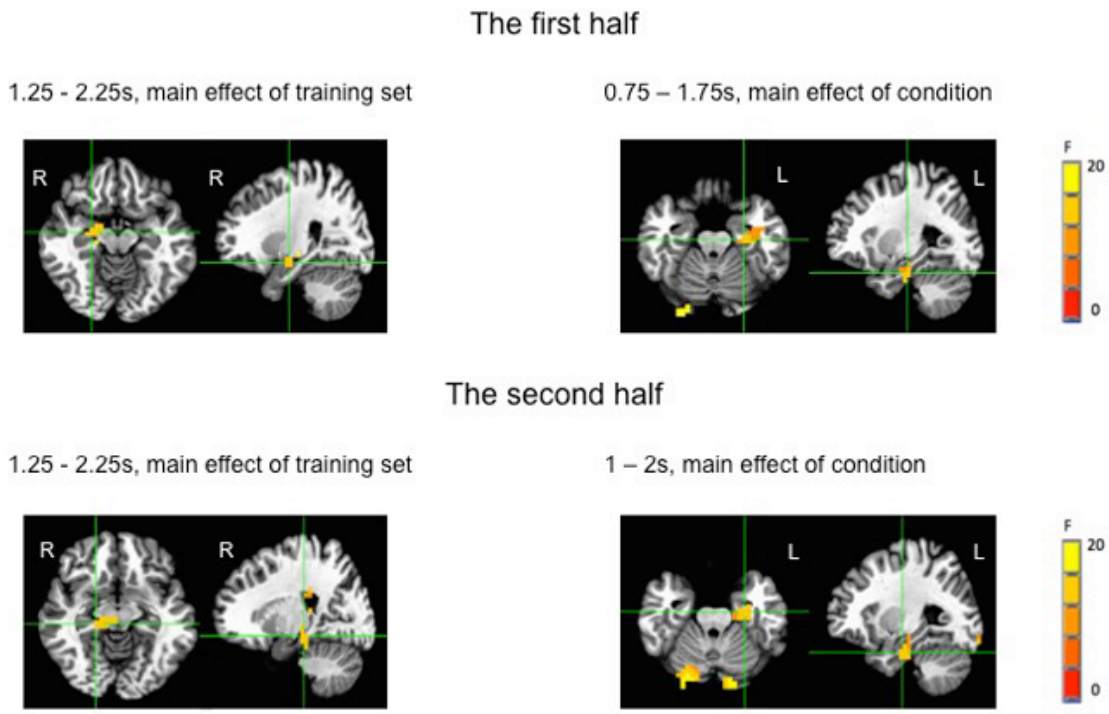

Figure 6. Whole brain images of split half analyses ($p<0.05$, small volume corrected). The **upper panel** showed the results of the first half of the participants. There was a main effect of condition in 1.25 – 2.25s and main effects of condition in 0.5 – 1.5s and 0.75 – 1.75s (we only showed images of 0.75 – 1.75s for an example). The **lower panel** shows the results of the second half of the participants. There was a main effect of condition in 1.25 – 2.25s and main effects of condition in 1 – 2s, 1.25 –2.25s and 1.5 – 2.5s (we only showed images of 1 – 2s for an example).

The post hoc analyses for the frequency range of 1 – 4 Hz and 1 – 8 Hz did not show significant results.

Correlations between behavioral performance and theta source power. To test the third hypothesis, the cluster mean of pseudo-F values of environment encoding-related right hippocampal theta in the first training set in the time window

of the significant main effect of training set (1.25 – 2.25 s) was correlated with average path lengths in training set one and two respectively. We found a negative correlation between average path length in training set one and the pseudo-F value of right hippocampus in the same training set ($r = -0.5$, $p = 0.035$) (7A). We also found that path length in the second training set correlated significantly with pseudo-F value of right hippocampus in the first training set ($r = -0.57$, $p = 0.014$) as well (Fig. 7B). This result suggests that stronger right hippocampal theta during initial encoding of an environment is associated with better navigation performance (indexed by shorter average path length) in an environment both initially when it is new and subsequently when it is familiar. This finding is in line with previous reports that higher theta is associated with better performance (e.g. Staudigl & Hanslmayr, 2013; Kaplan et al., 2012).

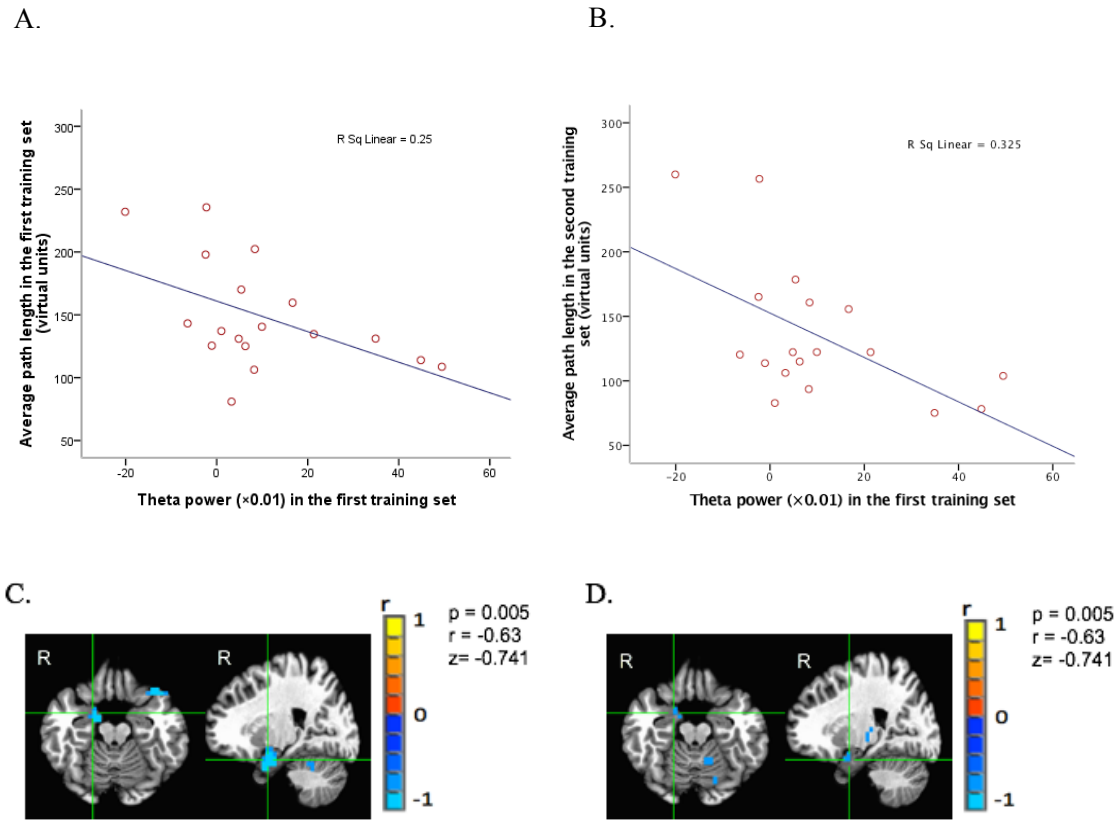

Figure 7. A. Cluster mean of theta power (i.e. pseudo-F values: theta power percentage change relative to the baseline) of environmental encoding related right hippocampal theta for each participant in the hidden platform condition in the first training set plotted against his average path length in the same condition in the same training set. **B.** Cluster mean of theta power (pseudo-F values) of environment layout encoding related right hippocampal theta for each participant in the hidden platform condition in training set one plotted against his average path length in the same condition in the second training set. **C.** Whole brain images of the correlation between theta power in the first training set in the hidden platform in the time window of 1.25 – 2.25s and average path length in the first training set, with the local maximum being in the right parahipp/hippocampus (Talairach coordinates x = 14, y = -5, z = -16). **D.** Whole brain images of the correlation between theta power in the first training set in the hidden platform in the time window of 1.25 – 2.25s and average path length in the second

training set, with the local maximum being in the right parahippocampus/hippocampus (Talairach coordinates x = 14, y = -5, z = -16).

For the post hoc analyses, we did not find significant correlations between right hippocampal theta in the second training set with average path length in either training set. These results suggest that hippocampus may function prominently only at the early stage of learning (Wolbers & Büchel, 2005). For the correlation between theta power in the hidden platform condition in the goal-oriented navigation related anterior left hippocampus/parahippocampus and average path length, no significant correlation was found as well, in line with previous findings from Cornwell et al. (2008a).

Finally, to investigate whether the correlation was only lateralized to the right hippocampus/parahippocampus and whether the correlation was only restricted to the first training set in the initial stage of learning, we then did a voxel-wise correlation between theta power in both training set with average path length in both training set respectively across the whole brain. We found there right hippocampal/parahippocampal theta in the first training set correlated with path length in both training sets ($p < 0.005$, uncorrected, local maxima were in the right hippocampus/parhippocampus: x = 14, y = -5, z = -16 and x = 14, y = -5, z = -16 for correlation between theta power in the first training set and average path length in the first training set and for correlation between theta power in the first training set and

average path length in the second training set respectively) (Fig. 6C & 6D). No correlation between theta from other parts of the hippocampus and parahippocampus and path length were found under the threshold of $p < 0.005$. For the correlation between theta power in the second training set and path length in both training sets, when $p < 0.005$, no single voxel in the bilateral hippocampi and parahippocampi was found to show correlation. The whole brain voxel-wise correlation confirmed that the correlation was only lateralized to right hippocampus and only occurred between right hippocampal theta in the initial encoding phase and navigation performance in both new and familiar environments.

Discussion

We investigated whether human hippocampal theta oscillations have a functional role in environmental encoding during spatial navigation in a virtual Morris water maze task. First, consistent with previous findings, we found that left anterior hippocampal/parahippocampal theta was stronger while navigating to the hidden platform relative to swimming randomly in a virtual pool. Second, in line with our hypotheses, we found evidence that right hippocampal/parahippocampal theta was stronger in the new relative to the familiar environment and the magnitude of right hippocampal/parahippocampal theta elicited during navigation in the new environment correlated with navigation performance in both the new and familiar environments.

The finding that anterior left hippocampal/parahippocampal theta was stronger in the hidden platform condition relative to the random swimming condition is consistent with the results of Cornwell et al. (2008a) who used a very similar experimental paradigm. These results confirm the robustness and specificity of anterior left hippocampal theta oscillations during goal-oriented spatial navigation in the human brain. The striking consistency of results between these two studies using different MEG systems with two independent cohorts of participants provides support for the contention that noninvasive MEG recordings of hippocampal theta are robust and reliable. Taken together with a small but growing body of MEG studies of the hippocampal theta rhythm (e.g. Riggs et al., 2009; Fuentemilla et al., 2010, 2014; Poch et al., 2011; Backus et al., 2016), our results also provide important confirmation of the hypothesis that the MEG-recorded theta rhythm indexes neurophysiological mechanisms that are functionally comparable to those previously measured with invasive recordings in the hippocampus of humans (e.g. Kahana et al., 1999; Caplan et al., 2001, 2003; Ekstrom et al., 2003, 2005; Jacobs et al., 2007; Vass et al., 2016) and animals (e.g. O'Keefe & Dostrosky, 1971; Harris et al., 2002; Mehta et al., 2002; Agarwal et al., 2016; Zhang et al., 2016). Importantly, the virtual Morris water maze task used in our experiment and that of Cornwell et al. (2008a) provided a behavioral context for spatial navigation that is highly comparable to the Morris water maze used to elicit and study theta oscillations in the extensively characterized rodent model (e.g. Kelemen et al., 2005; Olvera-Cortes, et al., 2004; 2012). The capability to

reliably and noninvasively measure hippocampal theta in humans now allows us to bridge the gap between animal and human models of hippocampal function, by systematically and rigorously characterizing the cognitive functions of the human theta rhythm in routine experimentation that does not rely on limited opportunities to invasively study human patients.

Our new finding that right hippocampal theta activation was greater in the first training set than in the second one in both hidden platform condition (cue rich environment) and random swimming condition (environment without cues), suggests an important role for the right hippocampus in encoding an environment in general. Since environmental layout was constant across training sets, we show that right hippocampal theta power was strongest when the requirement for environmental encoding was strongest (in the first training set), in line with the idea that hippocampal activation was prominent in the initial learning phase and decreased when performance improved (Wolbers & Buchel, 2005) and with the finding that right hippocampus was more active in processing new configuration/environment relative to familiar configuration/environment (Duzel et al., 2003; Doeller et al., 2008). This function of human right hippocampal theta in new environmental encoding is consistent with results from animal research (e.g. Jeewajee et al., 2008; Penley et al., 2013; see Burgess & O'Keefe, 2011 for a review) and provides a direct link between the human and animal studies. Our MEG results are also consistent with the fMRI results of Igloi et al. (2010), showing a time-dependent decrease in right

hippocampal activity during learning in a spatial navigation task. In addition, Kaplan et al. (2012) reported MEG theta changes (at the sensor level) when participants encoded a new environment during spatial navigation.

Notably, we found that stronger right hippocampal theta power during the first training set was correlated with better navigation performance in both the first and second training sets. These associations bolster the conclusion that right hippocampal theta plays a functional role in encoding configural properties of an environment. Those who exhibited relatively greater right hippocampal theta power during the first training set took relatively shorter paths to the hidden platform. This was true for performance in the first training set as well as the second one when a novel platform location was introduced in the same environment. This observation demonstrates that the correlation between right hippocampal theta during encoding and spatial navigation performance is not contingent on learning a specific location and therefore strongly argues for the functional role of right hippocampal theta is about encoding the whole environment. Robust encoding of the configuration of the environment to form a cognitive map of the space confers the flexibility to navigate efficiently to any location in that particular environment (Wolbers & Hegarty, 2010). This association is also consistent with previous studies linking the right hippocampus, more generally, to spatial navigation performance (e.g. Abrahams et al. 1997; Spiers et al., 2001; Burgess et al., 2002; Nedelska et al., 2012) and with previous reports that increased theta power was associated with successful/better memory formation in other

experimental paradigms (e.g. Staudigl & Hanslmayr, 2013; Hanslmayr et al., 2011; Osipova et al., 2006; Sederberg et al., 2003). However, the result that no correlation was found between right hippocampal theta in the familiar environment and path length, in conjunction with the result that in the familiar environment, there was an attenuation of right hippocampal theta power, indicates that the hippocampus might function prominently during the early stages of cognitive mapping (see Wolbers & Wiener, 2014 for a review).

Our results converge with a body of evidence that the right hippocampus is important in spatial navigation (Marguire et al., 1997; Bohbot et al., 1998; Gron et al., 2000; Maguire et al., 2000; Ekstrom et al., 2003), and further indicate that this may reflect a role in encoding an environment to facilitate navigation performance. There is some evidence that impairment of the right hippocampus is associated with impaired navigation performance. Cornwell et al. (2010) reported that depressed patients exhibited impaired performance in a virtual Morris water maze task and this impairment was related to reduced right hippocampal theta oscillations compared to healthy controls.

Taken together, our results indicate that left and right hippocampi may have different functional roles (Burgess et al., 2002), with right hippocampus playing a role in encoding an environment to form a cognitive map of the space and left hippocampus being involved in navigating to a specific location but not in

environmental processing. The left hippocampus is thought to play a role in associative processing (Igloi et al., 2010) and to mediate specific component processes of spatial navigation, such as binding the platform to its spatial location (Mitchell et al., 2000; Kessels et al., 2004; Cornwell et al., 2008a). Consistent with this hypothesis, our results show that left hippocampal theta was elicited with comparable magnitude in both training sets with the hidden platform presented in two different locations, and was not modulated by environmental novelty, adding another piece of evidence that left hippocampus was not sensitive to environment. Further work is required to nail down the potential functional dissociation of left and right hippocampi.

We note that all the effects observed in the current study were localized to the anterior portion of the hippocampus/parahippocampal cortices. Some authors have argued for functional specialization along the longitudinal axis of the hippocampus in both rodents (see Fanselow & Dong, 2010 for a review) and humans (see Poppenk et al., 2013 for a review). While no definitive conclusion on the specific functional differentiation between anterior and posterior portion of human hippocampus has been reached, our results fit with the proposal that anterior hippocampus may predominantly encode coarse, global representations and that encoding is more linked to anterior portion of the hippocampus (Poppenk et al., 2013).

Our results stand in contrast to those of a recent iEEG study (Park et al., 2014)

which reported bilateral hippocampal involvement during encoding of a new environment; further, these researchers reported that hippocampal theta power increased with increasing familiarity with the environment. There are two possible reasons for the discrepancies. First, Long et al. (2014) reported there existed temporal dynamics of the subsequent memory effect, with theta power increasing in the early encoding phase and decreasing in the late encoding phase. Different hippocampal theta power change patterns found in the current study and Park et al. (2014) might be due to difference in length of encoding phases. In Park et al., (2014), new environment was defined as the first trial in the learning phase, which can be regarded as very early encoding phase. In the current experiment, encoding effect was the average of the learning effect in the first training set, which contains 20 trials in hidden platform condition and random swimming condition respectively. Thus, the encoding effect reflected the average effect of very early encoding phase and later encoding phase. Second, in Park et al. (2014)'s study, target locations were constant in the new and familiar environments, so that the environment encoding was confounded with encoding a specific location within the environment. In our study, target location was dissociated from environmental familiarity in the first and second training sets. Thus, bilateral hippocampal activation found in Park et al. (2014) might reflect both encoding of new environment and location within that environment.

One may query whether the right hippocampal theta that was observed is related to general novelty processing instead of environmental novelty processing. However,

the correlation between right hippocampal theta power in the first training set and spatial navigation performance in both training sets argues against this possibility and suggests a more specific association with learning the environment. If the right hippocampal theta was only for general novelty processing and had nothing to do with spatial processing, the chance of being able to observe a correlation with behavioral measures of spatial cognition would be extremely slim. To yield a more definitive conclusion in this regard, a third training set in a new environment is needed, in which we would predict a rebound in right hippocampal theta.

Co-registration errors and head movement introduce spatial uncertainty of hippocampal estimates and the peak theta power at the individual level. Although group-level statistics should average out these differences, since co-registration errors and head movement across participants are unlikely to be systematic in direction, the ability of MEG to differentiate source signals from the hippocampus versus parahippocampus is questionable, and the clusters of differential power observed here generally spanned both structures. This is an important limitation given evidence that hippocampus and parahippocampal cortices mediate distinct functions. For instance, Ekstrom et al. (2007, 2011) documented that the hippocampus and parahippocampus responded differentially to spatial and temporal order source retrieval. Aggleton and Brown (2006) argued that the role of parahippocampus relies on an item-based familiarity discrimination mechanism, while the function of the hippocampus concerns novel spatial arrangements of stimuli and associative and

contextual aspects of memory. Future development of source reconstruction techniques with higher spatial resolution will facilitate the functional differentiation of parahippocampal and hippocampal theta oscillations.

Conclusion

In the past several decades, numerous studies have attempted to determine the precise function and behavioral correlates of hippocampal theta oscillations (Ekstrom et al., 2014). Our study contributes to this literature by presenting evidence for the function of right hippocampal theta rhythm in environment encoding during navigation in humans, directly linking results from invasive studies in animals with results from noninvasive measurements in healthy humans. Most importantly, these results demonstrate a robust relationship between hippocampal theta rhythm and behavioral measures of spatial navigation performance.

Acknowledgements: This work was supported by Australian Research Council Grants CE110001021, DP1096160. The authors thank Mr. Steven Saunders for the help with the implementation of the virtual Morris water maze programme, Dr. Jie Yang and Dr. Xiangzhen Kong for discussion and comments on an early draft of the manuscript. The first author also express appreciations to the China Scholarship Council and Macquarie University for financial support.

References

Arai, M., Brandt, V., & Dabaghian, Y. (2014). The effects of theta precession on spatial learning and simplicial complex dynamics in a topological model of the hippocampal spatial map. *PLoS Comput Biol, 10(6),* e1003651. doi:10.1371/journal.pcbi.1003651

Abrahams S, Pickering A, Polkey CE, Morris RG. 1997. Spatial memory deficits in patients with unilateral damage to the right hippocampal formation. *Neuropsychologia 35*, 11-24.

Agarwal, G., Stevenson, I. H., Berenyi, A., Mizuseki, K., Buzsaki, G., & Sommer, F. T. (2014). Spatially distributed local fields in the hippocampus encode rat position. *Science, 344(6184)*, 626-630. doi:10.1126/science.1250444

Aggleton, J. P., & Brown, M. W. (2006). Interleaving brain systems for episodic and recognition memory. *Trends Cogn Sci, 10(10)*, 455-463. doi:10.1016/j.tics.2006.08.003

Attal Y., Schwartz D. (2013) Assessment of subcortical source localization using deep brain activity imaging model with minimum norm operators: A MEG Study. *PLoS ONE, 8*, e59856. doi:10.1371/journal.pone.0059856

Backus, A. R., Schoffelen, J. M., Szebenyi, S., Hanslmayr, S., & Doeller, C. F. (2016). Hippocampal-Prefrontal Theta Oscillations Support Memory Integration. *Curr Biol, 26(4),* 450-457. doi:10.1016/j.cub.2015.12.048

Bohbot, V. D., Kalina, M., Stepankova, K., Spackova, N., Petrides, M., & Nadel, L. (1998). Spatial memory deficits in patients with lesions to the right

hippocampus and to the right parahippocampal cortex. *Neuropsychologia*, *36*, 1217-1238.

Burgess, N., Maguire, E. A., & O'Keefe, J. (2002). The human hippocampus and spatial and episodic memory. *Neuron*, *35*, 625-641. doi:10.1016/S0896-6273(02)00830-9

Burgess, N., & O'Keefe, J. (2011). Models of place and grid cell firing and theta rhythmicity. *Curr Opin Neurol*, *21*, 1-11. doi:10.1016/j.conb.2011.07.002

Buzsaki, G. (2005). Theta rhythm of navigation: Link between path integration and landmark navigation, episodic and semantic memory. *Hippocampus*, *15*, 827-840. doi:10.1002/hipo.20113

Buzsaki, G. (2006). *Rhythms of the brain*. Oxford: Oxford University Press.

Buzsaki, G., Anastassiou, C. A., & Koch, C. (2012). The origin of extracellular fields and currents--EEG, ECoG, LFP and spikes. *Nat Rev Neurosci, 13(6)*, 407-420. doi:10.1038/nrn3241

Caplan, J. B., Madsen, J. R., Raghavachari, S., & Kahana, M. J. (2001). Distinct patterns of brain oscillations underlie two basic parameters of human maze learning. *J Neurophysiol*, *86*, 368-380.

Caplan, J. B., Madsen, J. R., Schulze-Bonhage, A., Aschenbrenner-Scheibe, R., & Kahana, M. J. (2003). Human theta oscillations related to sensorimotor integration and spatial learning. *J Neurosci*, *23*, 4726-4736.

Cheyne, D., Bostan, A. C., Gaetz, W., & Pang, E. W. (2007). Event-related beamforming: a robust method for presurgical functional mapping using MEG. *Clin Neurophysiol, 118*(8), 1691-1704.

Cornwell, B. R., Johnson, L. L., Holroyd, T., Carver, F. W., & Grillon, C. (2008a). Human hippocampal and parahippocampal theta during goal-directed spatial navigation predicts performance on a virtual Morris water maze. *J Neurosci*, *23*, 5983-5990. doi:10.1523/JNEUROSCI.5001-07.2008

Cornwell, B. R., Carver, F. W., Coppola, R., Johnson, L., Alvarez, R., Coppola, R., Manji H., Zarate Jr. C. A., & Grillon, C. (2008b). Evoked amygdala responses to negative faces revealed by adaptive MEG beamformers. *Brain Res*, *1244*, 103-112. doi:10.1016/j.brainres.2008.09.068

Cornwell, B. R., Salvadore, G., Colon-Rosario, V., Latov, D. R., Holroyd, T., Carver, F. W., & Grillon, C. (2010). Abnormal hippocampal functioning and impaired spatial navigation in depressed individuals: evidence from whole-head magnetoencephalography. *Am J Psychiatry*, *167*, 836-844. doi:10.1176/appi.ajp.2009.09050614

Cornwell, B. R., Arkin, N., Overstreet, C., Carver, F. W., & Grillon, C. (2012). Distinct contributions of human hippocampal theta to spatial cognition and anxiety. *Hippocampus, 22*(9), 1848-1859. doi:10.1002/hipo.22019

Cousijn, H., Tunbridge, E. M., Rolinski, M., Wallis, G., Colclough, G. L., Woolrich, M. W., . . . Harrison, P. J. (2015). Modulation of hippocampal theta and

hippocampal-prefrontal cortex function by a schizophrenia risk gene. *Hum Brain Mapp, 36(6)*, 2387-2395. doi:10.1002/hbm.22778

Cox, R. W. (1996). AFNI: software for analysis and visualization of functional magnetic resonance neuroimages. *Comput Biomed Res*, *29*, 162-173. doi:10.1006/cbmr.1996.0014

Dalal S, Jerbi K, Bertrand O, Adam C, Ducorps A, Schwarts D, Martinerie J, Lachaux J (2013): Simultaneous MEG-intracranial EEG: New insights into the ability of MEG to capture oscillatory modulations in the neocortex and the hippocampus. *Epilepsy Behav, 28*(2), 310-311. doi:10.1016/j.yebeh.2012.04.032

Doeller C. F., King J. A., Burgess N. (2008). Parallel striatal and hippocampal systems for landmarks and boundaries in spatial memory. *Proc Natl Acad Sci USA, 105*, 5915–5920.

Ekstrom, A. D., & Bookheimer, S. Y. (2007). Spatial and temporal episodic memory retrieval recruit dissociable functional networks in the human brain. *Learn Mem, 14(10)*, 645-654. doi:10.1101/lm.575107

Ekstrom, A. D., Caplan, J. B., Fields, T. A., Isham, E. A., Newman, E. L., Kahana, M. J., & Fried, I. (2003). Cellular networks underlying human spatial navigation. *Nature*, *425*, 184-188. doi:10.1038/nature01964

Ekstrom, A. D., Caplan, J. B., Ho, E., Shattuck, K., Fried, I., & Kahana, M. J. (2005). Human hippocampal theta activity during virtual navigation. *Hippocampus*, *15*, 881-889. doi:10.1002/hipo.20109

Ekstrom, A. D., Copara, M. S., Isham, E. A., Wang, W. C., & Yonelinas, A. P. (2011). Dissociable networks involved in spatial and temporal order source retrieval. *Neuroimage, 56(3)*, 1803-1813. doi:10.1016/j.neuroimage.2011.02.033

Ekstrom, A. D., & Watrous, A. J. (2014). Multifaceted roles for low frequency oscillations in bottom-up and top-down processing during spatial navigation and memory. *Neuroimage*, *85*, 667-677. doi:10.1016/j.neuroimage.2013.06.049

Duzel E., Habib R., Rotte M., Guderian S., Tulving E., and Heinze H.. (2003). Human Hippocampal and Parahippocampal Activity during Visual Associative Recognition Memory for Spatial and Nonspatial Stimulus Configurations. *J Neurosci, 23*(28), 9439-9444.

Fanselow, M. S., & Dong, H. W. (2010). Are the dorsal and ventral hippocampus functionally distinct structures? *Neuron, 65(1)*, 7-19. doi:10.1016/j.neuron.2009.11.031

Foster, B. L., Kaveh, A., Dastjerdi, M., Miller, K. J., & Parvizi, J. (2013). Human retrosplenial cortex displays transient theta phase locking with medial temporal cortex prior to activation during autobiographical memory retrieval. *J Neurosci, 33(25),* 10439-10446. doi:10.1523/JNEUROSCI.0513-13.2013

Fuentemilla, L., Barnes, G. R., Duzel, E., & Levine, B. (2014). Theta oscillations orchestrate medial temporal lobe and neocortex in remembering autobiographical memories. *Neuroimage, 85 Pt 2*, 730-737. doi:10.1016/j.neuroimage.2013.08.029

Fuentemilla, L., Penny, W. D., Cashdollar, N., Bunzeck, N., & Duzel, E. (2010). Theta-coupled periodic replay in working memory. *Curr Biol, 20(7)*, 606-612. doi:10.1016/j.cub.2010.01.057

Guitart-Masip, M., Barnes, G. R., Horner, A., Bauer, M., Dolan, R. J., & Duzel, E. (2013). Synchronization of medial temporal lobe and prefrontal rhythms in human decision making. *J Neurosci, 33(2),* 442-451. doi:10.1523/JNEUROSCI.2573-12.2013

Grön, G., Wunderlich, A. P., Spitzer, M., Tomczak, R., & Riepe, M. W. (2000). Brain activation during human navigation: gender-different neural networks as substrate of performance. *Nature Neurosci, 3*, 404 - 408. doi:10.1038/73980

Hanslmayr, S., Volberg, G., Wimber, M., Raabe, M., Greenlee, M. W., & Bauml, K. H. (2011). The relationship between brain oscillations and BOLD signal during memory formation: a combined EEG-fMRI study. *J Neurosci, 31(44)*, 15674-15680. doi:10.1523/JNEUROSCI.3140-11.2011

Harris, K. D., Henze, D. A., Hirase, H., Leinekugel, X., Dragoi, G., Czurko, A., & Buzsaki, G. (2002). Spike train dynamics predicts theta-related phase precession in hippocampal pyramidal cells. *Nature, 417(6890)*, 738-741. doi:10.1038/nature00808

Hillebrand, A., Singh, K. D., Holliday, I. E., Furlong, P. L., & Barnes, G. R. (2005). A new approach to neuroimaging with magnetoencephalography. *Hum Brain Mapp, 25*, 199-211. doi:10.1002/hbm.20102

Hung, Y., Smith, M. L., Bayle, D. J., Mills, T., Cheyne, D., & Taylor, M. J. (2010). Unattended emotional faces elicit early lateralized amygdala–frontal and fusiform activations. *Neuroimage*, *50*, 727-733. doi:10.1016/j.neuroimage.2009.12.093

Igloi, K., Doeller, C. F., Berthoz, A., Rondi-Reig, L., & Burgess, N. (2010). Lateralized human hippocampal activity predicts navigation based on sequence or place memory. *Proc Natl Acad Sci USA*, *107*, 14466-14471. doi:10.1073/pnas.1004243107

Jacobs, J. (2014). Hippocampal theta oscillations are slower in humans than in rodents: implications for models of spatial navigation and memory. *Philos Trans R Soc Lond B Biol Sci, 369(1635)*, 20130304. doi:10.1098/rstb.2013.0304

Jacobs, J., Kahana, M. J., Ekstrom, A. D., & Fried, I. (2007). Brain oscillations control timing of single-neuron activity in humans. *J Neurosci, 27(14)*, 3839-3844. doi:10.1523/JNEUROSCI.4636-06.2007

Jacobs, J., Weidemann, C. T., Miller, J. F., Solway, A., Burke, J. F., Wei, X. X., . . . Kahana, M. J. (2013). Direct recordings of grid-like neuronal activity in human spatial navigation. *Nat Neurosci, 16(9)*, 1188-1190. doi:10.1038/nn.3466

Jeewajee, A., Lever, C., Burton, S., O'Keefe, J., & Burgess, N. (2008). Environmental novelty is signaled by reduction of the hippocampal theta frequency. *Hippocampus, 18,* 340-348. doi:10.1002/hipo.20394

Kado, H., Higuchi, M., Shimogawara, M., Haruta, Y., Adachi, Y., Kawai, J., & Uehara, G. (1999). Magnetoencephalogram systems developed at KIT. *IEEE Trans. Appl. Supercond*, *9*, 4057-4062. doi:10.1109/77.783918

Kahana, M. J., Sekuler, R., Caplan, J. B., Kirschen, M., & Madsen, J. R. (1999). Human theta oscillations exhibit task dependence during virtual maze navigation. *Nature*, *399*, 781-784.

Kaplan, R., Doeller, C. F., Barnes, G. R., Litvak, V., Duzel, E., Bandettini, P. A., & Burgess, N. (2012). Movement-related theta rhythm in humans: coordinating self-directed hippocampal learning. *PLoS Biol*, *10*, e1001267. doi:10.1371/journal.pbio.1001267

Keil, J., Muller, N., Ihssen, N., & Weisz, N. (2012). On the variability of the McGurk effect: audiovisual integration depends on prestimulus brain states. *Cereb Cortex, 22*(1), 221-231. doi:10.1093/cercor/bhr125

Keil, J., Pomper, U., & Senkowski, D. (2015). Distinct patterns of local oscillatory activity and functional connectivity underlie intersensory attention and temporal prediction. *Cortex, 74*, 277-288. doi:10.1016/j.cortex.2015.10.023

Kelemen, E., Moron, I., & Fenton, A. A. (2005). Is the hippocampal theta rhythm related to cognition in a non-locomotor place recognition task? *Hippocampus, 15(4)*, 472-479. doi:10.1002/hipo.20071

Kessels, R. P., Hendriks, M. P., Schouten, J., Asselen, M. V., & Postma, A. (2004). Spatial memory deficits in patients after unilateral selective

amygdalohippocampectomy. *J Int Neuropsychol Soc*, *10*, 907-912. doi:10.1017/S1355617704106140

Isabella, S., Ferrari, P., Jobst, C., Cheyne, J. A., & Cheyne, D. (2015). Complementary roles of cortical oscillations in automatic and controlled processing during rapid serial tasks. *Neuroimage, 118*, 268-281. doi:10.1016/j.neuroimage.2015.05.081

Long, N. M., Burke, J. F., & Kahana, M. J. (2014). Subsequent memory effect in intracranial and scalp EEG. *Neuroimage, 84*, 488-494. doi:10.1016/j.neuroimage.2013.08.052

Maguire, E. A., Frackowiak, R. S., & Frith, C. D. (1997). Recalling routes around London: Activation of the right Hippocampus in taxi drivers. *J Neurosci*, *17*, 7103-7110.

Maguire, E. A., Gadian, D. G., Johnsrude, I. S., Good, C. D., Ashburner, J., Frackowiak, R. S., & Frith, C. D. (2000). Navigation-related structural change in the hippocampi of taxi drivers. *Proc Natl Acad Sci USA*, *97*, 4398-4403. doi:10.1073/pnas.070039597

Mehta, M. R., Lee, A. K., & Wilson, M. A. (2002). Role of experience and oscillations in transforming a rate code into a temporal code. *Nature*, *417*, 741-746. doi:10.1038/nature00807

Meltzer, J. A., Wagage, S., Ryder, J., Solomon, B., & Braun, A. R. (2013). Adaptive significance of right hemisphere activation in aphasic language

comprehension. *Neuropsychologia, 51*(7), 1248-1259. doi:10.1016/j.neuropsychologia.2013.03.007

Mitchell, K. J., Johnson, M. K., Raye, C. L., & D'Esposito, M. (2000). fMRI evidence of age-related hippocampal dysfunction in feature binding in working memory. *Brain Res Cogn Brain Res*, *10*, 197-206. doi:10.1016/S0926-6410(00)00029-X

Morris, R (May 1984). Developments of a water-maze procedure for studying spatial learning in the rat. *J neurosci methods, 11*, 47–60. doi:10.1016/0165-0270(84)90007-4

Moser, E. I., Kropff, E., & Moser, M. B. (2008). Place cells, grid cells, and the brain's spatial representation system. *Annu Rev Neurosci, 31,* 69-89. doi:10.1146/annurev.neuro.31.061307.090723

Moser, M. B., Rowland, D. C., & Moser, E. I. (2015). Place cells, grid cells, and memory. *Cold Spring Harb Perspect Biol, 7(2)*, a021808. doi:10.1101/cshperspect.a021808

Muller R. (1996). A quarter of a century of place cell. *Neuron. 17,* 813-822. Nedeska, Z., Andel, R., Laczo, J., Vlcek, K., Horinek, D., Lisy, J., & Hort, J. (2012). Spatial navigation impairment is proportional to right hippocampal volume. *Proc Natl Acad Sci USA*, *109*, 2590-2594.

Muller, N., Keil, J., Obleser, J., Schulz, H., Grunwald, T., Bernays, R. L., . . . Weisz, N. (2013). You can't stop the music: reduced auditory alpha power and coupling between auditory and memory regions facilitate the illusory

perception of music during noise. *Neuroimage, 79*, 383-393. doi:10.1016/j.neuroimage.2013.05.001

Muller, N., & Weisz, N. (2012). Lateralized auditory cortical alpha band activity and interregional connectivity pattern reflect anticipation of target sounds. *Cereb Cortex, 22*(7), 1604-1613. doi:10.1093/cercor/bhr232

O'Keefe, J., & Dostrovsky, J. (1971). The hippocampus as a spatial map. Preliminary evidence from unit activity in the freely-moving rat. *Brain Research*, *34*, 171-175. doi:10.1016/0006-8993(71)90358-1

O'Keefe, J., & Nadel, L. (1978). The hippocampus as a cognitive map. *Hippocampus*, *9*, 352-364.

Olvera-Cortes, E., Guevara, M. A., & Gonzalez-Burgos, I. (2004). Increase of the hippocampal theta activity in the Morris water maze reflects learning rather than motor activity. *Brain Res Bull, 62(5)*, 379-384. doi:10.1016/j.brainresbull.2003.10.003

Olvera-Cortes, M. E., Garcia-Alcantar, I., Gutierrez-Guzman, B., Hernandez-Perez, J. J., Lopez-Vazquez, M. A., & Cervantes, M. (2012). Differential learning-related changes in theta activity during place learning in young and old rats. *Behav Brain Res, 226(2),* 555-562. doi:10.1016/j.bbr.2011.10.019

Osipova, D., Takashima, A., Oostenveld, R., Fernandez, G., Maris, E., & Jensen, O. (2006). Theta and gamma oscillations predict encoding and retrieval of declarative memory. *J Neurosci, 26(28)*, 7523-7531. doi:10.1523/JNEUROSCI.1948-06.2006

Park, J., Lee, H., Kim, T., Park, G. Y., Lee, E. M., Baek, S., Ku, J., Kim, I. Y., Jang, D. P., & Kang, J. K. (2014). Role of low- and high-frequency oscillations in the human hippocampus for encoding environmental novelty during a spatial navigation task. *Hippocampus, 24,* 1314-1352.

Peirce, J. W. (2007). PsychoPy—psychophysics software in Python. *J Neurosci Methods*, *162*, 8-13. doi:10.1016/j.jneumeth.2006.11.017

Peirce, J. W. (2008). Generating stimuli for neuroscience using PsychoPy. *Front Neuroinformat*, *2*. doi:10.3389/neuro.11.010.2008

Penley, S. C., Hinman, J. R., Long, L. L., Markus, E. J., Escabi, M. A., & Chrobak, J. J. (2013). Novel space alters theta and gamma synchrony across the longitudinal axis of the hippocampus. *Front Syst Neurosci, 7*, 20. doi:10.3389/fnsys.2013.00020

Poch, C., Fuentemilla, L., Barnes, G. R., & Duzel, E. (2011). Hippocampal theta-phase modulation of replay correlates with configural-relational short-term memory performance. *J Neurosci, 31(19),* 7038-7042.

Poppenk, J., Walia, G., McIntosh, A. R., Joanisse, M. F., Klein, D., & Kohler, S. (2008). Why is the meaning of a sentence better remembered than its form? An fMRI study on the role of novelty-encoding processes. *Hippocampus, 18(9)*, 909-918. doi:10.1002/hipo.20453

Riggs, L., Moses, S. N., Bardouille, T., Herdman, A. T., Ross, B., & Ryan, J. D. (2009). A complementary analytic approach to examining medial temporal lobe sources using magnetoencephalography. *Neuroimage, 45(2)*, 627-642. doi:10.1016/j.neuroimage.2008.11.018

Robinson, S. E., Vrba, J. (1999). Functional neuroimaging by synthetic aperture magnetometry (SAM). In: *Recent advances in biomagnetism* (YoshimotoT, Kotani M, Kuriki S, Karibe, H., Nakasato N., eds), pp 302–305. Sendai, Japan: Tohoku UP.

Rutishauser, U., Ross, I. B., Mamelak, A. N., & Schuman, E. M. (2010). Human memory strength is predicted by theta-frequency phase-locking of single neurons. *Nature, 464(7290)*, 903-907. doi:10.1038/nature08860

Sakimoto, Y., Okada, K., Takeda, K., & Sakata, S. (2013). Transient decline in hippocampal theta activity during the acquisition process of the negative patterning task. *PLoS One, 8(7),* e70756. doi:10.1371/journal.pone.0070756

Sarvas, J. (1987). Basic mathematical and electromagnetic concepts of the biomagnetic inverse problem. *Phys Med Biol, 32*, 11-22.

Sederberg, P. B., Schulze-Bonhage, A., Madsen, J. R., Bromfield, E. B., McCarthy, D. C., Brandt, A., . . . Kahana, M. J. (2007). Hippocampal and neocortical gamma oscillations predict memory formation in humans. *Cereb Cortex, 17(5)*, 1190-1196. doi:10.1093/cercor/bhl030

Spiers, H. J., Burgess, N., Maguire, E. A., Baxendale, S. A., Hartley, T., Thompson, P. J., & O'Keefe, J. (2001). Unilateral temporal lobectomy patients show

lateralized topographical and episodic memory deficits in a virtual town. *Brain*, *124*, 2476-2489. doi:10.1093/brain/124.12.2476

Staudigl, T., & Hanslmayr, S. (2013). Theta oscillations at encoding mediate the context-dependent nature of human episodic memory. *Curr Biol, 23(12)*, 1101-1106. doi:10.1016/j.cub.2013.04.074

Suthana, N., Haneef, Z., Stern, J., Mukamel, R., Behnke, E., Knowlton, B., & Fried, I. (2012). Memory enhancement and deep-brain stimulation of the entorhinal area. *N Engl J Med, 366(6)*, 502-510.

Tallon-Baudry, C., Bertrand, O., Delpuech, C., Permier, J. (1997). Oscillatory gamma-band (30-70 Hz) activity induced by a visual search task in humans. *J. Neurosci. 17,* 722-734.

Tesche, C. D., & Karhu, J. (2000). Theta oscillations index human hippocampal activation during a working memory task. *Proc Natl Acad Sci USA*, *97*, 9191-924. doi:10.1073/pnas.97.2.919

Vass, L. K., Copara, M. S., Seyal, M., Shahlaie, K., Farias, S. T., Shen, P. Y., & Ekstrom, A. D. (2016). Oscillations Go the Distance: Low-Frequency Human Hippocampal Oscillations Code Spatial Distance in the Absence of Sensory Cues during Teleportation. *Neuron, 89(6)*, 1180-1186. doi:10.1016/j.neuron.2016.01.045

Wang, Y., Romani, S., Lustig, B., Leonardo, A., & Pastalkova, E. (2015). Theta sequences are essential for internally generated hippocampal firing fields. *Nat Neurosci, 18(2)*, 282-288. doi:10.1038/nn.3904

Wolbers T., Büchel C. (2005). Dissociable retrosplenial and hippocampal contributions to successful formation of survey representations. *J Neurosci 25,* 3333–3340.

Wolbers, T., & Hegarty, M. (2010). What determines our navigational abilities? *Trends Cogn Sci, 14(3)*, 138-146. doi:10.1016/j.tics.2010.01.001

Wolbers, T., & Wiener, J. M. (2014). Challenges for identifying the neural mechanisms that support spatial navigation: the impact of spatial scale. *Front Hum Neurosci, 8,* 571. doi:10.3389/fnhum.2014.00571

Wyble, B. P., Hyman, J. M., Rossi, C. A., & Hasselmo, M. E. (2004). Analysis of theta power in hippocampal EEG during bar pressing and running behavior in rats during distinct behavioral contexts. *Hippocampus, 14(5),* 662-674. doi:10.1002/hipo.20012

Zhang, L., Ma, X., Chen, G., Barkai, E., & Lin, L. (2016). Theta Rhythmic Clock-Like Activity of Single Units in the Mouse Hippocampus. *J Neurosci, 36(16),* 4415-4420. doi:10.1523/JNEUROSCI.3851-15.2016

Chapter four

High-gamma activity in the human hippocampus during inter-trial rest periods of a virtual navigation task

Abstract

In rodents, hippocampal cell assemblies formed during learning of a navigation task are observed to re-emerge during resting (offline) periods, accompanied by high-frequency oscillations (HFOs). This phenomenon is believed to reflect mechanisms for strengthening newly-formed memory traces. Using magnetoencephalography recordings and a virtual Morris water maze task, we investigated high-gamma (80 – 140 Hz) oscillations in the hippocampal region in humans during inter-trial rest periods in a virtual navigation task. We found right hippocampal gamma oscillations mirrored the pattern of theta power in the same region during navigation, varying as a function of environmental novelty. Gamma power during inter-trial rest periods was positively correlated with theta power during navigation and predicted faster learning of a new location as the environment became familiar. These findings suggest the existence of a 'replay mechanism' for memory consolidation in the human hippocampus.

Keywords: Hippocampus, high-gamma oscillations, replay, virtual spatial navigation, magnetoencephalography (MEG)

Introduction

The formation of spatial memories has been proposed to proceed in two stages (Buzsaki, 1989, 2015). In the initial encoding phase, during active exploration of an environment, a transient change of synaptic strengths in the hippocampus is formed accompanied by theta-band local field potential (LFP) oscillations. Subsequently, during 'offline' states, including slow-wave sleep and quiet wakefulness, the new synaptic network re-emerges, accompanied by high frequency oscillations (HFOs) which operate to potentiate and strengthen the synaptic changes and thereby consolidate the otherwise labile memory traces.

Invasive electrophysiological studies in rodents have shown that temporal spike sequences of place cells active during navigation reoccur (replay) when the animal is asleep or in a state of awake immobility after exploration accompanied by HFOs (O'Neill et al., 2010). Disruption of hippocampal HFOs impairs spatial learning (Gerrard et al., 2008; Girardeau et al., 2009; Jadhav et al., 2012), suggesting a causal relationship between HFOs and memory formation. Replay is also sensitive to environmental novelty (Carr et al., 2011). Following navigating in a new environment, the strength of place cell replay is stronger (Diba & Buzsaki, 2007; O'Neill et al., 2008) and HFO power is significantly higher (Cheng & Frank, 2008) than that following navigation in a familiar environment.

Evidence for learning-dependent replay in the human hippocampus is lacking. fMRI studies (Staresina et al., 2013; Tambini et al., 2010) have reported that regions involved in encoding are reactivated during offline states. However, the results concerning hippocampal reactivation after learning of a hippocampus-dependent task are mixed. Some studies have found the hippocampus was reactivated (Bergmann et al., 2012; Peigneux et al., 2006), while others have not (Deuker et al., 2013; Staresina et al., 2013). We reasoned that the discrepancy might be due to the possibility that hippocampal reactivation occurs immediately following each learning trial and is transient. Depending on the task, durations of hippocampal replay vary, such that for some tasks, hippocampal reactivation during offline rest/sleep after a block of learning trials might not be apparent. In the meanwhile, some neurophysiological work has been done using iEEG or MEG aiming to reveal the neurophysiological mechanism underlying the replay process. After learning a word list, Axmacher et al. (2008) recorded the brain activity of pre-surgery patients during a nap and observed high-gamma (80 – 140 Hz) bursts in the rhinal cortex and hippocampus, but only the high-gamma bursts in the rhinal cortex were correlated with the number of words retrieved in the post-nap test. Using MEG, Cornwell et al. (2014) observed that hippocampal high-gamma power during a 5-minute rest period after a block of spatial learning correlated with learning rate before rest, but not with the performance in the post-rest test phase. These results suggest that high-gamma might be relevant to replay process. However, since there was no control condition (e.g., a non-learning condition) in these studies, it is unclear whether the correlation is learning specific or

only reflects trait-related general cognitive ability.

Motivated by the animal models, we used magnetoencephalography (MEG) to examine whether hippocampal high-gamma band would show a "replay effect" during the short inter-trial rest period following each trial of spatial learning, MEG was recorded while participants performed two training sets of a virtual Morris water maze task. Each set included a hidden platform condition (the task was to find the hidden platform) and a random swimming condition (the task was aimlessly swimming in a pool without platform). Environment layouts of each condition in the two training sets were the same. In a previous report on data from the same experiment described in chapter three, we studied low-frequency theta (4 – 8 Hz) activity during navigation, finding that there was significantly greater theta power in right hippocampus in the first compared to the second training set, which was associated with environment encoding; there was significantly more left hippocampal theta in hidden platform condition than in random swimming condition, which was associated with encoding of the hidden platform location.

In the present analyses, I hypothesized that right and left hippocampal high-gamma during inter-trial period would mirror the pattern of right and left hippocampal theta during navigation respectively to replay the newly learned information, as shown in animal studies (e.g., Cheng & Frank, 2008) described above. I also reasoned that hippocampal high-gamma power during rest should correlate with

theta power during navigation, since replay is proportional to previous learning in rodents (Sutherland & McNaughton, 2000). Finally, I hypothesized that high-gamma power after navigating in new environment should correlate with learning performance in the familiar environment, since consolidation of newly learned environment to form a cognitive map of the space should facilitate flexible navigation to new locations in the same environment (Wolbers & Hegarty, 2010).

Materials and Methods

Participants and Task. Eighteen male participants (mean age = 29 years; range = 18 – 39 years) participated in the study. The study was approved by Macquarie University's human subjects ethics committee. All participants gave written informed consent. Analysis of data during active navigation was previously reported in chapter three. The current analysis investigated high-gamma during the inter-trial intervals (ITI) of the experiment when participants rested quietly following each trial of spatial navigation.

A detailed description of the experimental paradigm is in chapter three. In brief, naive participants performed two training sets of a virtual Morris water maze task. In each training set of the task, there were two conditions. In the hidden platform condition, participants needed to find a hidden platform submerged in the opaque water by using the visual cues on the walls surrounding the virtual pool. In the

random swimming condition, participants moved aimlessly in the same virtual pool (but with no visual cues on the walls). The environment of each condition in the two training sets was the same, thus the environment in the first training set was defined as new environment and that in the second one as familiar environment. Therefore, the difference between the two training sets allowed us to measure *learning of the environment* (chapter three), and the difference between hidden platform condition and random swimming condition provided an index of *goal-directed spatial navigation* (Cornwell et al., 2008). The rationale for removing the cues in the random swimming condition was to investigate whether hippocampal oscillations have a general role in environmental learning of both cue poor and cue rich environment. To avoid the possibility that environment learning was confounded with learning a specific location, the location of the hidden platform was changed and counterbalanced between the training sets.

In each training set, there were 40 trials including 20 hidden platform and 20 random swimming trials respectively, presented in alternating blocks of four trials. Between each trial, there was a 4.5 – 5.5s inter-trial interval (ITI) (Fig. 1), during which a gray screen was presented and participants rested quietly without movement.

Behavioral measures. The length of the path taken from the starting position to the hidden platform in each trial was recorded. Learning rate was computed as the average path length of the first block minus that of the last one, divided by the number

of blocks. A large positive value thus reflects rapid learning (Hopper et al., 2007).

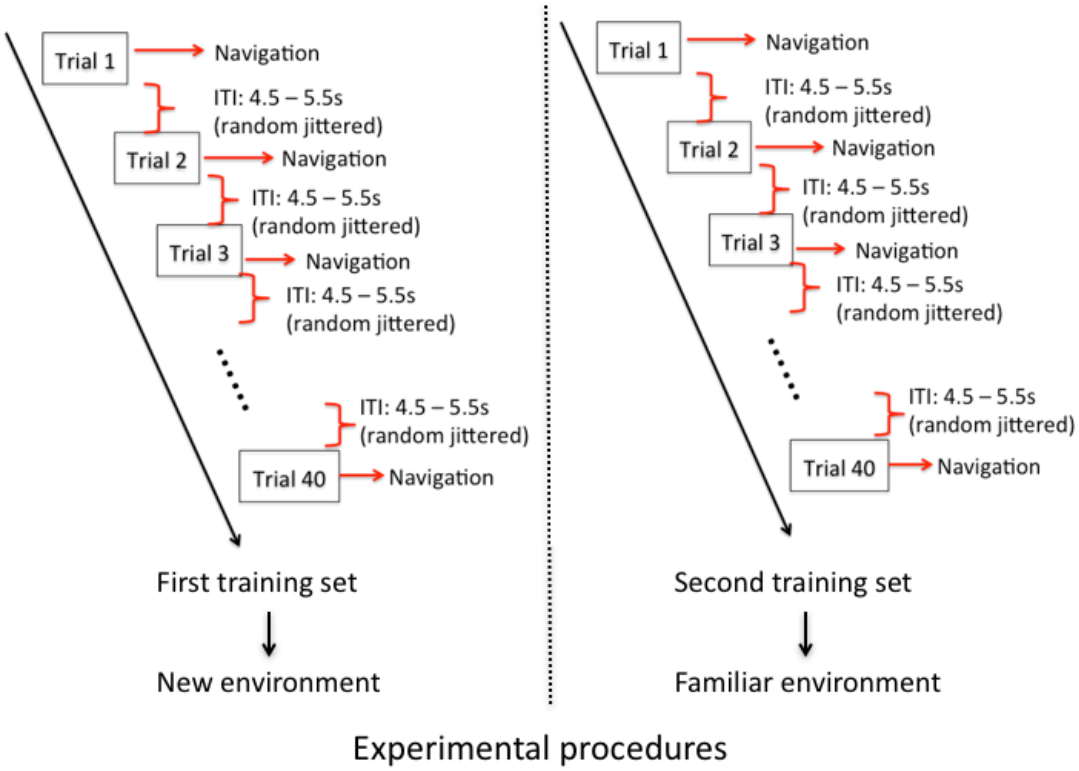

Figure 1. Experimental procedure. In each training set, there were 40 trials, including 20 hidden platform trials (the task was to find the hidden platform in a pool with four cues) and 20 random swimming trials (the task was to aimless swimming in a pool without visual cues and platform), which were alternatively presented (4 hidden platform trials, 4 random swimming trials, 4 hidden platform trials, 4 random swimming trials…). The interval between each trial (ITI) was 4.5 – 5.5 s (random jittered), during which a grey screen was presented and participants rested quietly without movement.

ITI: Inter-trial interval

MEG recordings. Recordings were made in a magnetically shielded room (Fujihara

Co. Ltd., Tokyo, Japan) with a 160-channel KIT system (Model PQ1160R-N2, Kanazawa, Japan) with superconducting quantum interference device (SQUID)-based first-order axial gradiometers (50-mm baseline; Kado et al., 1999; Uehara et al., 2003). Neuromagnetic signals were digitized continuously at a sampling rate of 1000 Hz filtered at 0.03 and 200 Hz. Before recordings, the locations of the five marker coils and three fiducial markers, and the participant's head shape were digitised with a pen digitizer (Polhemus Fastrack, Colchester, VT, USA). The five marker coils were energized before and after each training set to determine head movement and position within the MEG dewar.

MRI scans. High-resolution T1-weighted anatomical magnetic resonance images (MRIs) were acquired in a separate session at Macquarie University Hospital, using a 3T Siemens Magnetom Verio scanner with a 12-channel head coil. Images were obtained using 3D GR\IR scanning sequence with the following parameters: repetition time, 2000 ms; echo time, 3.94 ms; flip angle, 9 degrees; slice thickness, 0.93 mm; field of view, 240 mm; image dimensions, 512 × 512 × 208.

MEG analyses

High-gamma activities during offline rest period. The MEG data during the inter-trial intervals (ITI) were epoched (-4.5 – 0 s; 0 s was the onset of the next trial; 4.5 s was the shortest ITI across trials) and were labeled as *post hidden platform*

condition and *post random swimming* condition respectively. Sources were reconstructed using synthetic aperture magnetometry (SAM) beamformer analysis (Hillebrand et al., 2005; Robinson & Vrba, 1999) implemented in the BrainWave toolbox (version 3.0, http://cheynelab.utoronto.ca/). MEG has been shown to be able to reliably localize activity from the hippocampus in both simulation studies (e.g., Attal et al., 2007; Chupin et al., 2002; Meyer et al., 2017; Quraan et al., 2011; Stephen et al., 2005) and empirical experiments (e.g., Backus et al., 2016; Cornwell et al., 2008; Riggs et al., 2009; Tesche & Karhu, 2000). Recently, Crespo-Garcia et al. (2016) have shown agreement between simultaneous intracranial depth recordings and MEG virtual sensor recordings of hippocampal activity.

Due to the 1/f power law, in general, high-gamma power is harder to investigate as compared to low frequency power. Nevertheless, many previous studies have shown that high-gamma was successfully detected by MEG (e.g., Cheyne et al., 2008; Cheyne & Ferrari, 2013; Cornwell et al., 2014; Muthukumaraswamy, 2013 for a review). In the case of the hippocampus, an important reason is that invasive recordings in animal models show substantially greater power for high frequency gamma during rest/sleep than for low frequency theta during navigation (Buzsaki, 2015).

Beamformer source reconstruction is achieved by first defining a source space of volumetric grids encompassing the whole head. SAM operates by constructing an

adaptive spatial filter (beamformer weights) for each grid location, based on a combination of lead fields calculated from the forward solution and the data covariance matrix. Beamformer weights are convolved with the MEG sensor data to obtain a source signal for each grid element. Since the output of the spatial filter contains both the signal of interest and noise, it is necessary to estimate the noise level and normalize the output beamformer signal to obtain a relatively 'pure' neural signal. One commonly used method of normalization (e.g. Cornwell et al., 2014; Perry, 2015). uses a pseudo-Z metric (Robinson & Vrba, 1999; Vrba & Robinson, 2001), which divides the absolute source power of a single state by a noise estimate. Another normalization approach (e.g. Cornwell et al., 2012; Isabella et al., 2015) uses a pseudo-F or pseudo-T metric, which computes the percentage change (pseudo-F) or absolute change (pseudo-T) of the signal power in an active state relative to a control state so as to implicitly control the noise level (under the assumption that the two states have similar noise levels).

In the present analysis, the source power of high-gamma activity during inter-trial interval (ITI) was computed using a pseudo-Z metric because we were interested in estimating spontaneous high-gamma power during ITI rest period (as opposed to event-related power changes). The forward model in the current analysis was a single sphere volume conduction model (Lalancette et al., 2011; Sarvas, 1987) derived from the individual MRIs. Data covariance matrices were calculated for the whole epoch for the frequency band of 80 – 140 Hz during ITI, the same frequency

range as used in Axmacher et al. (2008) and Cornwell et al. (2014). Thus the length of the covariance matrix in the *post hidden platform* condition was 20 trials × 4.5s/trial = 90s and that in the *post random swimming* condition was 19 trials × 4.5s/trial = 85.5s. In the latter, there were 19 trials instead of 20, because the last trial of the experiment was always a random swimming trial and the experimental program aborted after the completion of the last trial. The slight difference in covariance window length for *post hidden platform* condition and *post random swimming* condition was not expected to significantly influence source estimation. Brookes et al. (2008) demonstrated that if the bandwidths of the estimated frequency band was > 50 Hz, and when covariance window length amounted to 40 s, the accuracy of source estimation would be very high and increasing the covariance window length would not greatly improve the accuracy of source estimation. Source power was estimated across the entire 3D source space at a resolution of 4×4×4 mm.

The resulting volumetric SAM images were warped to a standard Talairach template space and analyzed with Analysis of Functional Neuroimaging (AFNI) software (Cox, 1996; http://afni.nimh.nih.gov/afni). To address the first hypothesis, i.e., whether right and left hippocampal offline high-gamma mirror the pattern of right and left hippocampal theta activity during navigation respectively, first, we defined an ROI in the right hippocampus and parahippocampus[1], showing a new environment encoding effect in chapter three during navigation in theta frequency band and two

[1] For simplicity, I used right hippocampal ROI to refer to the ROI in the right hippocampus and parahippocampus.

ROIs (because this effect occurred in two time windows: 1 – 2 s and 1.5 – 2.5 s) in the left hippocampus and parahippocampus[2], which showed hidden platform encoding effect during navigation in theta frequency band in chapter three. The cluster mean of high-gamma power (pseudo-Z values) during ITI from the above ROIs was extracted from each condition and training sets. Then we compared the cluster mean of rest high-gamma in the right hippocampal ROI in *post hidden platform* and *post random swimming* condition in the first training set with those in the second training set using paired t test using IBM SPSS (version 23) to see whether right hippocampal rest high-gamma was significantly larger in the first training set relative to the second one, as shown in right hippocampal theta during navigation. We also compared the cluster mean of rest high-gamma in the two left hippocampal ROIs in *post hidden platform* condition with that in *post random swimming* condition in each training set using paired t test to find out whether left hippocampal rest high-gamma in the *post hidden platform* condition was significantly larger than that in *post random swimming* condition as seen in left hippocampal theta during navigation.

To address the concern that the effect seen in the above ROIs was due to signal leakage from cortical regions, we performed a 2 (condition: post hidden platform vs. post random swimming) × 2 (training set: 1^{st} vs. 2^{nd}) within-subject ANOVA analysis for each voxel across the whole brain to see whether the source image was focal with the local maximum being in the hippocampus. False positives were controlled by

[2] I referred the ROI in the left hippocampus and parahippocampus as left hippocampal ROI.

using small volume FDR correction method in a mask containing bilateral hippocampi and parahippocampi with the threshold of $p < 0.05$ (corrected).

Sliding window analyses. Previous animal studies have reported that high frequency oscillations (HFOs) are transient phenomena (Ego-Stengel & Wilson, 2010; Girardeau et al., 2009; Logothetis et al., 2012; Siapas & Wilson, 1998). To find out which analysis time window showed the most dominant effects, beamformer analyses were performed using a sliding window method, i.e., a sliding window of 2 s were advanced in 0.5s steps from -4.5 – 0 s. A length of 2 s was chosen for the sliding window, because we need to balance the accuracy of beamformer analyses (Brookes et al., 2008) and the sensitivity of detection. Thus, the covariance matrix of each sliding window was 20 trials * 2s/trial = 40s and 19 trials * 2s/trial = 38s for *post hidden platform* and *post random swimming* condition respectively. This step resulted in six volumetric beamformer images. Those images were normalized to a standard Talairach space as in the analyses for the whole time window. A 2 (condition: post hidden platform vs. post random swimming) × 2 (training set: 1st vs. 2nd) within-subject ANOVA was performed on each of these images with small volume FDR correction in the mask as used in the primary analyses to control multiple comparisons problems. From the technical point of view, sliding window analyses can also test whether the results from the whole-time window can be replicated.

Time frequency plots. The time frequency representations (TFRs) were constructed for the peak voxel of the hippocampal region showing significant main effect revealed by ANOVA analyses for the whole time window. To accomplish this, a five-cycle wavelet was convolved with the beamformed source activity over a frequency range of 30 – 200 Hz in 1 Hz steps from -4.5 – 0 s using the formula of

$$w(t, f_0) = A \exp(-t^2/2\sigma_t^2) \exp(2i\pi f_0 t).$$

Wavelets were normalized so that the total energy was 1, with the normalization factor A being equal to:

$$(\sigma_t \sqrt{\pi})^{-1/2}.$$

The final TFRs were presented as the power change in one condition/training set relative to another.

Post-hoc analyses

Low-gamma activities during offline rest period. To explore whether the effects seen during inter-trial period can also be seen in low-gamma band (30 – 80 Hz), we performed beamformer analyses for 30 – 80 Hz. Group analyses with the same significance threshold were performed as for the frequency band of 80 – 140 Hz.

High-gamma activities during navigation. To explore whether a similar effect during inter-trial period could also be seen during active navigation, MEG data were

epoched into 0 – 4 s (0 s was the trial onset, 4 s was the fastest time from the starting point to the hidden platform among all trials and participants) for each condition (hidden platform and random swimming condition). Beamformer images were computed for the frequency range of 80 – 140 Hz for this period. Then, the standardized beamformer images were analysed with a 2 (condition: hidden platform vs. random swimming) × 2 (training set: 1st vs. 2nd) within-subject ANOVA to see whether there was a similar effect as seen during inter-trial period. The same significance threshold was employed as used for the analyses of high-gamma band during inter-trial rest period.

To further explore whether there was an increase in high-gamma power during inter-trial rest period compared with navigation period as reported in rodent study (Buzsaki, 2015), for the ROI which showed significant 'replay' effect in the inter-trial rest period, we extracted the cluster mean of high-gamma power during navigation period from this ROI. We then performed a paired t-test to compare high-gamma power between offline rest period and navigation period.

Correlational analyses

High-gamma activities during rest versus subsequent navigation performance. To test the hypothesis that environment replay-related right hippocampal high-gamma power in the new environment should predict subsequent navigation performance in

the familiar environment, the right hippocampal high-gamma power increase in the *post hidden platform* condition relative to navigation period in *hidden platform* condition in the new environment (the first training set) was correlated with path lengths and learning rate in the hidden platform in the familiar environment (the second training set) using Pearson correlation analyses implemented in IBM SPSS (version 23) respectively. We did not correlate left hippocampal high-gamma power with navigation performance because in chapter three, only environment encoding-related right hippocampal theta showed a correlation with navigation performance. For exploratory purposes, if left hippocampus exhibited replay effect, we would also correlate left hippocampal high-gamma power with path lengths and learning rate in *hidden platform* condition.

High-gamma activities during rest versus theta during navigation. To address the third research question, i.e., whether higher replay related-hippocampal high-gamma power during inter-trial rest period corresponded to higher encoding related-hippocampal theta power during navigation, for the hippocampal ROI which showed a significant replay effect, the power change of high-gamma (difference in pseudo-Z values) in the ROI in *post hidden platform* and *post random swimming* condition during inter-trial rest period relative to that in *hidden platform* and *random swimming* condition during navigation was correlated with power change of theta (pseudo-F value as calculated in chapter three) in the same ROI in *hidden platform* condition and *random swimming* condition relative to pre-trial baseline in the

corresponding time window (the time window showing significant encoding effect) respectively. However, considering that the value of the power change used for correlation analyses above contained both baseline power and power of interest, if there was no significant correlation, it might not necessarily mean there was no correlation between the 'pure' power of the two frequency bands in each time period. Then we correlated the pure power of high-gamma (pseudo-Z values) in the ROI in the inter-trial rest period with the pure power of theta (pseudo-Z values) in the same ROI during navigation in the time window showing significant encoding effect in chapter three. The method of computing pseudo-Z images for theta during navigation was the same as used for computing pseudo-Z images for offline high-gamma. Since the time window showing significant encoding effect was only 1s long, the data used for computing pseudo-Z image for theta was only 20 trials * 1s/trial = 20s for both hidden platform and random swimming condition respectively. The signal-to-noise ratio might be low. If there was a significant correlation, to confirm that the correlation was not due to noise or leakage from cortical surface, cluster mean of offline high-gamma in the ROI was correlated voxel-wise with pseudo-Z image across the whole brain to make sure the correlation effect was not spanning everywhere and constrained in the region of interest. The significance threshold was set as $p < 0.005$ (uncorrected).

Results

High-gamma during rest. High-gamma power in the right hippocampal region in the inter-trial rest period in training set one was significantly larger than that in training set two ($t(17) = 2.257$, $p = 0.02$ for *post hidden platform* condition and $t(17) = 2.153$, $p = 0.046$ for *post random swimming* condition; Fig. 2A). However, no significant difference was found between offline high-gamma power in the left hippocampal ROI regions following hidden platform trials and that following random swimming trials. These results were confirmed by a whole brain 2 (conditions: post hidden platform vs. post random swimming) × 2 (training sets: first vs. second) repeated measures ANOVA analysis, which revealed a significant main effect of training set ($p < 0.05$, FDR corrected, peak voxel in right hippocampus, Talairach coordinates: x = 18 y = -5 z = -8) (Fig. 2C), with the power of hippocampal high-gamma in the first training set being significantly larger than that in the second one. No significant main effect of condition and no significant interaction between condition and training set were found in bilateral hippocampi. These results showed environmental learning-related right hippocampus accompanied by high-gamma band during inter-trial period exhibited the same power change of theta activities during navigation.

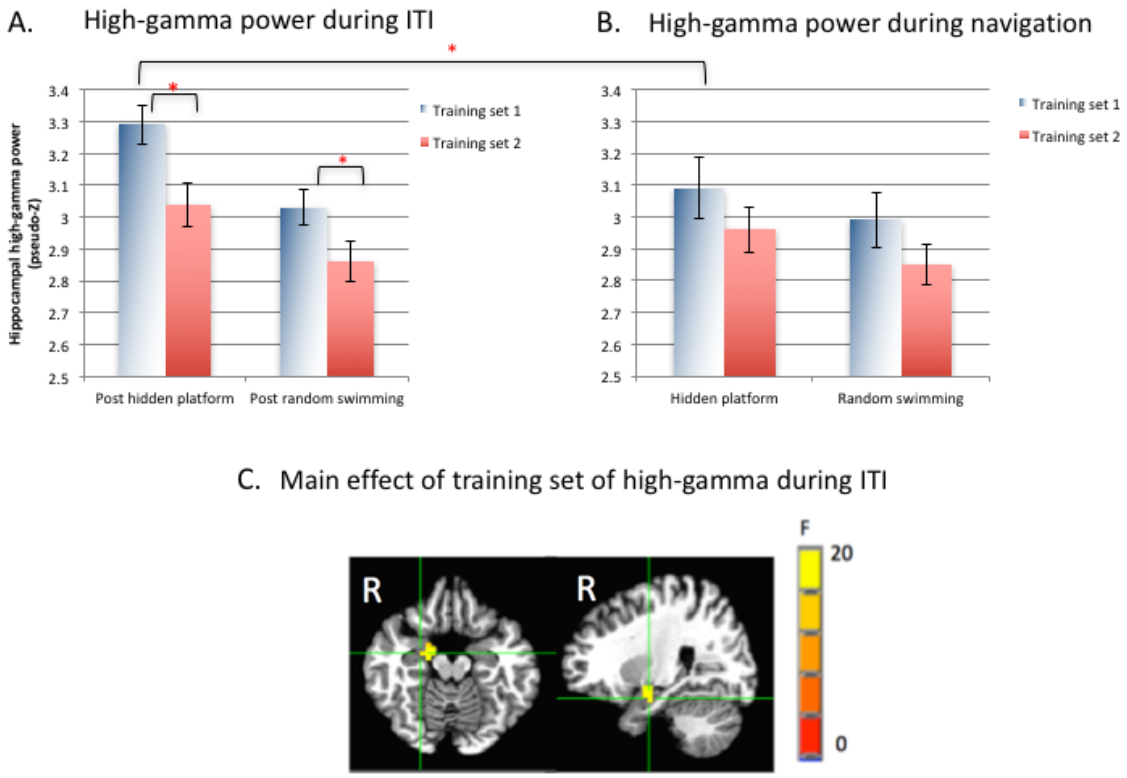

Figure 2. A. Cluster mean of high-gamma power (pseudo-Z values) during inter-trial rest period (ITI) (-4.5 – 0 s) in the encoding-related right hippocampal region (right hippocampal ROI) in the first and second training set for both *post hidden platform* condition and *post random swimming* condition. In both conditions, right hippocampal high-gamma power during rest in the first training set was significantly higher than that in the second training set. **B.** Cluster mean of high-gamma power (pseudo-Z values) during navigation period (0 – 4s) in the right hippocampal ROI in the first and second training set for both *hidden platform* and *random swimming* condition. For both conditions, no significant difference was found between right hippocampal high-gamma power in the first vs. second training set during this period. Paired t test showed right hippocampal high-gamma power in the *post hidden platform* condition during rest in the first training set was significantly higher than that in *hidden platform* condition during navigation in the first training set. **C.** Whole brain images of

main effect of training set during rest. The peak voxel is in the right hippocampus (peak voxel: Talairach coordinates x = 18 y = -5 z = -8).

Error bar represents standard errors. * represents $p < 0.05$.

Sliding window analyses showed similar results as in the primary analysis above. In the time window of -2.5 – -0.5 s and -4.5 – -2.5 s, there was a significant main effect of training set in the right hippocampus ($p< 0.05$, FDR corrected. We did not show images here because they were similar to Fig. 2C). TFRs (Fig. 3) also confirmed that there were more high-gamma increase during inter-trial period following exposure to new environment than following familiar one. Visual inspection revealed that the strongest high-gamma increase occurred in the time window of -2.5 – -0.5 s.

Other brain regions showing significant main effect of training set were left thalamus (peak: Talairach coordinates x= -2, y= -17, z= 0), left superior parietal lobule (peak: Talairach coordinates x= -18, y= -53, z= 44) and left posterior cingulate gyrus (peak: Talairach coordinates x= -2, y= -41, z= 28).

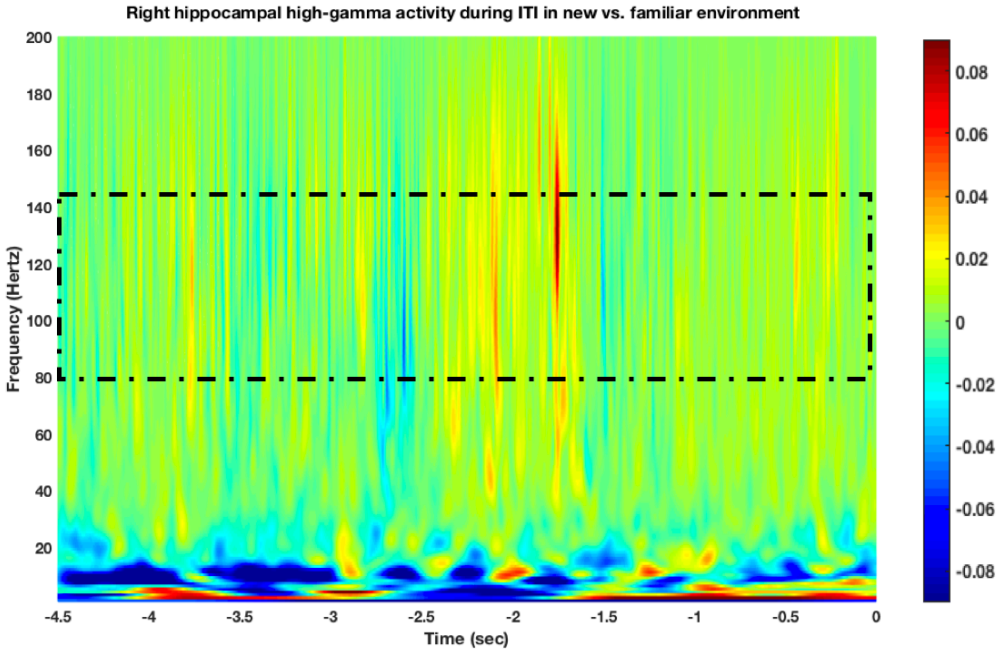

Figure 3. The time frequency representations of the peak voxel in the right hippocampus. This plot depicts the power change in first training set relative to the second one during inter-trial rest period of -4.5 – 0 s. The black rectangular shows more high-gamma (80 – 140 Hz) bursts during inter-trial rest period in the first relative to the second training set as revealed by SAM beamformer analysis. The TFRs show that the duration of high-gamma power increase is brief and is around 100ms, in line with the duration of animal ripples.

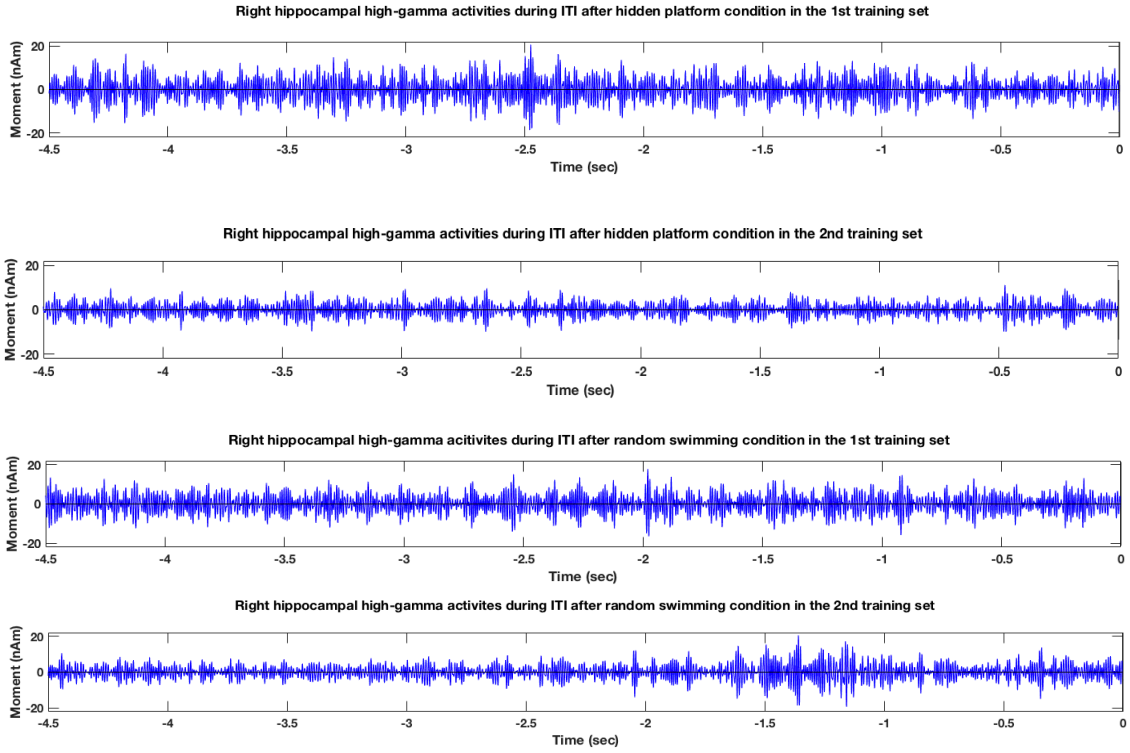

Figure 4. Band-pass filtered (80 – 140 Hz) virtual sensor activities of the peak voxel of the right hippocampus for one individual participant during ITI in each training set and condition.

Post-hoc analysis results

Low-gamma activities during rest. No significant results were found for low-gamma band of 30 – 80 Hz, supporting the specificity of the effects to the high-gamma range.

High-gamma activities during navigation. No significant results were found for high-gamma during navigation, which may suggest that when theta was the most dominant LFP, there was no significant effect for high-gamma rhythm during

navigation (Fig. 2B). Direct comparison of high-gamma power during inter-trial rest period and that during navigation in the right hippocampal ROI showed that high-gamma power in the *post hidden platform* condition during rest in the first training set was significant higher ($t= 3.072$, $p= 0.007$, Fig. 2A & 2B) than that during navigation in the *hidden platform* condition. No significant difference was found for the second training set, indicating that replay effect was most apparent following navigating in the new environment.

No significant difference was found between high-gamma power in the *post random swimming* condition and that during navigation in the *random swimming* condition in both training sets, which might suggest although in *post random swimming* condition, right hippocampal high-gamma power showed the same pattern of right hippocampal theta power during navigation, the replay effect in inter-trial period following navigation with low learning demands was not as salient as that following navigating with high learning demands (Eschenko & Sara, 2008; Girardeau et al., 2014). This was confirmed by the result of direct comparison between the high-gamma power difference between post hidden platform and hidden platform condition (Diff_H) in the first training set and the high-gamma power difference between *post random swimming* and *random swimming* condition (Diff_R) in the first training training set, which showed the Diff_H in the first training set was significantly larger than Diff_R in the first training set ($t(17) = 2.264$, $p= 0.037$). No significant difference was found between Diff_H and Diff_R in the second training

set.

Correlation Results

Right hippocampal high-gamma during rest vs. navigation performance. Consistent with our hypothesis, there was a significant correlation between the power increase of high-gamma in the inter-trial rest period in *post hidden platform* condition relative to that during navigation in *hidden platform* condition in the right hippocampal ROI in the first training set with learning rate in the second training set ($r= 0.601$, $p= 0.004$, one-tailed Fig. 5). No correlation was found between high-gamma power increase in the first training set with path length in the second training set. This might mean high-gamma is more sensitive to learning rate compared to path lengths as shown in Cornwell et al. (2014). The significant correlation indicates navigator who shows higher high-gamma power will learn the hidden platform location more quickly in the familiar environment as indicated by larger learning rate.

To exclude the possibility that the correlation only reflected the general relationship between high-gamma power and behavioral performance across subjects, we also correlated learning rate in the second training set with the right hippocampal high-gamma power change in the inter-trial rest period in *post hidden platform* condition relative to that in *hidden platform* condition in the ROI in the second

training set, when consolidation requirement decreased indexed by decreased high-gamma power as shown in above analyses and improved navigation performance in the second training set as shown in chapter three. No significant correlation was found, confirming that the correlation between replay-related high-gamma power and subsequent learning performance is functional relevant.

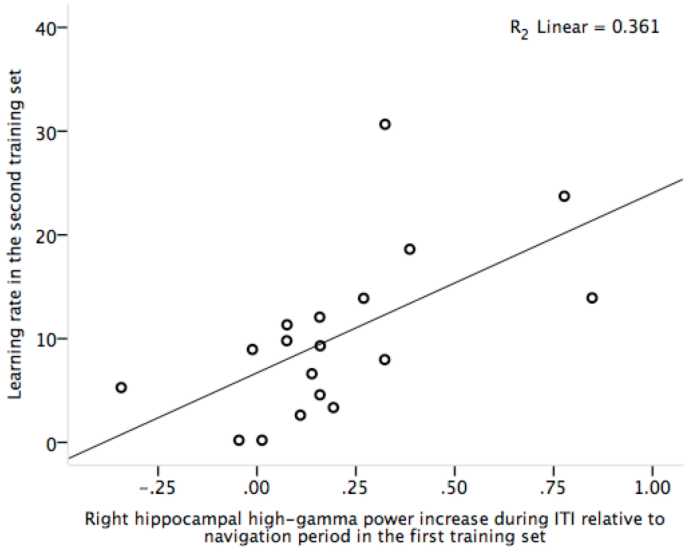

Figure 5. Right high-gamma power increase in the *post hidden platform* condition during rest relative to that in the *hidden platform* condition during navigation in the first training set in the right hippocampal ROI (x-axis) of each participant plotted against his learning rate during navigating in the second training set (y-axis).

ITI: inter-trial-interval

Right hippocampal high-gamma during rest vs. right hippocampal theta during navigation. No significant correlation was found between the power change

(difference in pseudo-Z values) of high-gamma in *post hidden platform* condition relative to that in *hidden platform* condition in the right hippocampal ROI in the first training set with the power change of theta (pseudo-F values computed in Pu et al. (2017) in *hidden platform* condition relative to pre-trial baseline in the first training set when the environment was new and the learning requirement was maximum. Since power change contains power information of both baseline period and the period of interest, we then investigated whether there was a significant correlation between the 'pure' power in the two periods of interest. To do so, we correlated the cluster mean (pseudo-Z values) of high-gamma in the right hippocampal ROI in inter-trial rest period of -4.5 – 0 s in *post hidden platform* condition in the first training set and the cluster mean (pseudo-Z values) of theta power in the same right hippocampal ROI in the hidden platform condition in the time window of 1.25 – 2.25s (this time window showed significant environmental encoding effect in chapter three) during navigation.

We found a significant correlation ($r = 0.406$, $p = 0.046$, one tailed). We also correlated high-gamma power in the time window (-2.5 – -0.5s), which showed the strongest high-gamma increase with theta power in 1.25 – 2.25s. As expected, the correlation was significant and even stronger ($r = 0.53$, $p = 0.017$, one-tailed, Fig. 6A). Voxel wise correlation analysis confirmed that the significant effect was focal with the local maximum in the right hippocampus (Fig. 6B). These correlations support the conclusion that spontaneous high-gamma power in the inter-trial rest period was

proportional to previous learning indicated by the strength of right hippocampal theta. No significant correlation was found between offline high-gamma power in the second training set and online theta power in the second training set, when learning requirement decreased, suggesting the significant correlation seen above is learning dependent.

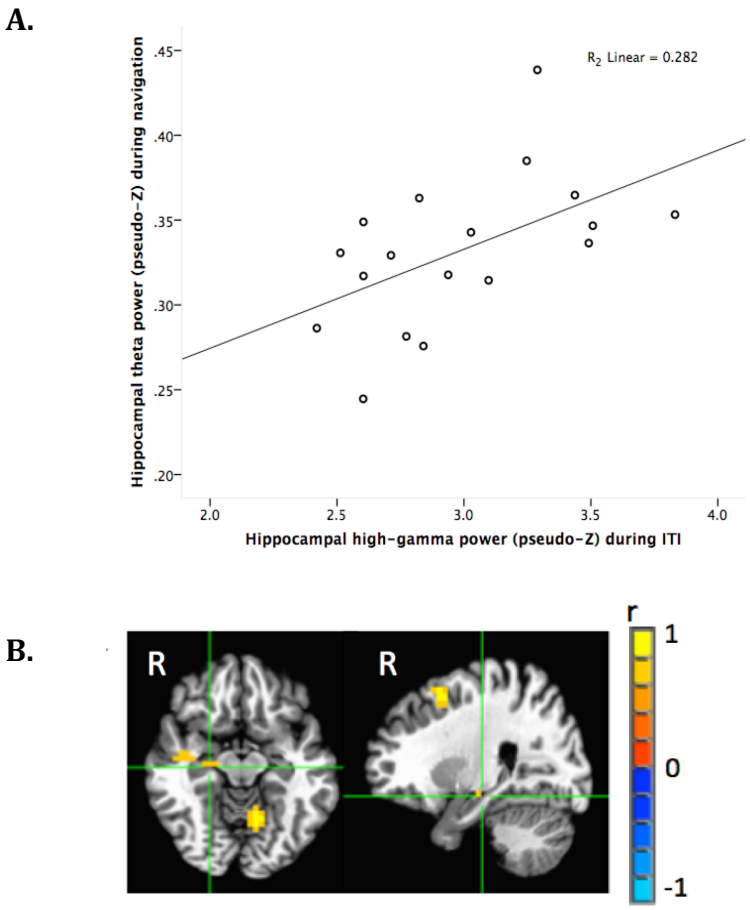

Figure 6. A. Cluster mean of high-gamma power (pseudo-Z values) in the right hippocampal ROI during inter-trial rest period (ITI) of -2.5 – -0.5s (the time window showed the strongest high-gamma effect in the time frequency representations in Fig. 3), plotted against cluster mean of theta power (pseudo-Z values) in the same region during navigation in the time window of 1.25 – 2.25s when there was an environmental encoding effect as shown in

chapter three. **B.** Whole brain images of correlation between cluster mean of high-gamma power (pseudo-Z values) in the right hippocampal ROI in the time window of -2.5 – -0.5s and theta power (pseudo-Z values) in the time window of 1.25 – 2.25s in each voxel across the whole brain. Threshold is set at $p<0.005$ (uncorrected). The local maximum is at right hippocampus (peak voxel: Talairach coordinates x = 26, y = -17, z = -8).

ITI: Inter-trial interval

No significant correlation was found between high-gamma power during rest in *post random swimming* condition and theta power in *random swimming* condition. Voxel wise correlation did not yield significant correlation in any voxels in the bilateral hippocampi as well. These results might indicate although offline high-gamma power in inter-trial rest period in *post random swimming* condition showed the same pattern as theta during navigation in *random swimming* condition as a function of environmental novelty, the faithfulness of 'replay' following spatial navigation in simple environment with low encoding requirement and with low learning requirement is low, in line with findings from animal literature (Kentros et al., 2004) that faithful retrieval of a mouse's hippocampal representation of an environment increased as task demands increased.

Discussion

Using MEG, we found the right hippocampal high-gamma power after

navigation in the new environment was significantly stronger than that in the familiar one, which reflected the same power change pattern of encoding related right hippocampal theta oscillations during navigation as shown in chapter three. This result is in line with the prediction of two-stage model for memory formation (Buzsaki, 2015) and animal studies (Ambrose et al., 2016; Davidson et al., 2009; Dupret et al., 2010; Jackson et al., 2006; Jadhav et al., 2012; Karlsson & Frank, 2009; Singer & Frank, 2009, refer to Roumis & Frank, 2015 for a review) and suggests that human high frequency oscillations may play an important role in replay of recently learnt information accompanied by theta oscillation. Greater offline high-gamma power after exposure to the new environment than to the familiar one also suggests that replay strength is stronger after navigation in new environment, consistent with results from animal studies that relative to a familiar environment, neuronal replay in a new environment is stronger and more easily to be detected (Foster & Wilson, 2006; O'Neill et al., 2008) and high frequency LFP in a new environment is stronger (Cheng & Frank, 2008; Csicsvari et al., 2007).

Our data further showed the high-gamma related learning-dependent reaction effect did not occur during navigation period, when the theta rhythm was the most dominant LFP; high-gamma power after navigation in *post hidden platform* condition in the new environment was significantly larger than that during navigation in *hidden platform* condition in new environment, in line with idea that during offline states, high frequency oscillations is the most dominant LFP and replay often occurs when

animals were disengaged with external environment (Buzsaki, 2015). In the familiar environment, where the learning and consolidation requirement decreased, indexed by improved navigation performance as shown in chapter three, no high-gamma power increase was found during rest period relative to navigation period, suggesting that the high-gamma increase in the new environment is learning dependent (Cheng & Frank, 2008). Although rest high-gamma after *random swimming* trials showed a power change in the new vs. familiar environment, resting high-gamma increase following navigating in *hidden platform* trials relative to that during navigating in *hidden platform* trials in the new environment was significantly larger than resting high-gamma increase after navigating in *random swimming* trials relative to that during navigating in *random swimming* trials. This suggests that replay strengths are stronger after navigation in a more complex environment with higher learning requirements, which is in agreement with the finding that replay strengths vary as a function of task demands (Eschenko & Sara, 2008; Girardeau et al., 2014).

The present results complement previous studies (Cornwell et al., 2014; Axmacher et al., 2008) by showing that the same hippocampal region used for encoding exhibited replay effect accompanied by high-gamma oscillations during offline states, thus supporting the role of hippocampal high-gamma in replay of previously learned experience. These results also support previous fMRI studies (Deuker et al., 2013; Peigneux et al., 2006; Staresina et al., 2013; Tambini et al., 2010; Vincent et al., 2006), which showed experience-dependent reactivation during

wakefulness or sleep and provides a neurophysiological mechanism underlying the reactivation. The current results might also help explain why some studies have not found hippocampal reactivation during offline states after learning. Because the onset of hippocampal reactivation occurs immediately after each learning trial as shown in our data and decays over the course of high frequency oscillations (Colgin, 2016; Kudrimoti et al., 1999), during which information is being transferred to neocortex. Therefore, hippocampal reactivation might not be strong and salient after a whole block of learning. Further study could investigate how this issue of how persistent high-gamma hippocampal replay is.

High frequency oscillations measured using MEG are easily confounded by muscle artifacts. However, source localization algorithms based on spatial filters can differentiate cognitive processing source from cortical or subcortical areas with artifactual sources (Dalal et al., 2011). Several checks support our contention the high-gamma effects observed in the current study are not artefactual. First, the analyses were performed during the inter-trial period when participants were instructed to rest quietly and to minimize movement. Second, there was no significant high-gamma effect during active navigation epochs which are more likely to be contaminated by muscle artifacts because participants pressed buttons to move in the virtual pool. Third, the spatial map of the effect was focal and localized unilaterally to right hippocampus, and TFRs showed relatively narrow band power changes. Muscle artifact, in contrast, tends to span large spatial regions and broad frequency ranges

(from 30 to 200 Hz or higher; Muthukumaraswamy, 2013).

Consistent with our hypothesis that replay is proportional to encoding, our data showed that offline high-gamma power after navigating in the *hidden platform* condition in the new environment was positively associated with theta power during navigation in *hidden platform* condition in the new environment, when learning requirement was strongest. Together with the finding that the same hippocampal region used for encoding was reactivated during rest period, the correlation provides further evidence that high-gamma during rest is modulated by previous learning experience to accurately reinforce the newly formed labile memory traces (e.g., Davidson et al., 2009; Skaggs & McNaughton, 1996; Wilson & McNaughton, 1994). A comparable correlation was not found for familiar environments with decreased learning requirements, indicating that the correlation seen in new environment is learning induced, rather than an intrinsic relationship between gamma and theta power. The random swimming condition, where learning requirements were low, showed no significant correlation between theta and high-gamma in both training sets, suggesting although replay is automatic, the degree of replay faithfulness may vary as a function of encoding requirement. This is corroborated by the findings of a rodent study (Kentros et al., 2004), showing that the faithful retrieval of a mouse's hippocampal representation of an environment increases as task demands increase and place cell stability tightly covaries with attention to the available spatial cues.

Further, we observed that right hippocampal high-gamma power increase in *post hidden platform* condition in the first training set relative to that during navigation in hidden platform condition in the first training set correlated with learning rate in the *hidden platform* condition in the second training set in the same environment. This correlation bolsters the argument that the functional role of right hippocampal high-gamma replay is memory consolidation. As indexed by higher gamma power, navigators with stronger memory consolidation of the environment during the offline state after new environment learning learned more quickly in the second training set where the environment was the same, even though the hidden platform location changed. Good consolidation of the environment to form a cognitive map can facilitate flexible navigation to any place in the same environment (Wolbers & Hegarty, 2010). This correlation is also consistent with observations from human fMRI studies showing that reactivation strength of the hippocampus predicts subsequent memory performance (Bergmann et al., 2012; Peigneux et al., 2006). The direction of the correlation is consistent with the results of Axmacher et al., 2008; Cornwell et al., 2014), showing that stronger high-gamma power corresponded to better memory performance. No correlation was found between high-gamma power during rest in the second training set (where consolidation requirement decreased) with learning rate in this training set, indicating the significant correlation seen above is learning specific.

It is noteworthy that the effects described in the current study were confined to

right hippocampus. In contrast, in our previous findings, navigation related theta effects were found in both left hippocampus (implicated in binding the external cues to the platform location) and right hippocampus (associated with encoding the environment to form the cognitive map of the space). While non-significant results do not confirm the null hypothesis, this is consistent with the notion that replay is selective, such that not every aspect of learning would be replayed (Deuker et al., 2013). However, the mechanism underlying this replay selection is still unclear. Reactivation during awake rest and sleep is more complicated than expected (Buzsaki, 2015). Recent studies (Gupta et al., 2010; Wu & Foster, 2014) have pointed out that the function of replay is not just consolidating previous experience but also helping to construct a Tolmanian cognitive map of the environment, which would result in flexible routes to the goal location on subsequent trials. Thus, the replay might not necessarily be location dependent (O'Neill et al., 2006). This might help explain why only the right hippocampus region was reactivated in our data. Moreover, this work might provide some insights into the reason why right hippocampus is believed to be important in spatial cognition in general (Cornwell et al., 2010; Jacobs et al., 2009; Maguire et al., 1998; Nedelska et al., 2012). More research is needed in the future to investigate the selective nature of hippocampal replay.

In sum, using a highly translational experimental task, we show as reported in animal studies, in the rest periods immediately following each spatial learning trial, human hippocampal high-gamma activity is evident and mirrors the power change

pattern of theta rhythms during encoding; high gamma power is proportional to theta magnitude and is predictive of subsequent performance. These findings link human data with animal models and advance our understanding of the neurophysiological mechanisms of human hippocampal replay in memory consolidation.

Acknowledgements: This work was supported by Australian Research Council Grants CE110001021, DP1096160. The author was financially supported by the China Scholarship Council and Macquarie University. We thank Dr. Suresh Muthukumaraswamy for helpful discussions about muscle artifacts and gamma activity.

References

Ambrose, R. E., Pfeiffer, B. E., & Foster, D. J. (2016). Reverse Replay of Hippocampal Place Cells Is Uniquely Modulated by Changing Reward. *Neuron, 91*(5), 1124-1136. doi:10.1016/j.neuron.2016.07.047

Attal, Y., Bhattacharjee, M., Yelnik, J., Cottereau, B., Lefevre, J., Okada, Y., . . . Baillet, S. (2007). Modeling and Detecting Deep Brain Activity with MEG & EEG. *Conf Proc IEEE Eng Med Biol Soc*, 4937-4940.

Axmacher, N., Elger, C. E., & Fell, J. (2008). Ripples in the medial temporal lobe are relevant for human memory consolidation. *Brain, 131*(Pt 7), 1806-1817. doi:10.1093/brain/awn103

Backus, A. R., Schoffelen, J. M., Szebenyi, S., Hanslmayr, S., & Doeller, C. F. (2016). Hippocampal-Prefrontal Theta Oscillations Support Memory Integration. *Curr Biol, 26*(4), 450-457. doi:10.1016/j.cub.2015.12.048

Bergmann, T. O., Molle, M., Diedrichs, J., Born, J., & Siebner, H. R. (2012). Sleep spindle-related reactivation of category-specific cortical regions after learning face-scene associations. *Neuroimage, 59*(3), 2733-2742. doi:10.1016/j.neuroimage.2011.10.036

Brookes, M. J., Vrba, J., Robinson, S. E., Stevenson, C. M., Peters, A. M., Barnes, G. R., . . . Morris, P. G. (2008). Optimising experimental design for MEG beamformer imaging. *Neuroimage, 39*(4), 1788-1802. doi:10.1016/j.neuroimage.2007.09.050

Buzsaki, G. (1989). Two-stage model of memory trace formation: a role for "noisy"

brain states *Neuroscience, 31*(3), 551-570.

Buzsaki, G. (2015). Hippocampal sharp wave-ripple: A cognitive biomarker for episodic memory and planning. *Hippocampus, 25*(10), 1073-1188. doi:10.1002/hipo.22488

Carr, M. F., Jadhav, S. P., & Frank, L. M. (2011). Hippocampal replay in the awake state: a potential substrate for memory consolidation and retrieval. *Nat Neurosci, 14*(2), 147-153. doi:10.1038/nn.2732

Cheng, S., & Frank, L. M. (2008). New experiences enhance coordinated neural activity in the hippocampus. *Neuron, 57*(2), 303-313. doi:10.1016/j.neuron.2007.11.035

Cheyne, D., Bells, S., Ferrari, P., Gaetz, W., & Bostan, A. C. (2008). Self-paced movements induce high-frequency gamma oscillations in primary motor cortex. *Neuroimage, 42*(1), 332-342. doi:10.1016/j.neuroimage.2008.04.178

Cheyne, D., & Ferrari, P. (2013). MEG studies of motor cortex gamma oscillations: evidence for a gamma "fingerprint" in the brain? *Front Hum Neurosci, 7*, 575. doi:10.3389/fnhum.2013.00575

Chupin, M., Baillet, S., Okada, Y. C., Hasboun, D., & Garnero, L. (2002). *On the detection of hippocampus activity with MEG*. Paper presented at the 13th International Conference on Biomagnetism, Germany.

Colgin, L. L. (2016). Rhythms of the hippocampal network. *Nat Rev Neurosci, 17*(4), 239-249. doi:10.1038/nrn.2016.21

Cornwell, B. R., Arkin, N., Overstreet, C., Carver, F. W., & Grillon, C. (2012).

Distinct contributions of human hippocampal theta to spatial cognition and anxiety. *Hippocampus, 22*(9), 1848-1859. doi:10.1002/hipo.22019

Cornwell, B. R., Johnson, L. L., Holroyd, T., Carver, F. W., & Grillon, C. (2008). Human hippocampal and parahippocampal theta during goal-directed spatial navigation predicts performance on a virtual Morris water maze. *J Neurosci, 28*(23), 5983-5990. doi:10.1523/JNEUROSCI.5001-07.2008

Cornwell, B. R., Overstreet, C., & Grillon, C. (2014). Spontaneous fast gamma activity in the septal hippocampal region correlates with spatial learning in humans. *Behav Brain Res, 261*, 258-264. doi:10.1016/j.bbr.2013.12.031

Cornwell, B. R., Salvadore, G., Colon-Rosario, V., Latov, D. R., Holroyd, T., Carver, F. W., . . . Grillon, C. (2010). Abnormal hippocampal functioning and impaired spatial navigation in depressed individuals: evidence from whole-head magnetoencephalography. *Am J Psychiatry, 167*(7), 836-844. doi:10.1176/appi.ajp.2009.09050614

Cox, R. W. (1996). AFNI: software for analysis and visualization of functional magnetic resonance neuroimages. *Comput Biomed Res, 29*, 162-173. doi:10.1006/cbmr.1996.0014

Crespo-Garcia, M., Zeiller, M., Leupold, C., Kreiselmeyer, G., Rampp, S., Hamer, H. M., & Dalal, S. S. (2016). Slow-theta power decreases during item-place encoding predict spatial accuracy of subsequent context recall. *Neuroimage, 142*, 533-543. doi:10.1016/j.neuroimage.2016.08.021

Csicsvari, J., O'Neill, J., Allen, K., & Senior, T. (2007). Place-selective firing

contributes to the reverse-order reactivation of CA1 pyramidal cells during sharp waves in open-field exploration. *Eur J Neurosci, 26*(3), 704-716. doi:10.1111/j.1460-9568.2007.05684.x

Dalal, S., Vidal, J. R., Hamame, C. M., Ossamdpm, T., Betrand, O., Lachaux, J. P., & Jerbi, K. (2011). Spanning the rieh spectrum of the human brain: slow waves to gamma and beyond. *Brain Struct Funct, 216*, 77-84. doi:10.1007/s00429-011-0307-z

Davidson, T. J., Kloosterman, F., & Wilson, M. A. (2009). Hippocampal replay of extended experience. *Neuron, 63*(4), 497-507. doi:10.1016/j.neuron.2009.07.027

Deuker, L., Olligs, J., Fell, J., Kranz, T. A., Mormann, F., Montag, C., . . . Axmacher, N. (2013). Memory consolidation by replay of stimulus-specific neural activity. *J Neurosci, 33*(49), 19373-19383. doi:10.1523/JNEUROSCI.0414-13.2013

Diba, K., & Buzsaki, G. (2007). Forward and reverse hippocampal place-cell sequences during ripples. *Nat Neurosci, 10*(10), 1241-1242. doi:10.1038/nn1961

Dupret, D., O'Neill, J., Pleydell-Bouverie, B., & Csicsvari, J. (2010). The reorganization and reactivation of hippocampal maps predict spatial memory performance. *Nat Neurosci, 13*(8), 995-1002. doi:10.1038/nn.2599

Ego-Stengel, V., & Wilson, M. A. (2010). Disruption of ripple-associated hippocampal activity during rest impairs spatial learning in the rat.

Hippocampus, 20(1), 1-10. doi:10.1002/hipo.20707

Eschenko, O., & Sara, S. J. (2008). Learning-dependent, transient increase of activity in noradrenergic neurons of locus coeruleus during slow wave sleep in the rat: brain stem-cortex interplay for memory consolidation? *Cereb Cortex, 18*(11), 2596-2603. doi:10.1093/cercor/bhn020

Foster, D. J., & Wilson, M. A. (2006). Reverse replay of behavioural sequences in hippocampal place cells during the awake state. *Nature, 440*(7084), 680-683. doi:10.1038/nature04587

Gerrard, J. L., Burke, S. N., McNaughton, B. L., & Barnes, C. A. (2008). Sequence reactivation in the hippocampus is impaired in aged rats. *J Neurosci, 28*(31), 7883-7890. doi:10.1523/JNEUROSCI.1265-08.2008

Girardeau, G., Benchenane, K., Wiener, S. I., Buzsaki, G., & Zugaro, M. B. (2009). Selective suppression of hippocampal ripples impairs spatial memory. *Nat Neurosci, 12*(10), 1222-1223. doi:10.1038/nn.2384

Girardeau, G., Cei, A., & Zugaro, M. (2014). Learning-induced plasticity regulates hippocampal sharp wave-ripple drive. *J Neurosci, 34*(15), 5176-5183. doi:10.1523/JNEUROSCI.4288-13.2014

Gupta, A. S., van der Meer, M. A., Touretzky, D. S., & Redish, A. D. (2010). Hippocampal replay is not a simple function of experience. *Neuron, 65*(5), 695-705. doi:10.1016/j.neuron.2010.01.034

Hillebrand, A., Singh, K. D., Holliday, I. E., Furlong, P. L., & Barnes, G. R. (2005). A new approach to neuroimaging with magnetoencephalography. *Hum Brain*

Mapp, 25(2), 199-211. doi:10.1002/hbm.20102

Hopper, A. N., Jamison, M. H., & Lewis, W. G. (2007). Learning curves in surgical practice. *Postgrad Med J, 83*(986), 777-779. doi:10.1136/pgmj.2007.057190

Isabella, S., Ferrari, P., Jobst, C., Cheyne, J. A., & Cheyne, D. (2015). Complementary roles of cortical oscillations in automatic and controlled processing during rapid serial tasks. *Neuroimage, 118*, 268-281. doi:10.1016/j.neuroimage.2015.05.081

Jackson, J. C., Johnson, A., & Redish, A. D. (2006). Hippocampal sharp waves and reactivation during awake states depend on repeated sequential experience. *J Neurosci, 26*(48), 12415-12426. doi:10.1523/JNEUROSCI.4118-06.2006

Jacobs, J., Lorolev, I. O., Caplan, J. B., Ekstrom, A., Litt, B., Baltuch, G., . . . Kahana, M. J. (2009). Right-lateralized brain oscillations in human spatial navigation. *J Cogn Neurosci, 22*(5), 824-836. doi:10.1162/jocn.2009.21240

Jadhav, S. P., Kemere, C., German, P. W., & Frank, L. M. (2012). Awake hippocampal sharp-wave ripples support spatial memory. *Science, 336*(6087), 1454-1458. doi:10.1126/science.1217230

Kado, H., Higuchi, M., Shimogawara, M., Haruta, Y., Adachi, Y., Kawai, J., & Uehara, G. (1999). Magnetoencephalogram systems developed at KIT. *IEEE Trans. Appl. Supercond, 9*, 4057-4062. doi:doi:10.1109/77.783918

Karlsson, M. P., & Frank, L. M. (2009). Awake replay of remote experiences in the hippocampus. *Nat Neurosci, 12*(7), 913-918. doi:10.1038/nn.2344

Kentros, C. G., Agnihotri, N. T., Streater, S., Hawkins, R. D., & Kandel, E. R. (2004).

Increased attention to spatial context increases both place field stability and spatial memory. *Neuron, 42*, 283-295. doi:10.1016/S0896-6273(04)00192-8

Kudrimoti, H. S., Barnes, C. A., & McNaughton, B. L. (1999). Reactivation of hippocampal cell assemblies: effects of behavioral state, experience, and EEG dynamics. *J Neurosci, 19*(10), 4090-4101.

Lalancette, M., Quraan, M., & Cheyne, D. (2011). Evaluation of multiple-sphere head models for MEG source localization. *Phys Med Biol, 56*(17), 5621-5635. doi:10.1088/0031-9155/56/17/010

Logothetis, N. K., Eschenko, O., Murayama, Y., Augath, M., Steudel, T., Evrard, H. C., . . . Oeltermann, A. (2012). Hippocampal-cortical interaction during periods of subcortical silence. *Nature, 491*(7425), 547-553. doi:10.1038/nature11618

Maguire, E. A., Burgess, N., Donnett, J. G., Frackowiak, R. S. J., Frith, C. D., & O'Keefe, J. (1998). Knowing where and geeting there: a huma navigation network. *Science, 280*, 921-924.

Meyer, S. S., Rossiter, H., Brookes, M. J., Woolrich, M. W., Bestmann, S., & Barnes, G. R. (2017). Using generative models to make probabilistic statements about hippocampal engagement in MEG. *Neuroimage*. doi:10.1016/j.neuroimage.2017.01.029

Muthukumaraswamy, S. D. (2013). High-frequency brain activity and muscle artifacts in MEG/EEG: a review and recommendations. *Front Hum Neurosci, 7*, 138. doi:10.3389/fnhum.2013.00138

Nedelska, Z., Andel, R., Laczo, J., Vlcek, K., Horinek, D., Lisy, J., . . . Hort, J. (2012). Spatial navigation impairment is proportional to right hippocampal volume. *Proc Natl Acad Sci U S A, 109*(7), 2590-2594. doi:10.1073/pnas.1121588109

O'Neill, J., Pleydell-Bouverie, B., Dupret, D., & Csicsvari, J. (2010). Play it again: reactivation of waking experience and memory. *Trends Neurosci, 33*(5), 220-229. doi:10.1016/j.tins.2010.01.006

O'Neill, J., Senior, T., & Csicsvari, J. (2006). Place-selective firing of CA1 pyramidal cells during sharp wave/ripple network patterns in exploratory behavior. *Neuron, 49*(1), 143-155. doi:10.1016/j.neuron.2005.10.037

O'Neill, J., Senior, T. J., Allen, K., Huxter, J. R., & Csicsvari, J. (2008). Reactivation of experience-dependent cell assembly patterns in the hippocampus. *Nat Neurosci, 11*(2), 209-215. doi:10.1038/nn2037

Peigneux, P., Orban, P., Balteau, E., Degueldre, C., Luxen, A., Laureys, S., & Maquet, P. (2006). Offline persistence of memory-related cerebral activity during active wakefulness. *PLoS Biol, 4*(4), e100. doi:10.1371/journal.pbio.0040100

Perry, G. (2015). The effects of cross-orientation masking on the visual gamma response in humans. *Eur J Neurosci, 41*(11), 1484-1495. doi:10.1111/ejn.12900

Pu, Y., Cornwell, B. R., Cheyne, D., & Johnson, B. W. (2017). The functional role of human right hippocampal/parahippocampal theta rhythm in environmental encoding during virtual spatial navigation. *Hum Brain Mapp, 38*(3), 1347-1361. doi:10.1002/hbm.23458

Quraan, M. A., Moses, S. N., Hung, Y., Mills, T., & Taylor, M. J. (2011). Detection and localization of hippocampal activity using beamformers with MEG: a detailed investigation using simulations and empirical data. *Hum Brain Mapp, 32*(5), 812-827. doi:10.1002/hbm.21068

Riggs, L., Moses, S. N., Bardouille, T., Herdman, A. T., Ross, B., & Ryan, J. D. (2009). A complementary analytic approach to examining medial temporal lobe sources using magnetoencephalography. *Neuroimage, 45*(2), 627-642. doi:10.1016/j.neuroimage.2008.11.018

Robinson, S. E., & Vrba, J. (1999). *Functional neuroimaging by synthetic aperture magnetometry (SAM)*

(T. Yoshimoto, M. Kotani, S. Kuriki, H. Karibe, & N. Nakasato Eds.). Sendai, Japan: Tohoku UP.

Roumis, D. K., & Frank, L. M. (2015). Hippocampal sharp-wave ripples in waking and sleeping states. *Curr Opin Neurobiol, 35*, 6-12. doi:10.1016/j.conb.2015.05.001

Sarvas, J. (1987). Basic mathmatical and electromagnetic concepts of the biomagnetic inverse problem. *Phys Med Biol, 32*, 11-22.

Siapas, A. G., & Wilson, M. A. (1998). Coordinated interactions between hippocampal ripples and cortical spindles during slow-wave sleep. *Neuron, 21*, 1123-1128.

Singer, A. C., & Frank, L. M. (2009). Rewarded outcomes enhance reactivation of experience in the hippocampus. *Neuron, 64*(6), 910-921.

doi:10.1016/j.neuron.2009.11.016

Skaggs, W. E., & McNaughton, B. L. (1996). Replay of neuronal firing sequences in rat hippocampus during sleep following spatial experience. *Science, 271*, 1870-1873.

Staresina, B. P., Alink, A., Kriegeskorte, N., & Henson, R. N. (2013). Awake reactivation predicts memory in humans. *Proc Natl Acad Sci U S A, 110*(52), 21159-21164. doi:10.1073/pnas.1311989110

Stephen, J. M., Ranken, D. M., Aine, C. J., Weisend, M. P., & Shih, J. J. (2005). Differentiability of simulated MEG hippocampal, medial temporal and neocortical temporal

epileptic spike activity. *J Clin Neurophysiol, 22*, 388-401. doi:10.1097/01.WNP.0000172141.26081.78

Sutherland, G. R., & McNaughton, B. L. (2000). Memory trace reactivation in hippocampal and neocortical neuronal ensembles. *Curr Opin Neurobiol, 10*, 180-186.

Tambini, A., Ketz, N., & Davachi, L. (2010). Enhanced brain correlations during rest are related to memory for recent experiences. *Neuron, 65*(2), 280-290. doi:10.1016/j.neuron.2010.01.001

Tesche, C. D., & Karhu, J. (2000). Theta oscillations index human hippocampal activation during a working memory task. *Proc Natl Acad Sci U S A, 97*(2), 919-924.

Uehara, G., Adachi, Y., Kawai, J., Shimogawara, M., Higuchi, M., Haruta, Y., &

Kado, H. (2003). Multi-channel SQUID systems for biomagnetic measurement. *IEICE Trans Electron, E86c*(43–54).

Vincent, J. L., Snyder, A. Z., Fox, M. D., Shannon, B. J., Andrews, J. R., Raichle, M. E., & Buckner, R. L. (2006). Coherent spontaneous activity identifies a hippocampal-parietal memory network. *J Neurophysiol, 96*(6), 3517-3531. doi:10.1152/jn.00048.2006

Vrba, J., & Robinson, S. E. (2001). Signal processing in magnetoencephalography. *Methods, 25*(2), 249-271. doi:10.1006/meth.2001.1238

Wilson, M. A., & McNaughton, B. L. (1994). Reactivation of hippocampal ensemble memories during sleep. *Science, 265*, 676-67.

Wolbers, T., & Hegarty, M. (2010). What determines our navigational abilities? *Trends Cogn Sci, 14*(3), 138-146. doi:10.1016/j.tics.2010.01.001

Wu, X., & Foster, D. J. (2014). Hippocampal replay captures the unique topological structure of a novel environment. *J Neurosci, 34*(19), 6459-6469. doi:10.1523/JNEUROSCI.3414-13.2014

Chapter five

Gender differences in navigation performance are associated with differential theta and high-gamma activities in the hippocampus

Abstract

Gender differences in spatial navigation are well-established, but the brain mechanisms responsible for these differences are unclear. Hippocampal theta (4 – 8 Hz) and high-gamma rhythms (80 – 140 Hz) are thought to play an important role in online encoding and offline consolidation respectively. This study examined whether gender differences in navigation performance are associated with differences in these two rhythms. We measured brain activity with whole-head magnetoencephalography (MEG) and analysed theta activity in males and females during navigation in a virtual Morris water maze, and high-gamma activity during inter-trial rest periods. Behavioural results showed clear gender differences: males scored significantly higher on the Santa-Barbara-Sense-of-Direction Scale; and were significantly faster than females in the water maze task. Males, but not females, showed significantly improved performance in the familiar environment compared to the new environment in the water maze task. MEG results for the two groups showed comparable left hippocampal theta rhythm magnitudes during goal-oriented navigation processing. However, there were gender differences in right hippocampal activities in environmental learning processing. In the new environment, right hippocampal magnitudes were similar between the two groups, but in the familiar environment, males exhibited a significant decrease in right hippocampal theta power during navigation, while females showed no change. After navigating in the new environment during inter-trial rest periods, males showed significantly higher right hippocampal high-gamma power than females. These results suggest that hippocampal theta during navigation and high gamma activities during rest might be responsible for behavioral differences in navigation performance of males and females. The study provides evidence for the functional importance of human hippocampal rhythms during spatial learning.

Keywords: Gender difference, spatial navigation, hippocampus, theta rhythms, high-gamma rhythms

Introduction

Gender differences in spatial ability and performance are well-established both in animals and humans (e.g., Astur et al., 2004; Blokland et al., 2006; Jones et al., 2003; Newhouse et al., 2007). However, the brain mechanisms underlying gender differences in spatial ability are largely unknown (Wolbers & Hegarty, 2010). An obvious candidate is the hippocampal formation (HF), known to be crucially important for spatial navigation in animals and humans (Buzsaki & Moser, 2013; O'Keefe & Nadel, 1978). In rodents, navigation is associated with slow rhythmic theta oscillations, dominating the local field potential (LFP) of the HF (e.g., Buzsaki, 2002). Theta oscillations are thought to bring together and link cell assemblies into a temporal range where they can be modulated by synaptic plasticity (Buzsaki & Moser, 2013). During offline states, including rest and sleep, high frequency oscillations (HFOs) are the dominant LFP and cell assemblies activated during navigation are reactivated (Buzsaki & Lopes da Silva, 2012). HFOs are thought to be crucial in strengthening the synaptic changes brought about during navigation (i.e., consolidation) (Buzsaki, 1989, 2015). The current study aimed to investigate whether gender differences in behavioral performance are reflected in one or both of these hippocampal rhythms, which are associated with different stages of spatial learning (Buzsaki, 2015).

Behavioural studies have repeatedly demonstrated gender differences in spatial

ability and performance, with males showing an advantage over females in psychometric measures of ability and in spatial tasks (e.g., Astur et al., 1998; Hao et al., 2016; Hegarty et al., 2006; Moffat et al., 1998; Mueller et al., 2008; Ross et al., 2006; Wegman et al., 2014, see Maguire et al., 1999 for a review). However, neuroimaging studies of gender differences in spatial cognition are still lacking. Such studies have focused on differences in brain activity during active navigation, with mixed results. For instance, an fMRI study (Gron et al., 2000) found that males showed bilateral hippocampal activation during navigation, while females showed only right hippocampal activation. In contrast, another fMRI study (Blanch et al., 2004) reported no gender differences in brain activation during spatial navigation; notably, however, this study failed to find hippocampal activation in either gender. To our knowledge, no neuroimaging studies have investigated whether there are gender differences in brain activities during the offline period after spatial learning, when replay of newly learned information may support consolidation (Buzsaki, 2015; Carr et al., 2011).

In the present study, we measured the brain responses of a group of female participants using a whole-head magnetoencephalography (MEG) system when they were performing a virtual Morris water maze task (Morris, 1984). In our previous reports on male participants (chapters three and four), we have shown that they exhibited stronger left hippocampal theta power during active navigation relative to random swimming (i.e. encoding the hidden platform position); and more right

hippocampal theta power in the new relative to familiar environment (i.e. encoding the environment). During rest periods after each trial of spatial learning, right hippocampal high-gamma showed the same power change as right hippocampal theta during navigation (i.e. replaying the newly learned environment for consolidation). Here we compared data from the male participants, described in the previous chapters three and four, to data from the group of female participants. We wished to examine whether the gender differences in their behavioral performance are associated with gender differences in theta and high-gamma oscillations. We reasoned that if hippocampal theta and high-gamma are functionally important for spatial navigation, they should reflect the robust gender differences in performance. We predicted that behavioral differences should be reflected in one or both of these oscillatory responses to spatial learning.

Methods

Participants. Eighteen right-handed healthy male and female participants (mean age in years: male 29.0 ± 5.1, female 27.9 ± 5.0; years of education: males 20.0 ± 3.3, females 19.1 ± 3.0). All experimental procedures were approved by the Human Research Ethics Committee of Macquarie University. Two female participants were excluded from MEG data analyses due to excessive head movement (pre-post head movement of pre-post recording > 4 mm). The rest of the sixteen females (mean age in years: 27.8 ± 4.9, mean years of education: 19.8 ± 2.9) were matched with the

eighteen male participants for age and education. The behavioral data analyses included all 18 females. The male data have been reported in chapters three and four. Here we focused on comparing males and females.

All the female participants had a regular menstrual cycle with a mean cycle length of 24 – 30 days. The eighteen females were evenly distributed in three different menstrual cycle phases by self-reports (six in the menstrual phase (cycle day 1 – 5), six in follicular phase (cycle day 6 – 12), six in luteal phase (cycle day 14 – 29). For the sixteen participants used in MEG data analyses, five were in the menstrual phase, six in follicular phase, and five in luteal phase. They were not pregnant and did not take any contraceptives or other hormone drugs at the time of testing.

Virtual Morris water maze task. This paradigm was described in detail in chapter three. Briefly, naïve participants did two repeated training sets in a virtual version of the Morris water maze task commonly used to elicit and study hippocampal activities in the extensively characterized rodent model (e.g., Kelemen et al., 2005; Olvera-Cortes et al., 2012). In humans, the virtual Morris water maze has been shown to elicit hippocampal rhythms measured by MEG (e.g., Cornwell et al., 2008; Cornwell et al., 2010). Behaviourally, the virtual Morris water maze has also been shown to reveal robust gender differences in virtual place learning (Astur et al., 1998; Astur et al., 2004). Participants navigated by pressing buttons on a button box (Current Designs Co. Ltd., Philadelphia, USA) using their right hand. In each training

set, they needed to find a hidden platform fixed in a goal location from different starting positions in the hidden platform condition by using the external landmarks attached on the pool wall; or they needed to move aimlessly in the random swimming condition. The contrast of the two conditions provided an index of goal-oriented navigation via binding of the goal location to external cues (Cornwell et al., 2008). We kept the environment layout of each condition of the two training sets constant to measure environmental encoding from training set one to two (chapter three). Thus, the environment in the first training set was defined as a new environment and that in the second one as a familiar environment. The positions of the hidden platform location in the two training sets were different and counterbalanced, to avoid environmental learning being confounded by learning a specific location in the environment. In each training set, there were five blocks of 5 trials for each condition respectively and were alternatively presented.

Control condition. To control the differences in interacting with the computer program between the two groups, after the MEG recording, participants were required to do ten trials of visible platform condition, where they needed to swim to a visible platform in a virtual Morris water maze with a different set of cues attached on the wall from different starting positions of the pool as quickly as possible by pressing buttons (Astur et al., 1998).

Psychometric task. Participants completed the Santa Barbara sense of direction scale

(SBSOD; Hegarty et al., 2002), a standardized self-report scale of spatial abilities. It consisted of 15 items, such as "I can usually remember a new route after I have traveled it only once" and "I do not have a very good 'mental map' of the environment". Participants were instructed to choose to what extent they agree or disagree with the statement in a 7-point Likert-type scale. The higher score of this scale indexes the better perceived sense of direction (https://labs.psych.ucsb.edu/hegarty/mary/content/santa-barbara-sense-direction-scale). The scale has been shown to have good test-retest reliability (two-administration correlation was 0.91) and highly correlated with objective measures of spatial abilities based on different types of learning experience (Hegarty et al., 2002; Wegman & Janzen, 2011).

Data acquisition.

MEG recording. Neuromagnetic responses were recorded at the KIT-Macquarie Brain Research Laboratory, Macquarie University, Sydney. The MEG system (Model PQ1160R-N2, KIT, Kanazawa, Japan) contained 160 coaxial first order gradiometers (50-mm baseline; Kado et al., 1999; Uehara et al., 2003) in a magnetic shielding room (Fujihara Co. Ltd., Tokyo, Japan). Before MEG measurements, the 3D locations of five head position indicators, the three fiducial landmarks (the nasion and bilateral preauricular points) and head shape were measured with a pen digitizer (Polhemus Fastrack, Colchester, VT, USA). Head position relative to the MEG sensors was

measured by energizing the five marker coils both before and after each of the recording. Continuous data were acquired with a sampling rate of 1000 Hz.

MRI recording. High-resolution T1-weighted anatomical magnetic resonance images (MRIs) were acquired at Macquarie University Hospital, using a 3T Siemens Magnetom Verio scanner with a 12-channel head coil. Those anatomical images were obtained using 3D GR\IR scanning sequence with the following parameters: repetition time, 2000 ms; echo time, 3.94 ms; flip angle, 9 degrees; slice thickness, 0.93 mm; field of view, 240 mm; image dimensions, 512 × 512 × 208.

Data analysis.

MEG source reconstruction. Source localization analyses were performed using the synthetic aperture magnetometry (SAM) beamformer (Robinson & Vrba, 1999) implemented in a Matlab toolbox – BrainWave (Version 3.0; http://cheynelab.utoronto.ca/brainwave). SAM is a non-linear 'beamforming' technique based on fixed-aperture radar technology (Dymond et al., 2014). It estimates source power within specific time and frequency windows across the whole brain. Source space is parsed into a three-dimensional grid with optimum spatial filter (beamformer weights) specified for each grid point (voxel) (Hillebrand et al., 2005). Localizing hippocampal activity with MEG beamformer has been shown to be successful in both simulation studies (e.g., Meyer et al., 2017; Quraan et al., 2011;

Stephen et al., 2005) and empirical studies (e.g., Backus et al., 2016; Cornwell et al., 2008; Riggs et al., 2009).

Estimation of navigation-related theta oscillations. A detailed description of analyses can be found in chapter three. Briefly, MEG data were epoched from -1 – 4 s relative to trial onset (4 s was the fastest time from the starting point to finding the hidden platform of two participants (one female and one male)). A single sphere forward head model (Lalancette et al., 2011; Sarvas, 1987) was derived by fitting the sphere to the inner skull surface of each individual's MRI extracted by the Brain Extraction Tool (Smith, 2002) in FSL. Beamformer weights were generated for the theta frequency (4 – 8 Hz) range. Sets of beamformer weights were computed for the entire brain at 4 mm isotropic voxel resolution without regularization of the covariance matrix. Source power at each voxel was normalized to that of the pre-trial baseline to control the noise and to capture the navigation-related power change relative to pre-trial period (event-related perturbation of theta power). Source power (quantified as a pseudo-F ratio) was estimated for 1s time windows using sliding windows in 250 ms increments (one theta cycle) after the trial onset (i.e. active window, e.g. 0 - 1s, 0.25 - 1.25 s, 0.5 - 1.5 s,..., 2.75 - 3.75 s), relative to the 1s pretrial baseline window. This generated a set of individual SAM images consisting of a volume of pseudo-F ratios. Sliding windows were required to detect the highly transient theta power change (e.g., Arai et al., 2014; Foster et al., 2013; Wyble et al., 2004).

Estimation of spontaneous high-gamma oscillations during inter-trial rest period. For more information on high-gamma power estimation, please refer to chapter four. Briefly, MEG data were epoched into -4.5 – 0 s (0 s was the onset of the next trial; 4.5 s was the shortest ITI across trials) and the epochs were grouped and labeled as *post hidden platform condition* and *post random swimming condition*. Since we were interested in spontaneous high-gamma power as opposed to event-related perturbation, source power at each grid location was estimated by normalizing a noise estimate instead of baseline power (called pseudo-Z ratio). Normalization has to be done to obtain a relatively 'pure' signal of interest, because the output of beamformer contains a certain amount of noise (Robinson & Vrba, 1999). This procedure resulted in a SAM image of a volume of pseudo-Z ratios for each condition and each training set.

Group statistics. Individual SAM images were first normalized to a Talairach brain template using Analysis of Functional NeuroImages software (AFNI; Cox, 1996; http://afni.nimh.nih.gov/afni). This was achieved by registering each participant's anatomical MRI to this brain template and a set of warping parameters was obtained, which was then applied to this participant's SAM images for normalization. To unveil the similarities and differences of the two groups, we first separately analyzed females and males using condition by training set within-subject ANOVA to see the brain activation patterns of theta and high-gamma activities and then directly compared the two groups (e.g., Gron et al., 2000; Konishi et al., 2013) to see whether there was a

significant group difference. Multiple comparison issues of voxel wise analyses were controlled by using small volume FDR correction ($p < 0.05$) in a mask containing bilateral hippocampi and parahippocampi.

Post-hoc comparison between high-gamma power during ITI and navigation period. In males, we reported that there was an increase during ITI in the first training set after hidden platform condition vs. navigation period in the first training. To investigate whether females also showed similar patterns, we estimated the high-gamma power during navigation period (0 – 4s) as what we did for high-gamma power estimation for ITI in females. We also carried out a within-subject ANOVA to see whether there was any significant effect for high-gamma power during ITI and navigation period for females.

Time frequency representations (TFRs)

Time course of navigation-related theta rhythms. The theta power time course of the peak voxel showing a group difference in the hippocampus was constructed to reveal the time-varying change of hippocampal theta oscillations in males and females. First, we reconstructed the source waveform of the voxel we specified from -1 – 4 s. Then, a five-cycle Morlet wavelet frequency transformation was performed on single trial source activity over a frequency range of 4 – 8 Hz in 1 Hz steps using the formula:

$$w(t, f_0) = A \exp(-t^2/2\sigma_t^2) \exp(2i\pi f_0 t).$$

Wavelets were then normalized so that the total energy was 1, with the normalization factor A being equal to: $(\sigma_t\sqrt{\pi})^{-1/2}$ (Tallon-Baudry et al., 1996). A convolution of the complex wavelet with the MEG source waveform was then derived and the magnitude of this convolution was used to create each TFRs. The value was then converted to percentage change in power relative to the pre-trial baseline (-1 – 0 s). Theta power change relative to baseline was collapsed over 4 – 8 Hz frequency bins and plotted over time to obtain the time course of theta power change (Isabella et al., 2015).

TFRs for spontaneous high-gamma activities. TFRs of the peak voxel showing a group difference was constructed. The main procedure was similar to that for the theta time course described above. A five-cycle Morlet wavelet transformation was performed on single trial source activity over a frequency range of 30 – 200 Hz over the period of -4.5 – 0, normalized across the frequency range so that total energy summed to 1. The final TFRs were presented as the difference between the two groups.

Correlation with behavioral performance. To further confirm that theta and high-gamma power have a functional property in spatial learning, we collapsed males and females and correlated theta power change during navigation relative to ITI baseline in the first training set, where learning requirement was maximum, with the

average path lengths in the hidden platform condition in both training sets across the whole brain. Because encoding related hippocampal theta rhythm should facilitate flexible navigation in the same environment (Wolbers & Hegarty, 2010). We also correlated high-gamma power change during ITI relative to navigation in the first training set with learning rate of path lengths in the subsequent training set two, because consolidation related high-gamma during rest/sleep should correlated with quicker learning in the subsequent spatial learning in the same environment. The significance threshold was set at $p = 0.05$ (uncorrected).

To confirm that the correlation seen for the whole group collapsed across the two genders was not driven by two opposite correlation patterns of each gender, we plotted scattered plots for a visual check and also compared the correlation coefficiencies of the two genders to see whether there was a significant difference between the two groups. The comparison of correlation coefficiency followed the standard procedure described by Cohen and Cohen (1983) which does the Fisher r-to-z transformation, and then calculates a value of z that can be applied to assess the significance of the difference between two correlation coeofficients found in two independent samples (http://vassarstats.net/rdiff.html). The significance threshold was set at $p = 0.05$.

Correlation between high-gamma and theta. Based on the effect of group comparison above, in order to confirm whether it is the case that the more

high-gamma power during ITI in the first training set was, the less theta power during navigation in the second training set was, we extracted the hippocampal theta power change during navigation relative to ITI baseline from the region which showed group differences in the right hippocampus and correlated that with high-gamma power change during ITI relative to navigation in the first training set across the whole brain. The significance threshold was set at p = 0.05 (uncorrected). Comparison between correlation coefficiencies between the two groups was made to make sure no significant difference between the two groups.

Results

Behavioral results

SBSOD Scale. Independent samples t test showed that females had significantly lower scores than males (t(27.886) = -3.537, p = 0.001, Cohen's d = 1.05; Fig. 1A). This is in accordance with previous findings (e.g., Hao et al., 2016; Hegarty et al., 2006).

Visible platform condition. Average latency over the ten visible platform trials was not significantly different between the two groups (t(17.018) = -1.003, p = 0.330), indicating that there were no systematic differences (e.g. motivational) between females and males in terms of how they interacted with the computer programme

(Astur et al., 1998).

Performance in virtual Morris water maze task.

Movement onset (from the picture showing up to the movement onset in each trial) of the two groups were marginally different (main effect of gender, $F(1,34) = 4.057$, $p = 0.052$, $\eta^2 = 0.107$), with females being slightly slower than males to move in the task.

We then performed a two (gender: females vs. males) × two (training set: one vs. two) mixed design ANOVA to directly compare the average latency and path lengths from movement onset to the time point of finding the hidden platform in the two groups. We found a main effect of gender ($F(1,34) = 7.37$, $p = 0.01$, $\eta^2 = 0.178$) and an interaction between gender and training set ($F(1,34) = 4.33$, $p = 0.045$, $\eta^2 = 0.113$) (Fig. 1B). Simple effect analyses confirmed that males required significantly less time to find the platform in the second training set compared to the first training set ($F = 5.67$, $p = 0.023$), while females did not show any improvement ($F = 0.31$, $p = 0.579$). Males were significantly faster than females in both training sets ($F = 4.17$, $p = 0.049$ and $F = 8.65$, $p = 0.006$ for training set one and two). (The subset of 16 participants used for MEG analyses were subjected to the same analysis, with no differences in the statistical inferences reported for the total 18 female participants).

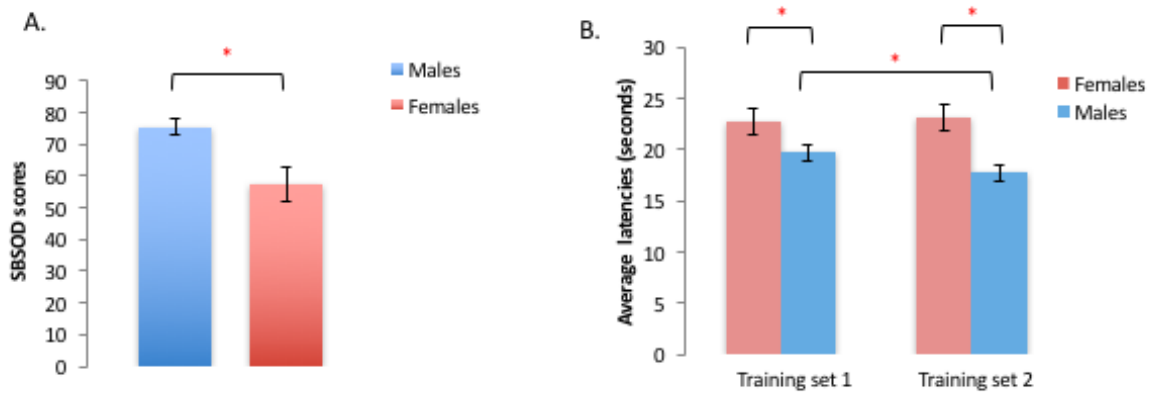

Figure 1. A. Score of Santa Barbara sense of direction (SBSOD) of females and males. **B.** Average latency in each condition and training set taken by the two groups. * represents $p < 0.05$.

For path lengths, we found a significant interaction between gender and training set ($F(1,34) = 5.29$, $p = 0.031$, $\eta^2 = 0.13$). Males showed significantly shorter path lengths in the second training set ($t(17)=2.329$, $p=0.032$) than that in the first one as reported in chapter three, while females did not showed no difference between training sets ($t(17)=0.596$, $p = 0.559$).

Overall, the behavioural results show clear gender differences, with males having higher scores on the sense of direction scale and faster performance on the maze task. Males also showed significantly improved performance in the familiar versus new environments, while females did not, in line with the idea that males and females differ in how they process environmental cues (e.g., Sandstrom et al., 1998; Saucier et al., 2002; Chai & Jacobs, 2009; Iachini et al., 2005; Lawton, 1994; Mueller

et al., 2008).

MEG results

Theta activation pattern of males and females during navigation. Males' theta results have been reported in chapter three. Briefly, there was a main effect of condition in the anterior left hippocampus and parahippocampus in the time window of 1 - 2s, 1.5 - 2.5s and there was a main effect of training set in the right hippocampus in the time window of 1.25 – 2.25s. For females, two (conditions: hidden platform vs. random swimming condition) × two (training sets: first vs. second) repeated measures ANOVAs demonstrated that there was a main effect of condition in the anterior left hippocampus and parahippocampus in the time window of 2 - 3s ($p < 0.05$, corrected, peak voxel at left parahippocampus: Talairach coordinate x= -18 , y= -17, z= -16), with left hippocampal theta being greater in the hidden platform condition than in the random swimming condition (Fig. 2A & B). No significant main effect of training set, or interaction between training set and condition, was found in any time window for females (Fig. 3A).

High-gamma activation pattern of males and females during rest. Males' high-gamma results have been reported in chapter four. There was a main effect of training set in the right hippocampal high-gamma activities, mirroring the power change pattern of navigation-related right hippocampal theta rhythms in the new

versus familiar environment. For females, no significant main effect of training set was found for rest high-gamma activities during the inter-trial rest period (Fig. 5A). This echoed the result that in females no significant main effect of training set was found for theta oscillations during navigation. No other significant results were found for females for resting high-gamma activities. We further computed high-gamma power during navigation period for females and compared that with that during ITI. No single voxels were found when original p = 0.05 (uncorrected) for high-gamma power between the two time periods (Data not shown), while as shown in chapter four, there was a significant increase in high-gamma power during ITI after hidden platform condition in the first training set relative to that during navigation in the hidden platform condition in the first training set.

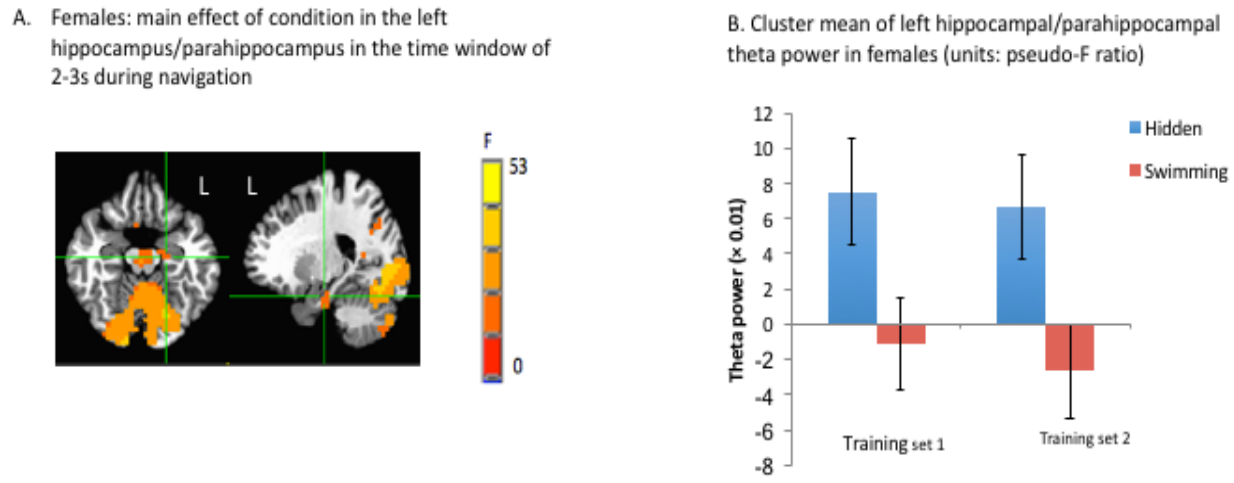

Figure 2. Images of hippocampal activation of females. A. Main effect of condition in the anterior left hippocampus (peak voxel: x = -18, y = -17, z = -16) in the time window of 2 - 3s. B. The cluster mean of theta power (pseudo-F values) in anterior left hippocampus in each condition and each training set in the time window of 2 - 3s.

Direct comparison of the two groups.

Left hippocampal theta during navigation. Since both groups showed a significant main effect of condition in the left hippocampus and parahippocampus, the cluster mean (pseudo-F values) of the voxels showing a significant effect in each group in the corresponding time window was extracted to directly compare activations in the two groups. Since this effect was the contrast between hidden platform condition and random swimming condition, and there was no condition by training set interaction in either group, we collapsed the power of the cluster mean of the left hippocampal and parahippocampal theta power in training set one and two together for each group and compared the value of the two groups using independent sample t-test. No significant difference was found between the two groups.

Right hippocampal theta during navigation. Since females did not show any significant environmental learning effect in any of the voxels in bilateral hippocampi, defining an ROI in the right hippocampus showing a significant effect in male group and extracting theta power from females for group comparison may cause bias (Vul et al., 2009). So voxel wise comparisons between the two groups were performed and corrected as in the previous analyses above. Moreover, since the environmental learning effect was obtained through subtraction of the two training sets, to investigate where the group difference came from (1^{st} or 2^{nd} training set), a two

(gender: females vs. males) × two (conditions: hidden platform condition vs. random swimming condition) mixed design ANOVA was performed for training set one and two respectively. We averaged all the time windows of females together, because no single time window in females showed a significant main effect of training set and compared theta power in the average time window with that of males in the time window of 1.25 – 2.25s for training set one and two respectively. We found no significant difference in the first training set, but a significant main effect of gender in the right hippocampus in the second training set ($p < 0.05$, corrected, peak voxel in the right hippocampus, Talairach coordinate x = 26, y = -25, z = -4) (Fig. 3B & 3C), with females having significantly higher right hippocampal activation than males. No other significant effect was found for both training sets.

A. No significant main effect of training set for theta rhythms during navigation in females

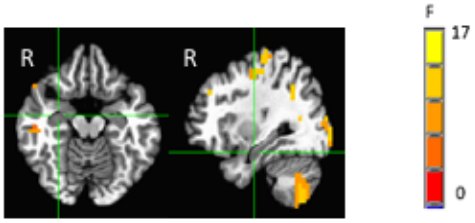

B. A significant gender difference for theta rhythms in the ***second*** training set

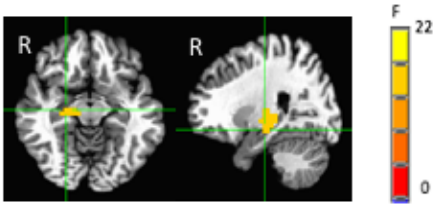

C. Cluster mean of right hippocampal theta power (units: pseudo-F ratio) in both groups in the ***second*** training set

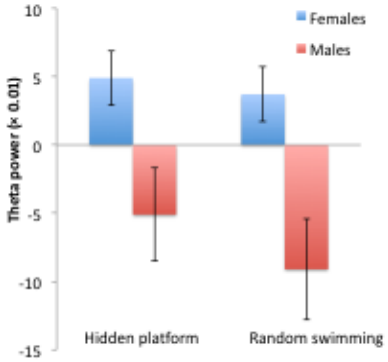

Figure 3. A. Females showed no main effect of training set in the hippocampus for theta oscillations during navigation. **B.** Main effect of gender (1.25 - 2.25s of males vs. average time window of females) in the right hippocampus (peak voxel: x = 26, y = -25, z = -4) for the second training set for theta oscillations during navigation. **C.** The cluster mean of theta power in the right hippocampal region showing gender difference in each condition in males and females in the second training set.

We then plotted the time course of the peak voxel showing main effect of gender in the right hippocampal region for both males and females (Fig. 4. the last few hundred milliseconds were trimmed because of edge effects, Kaplan et al., 2012). The time course of right hippocampal theta activities confirmed that in the first training set, when the environment was new, right hippocampal theta activity was similar in the two groups; in the second training set, where the familiarity degree of the environment decreased, right hippocampal theta power of male participants decreased, while females' right hippocampal theta magnitude was still high.

New environment

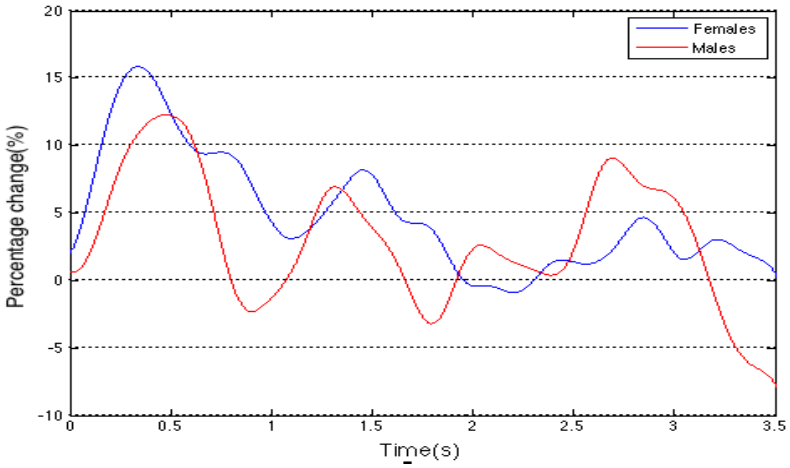

Familiar environment

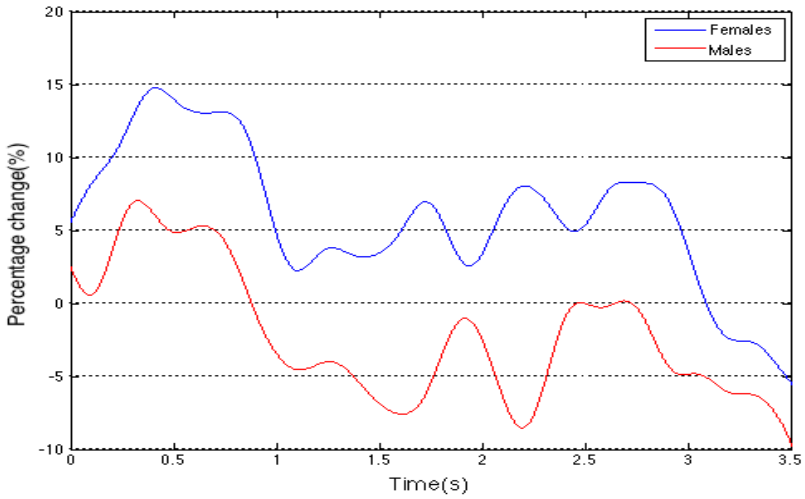

Figure 4. Time course of right hippocampal theta power (during navigation) percentage change relative to the baseline in training set one (new environment) and two (familiar environment) for males and females.

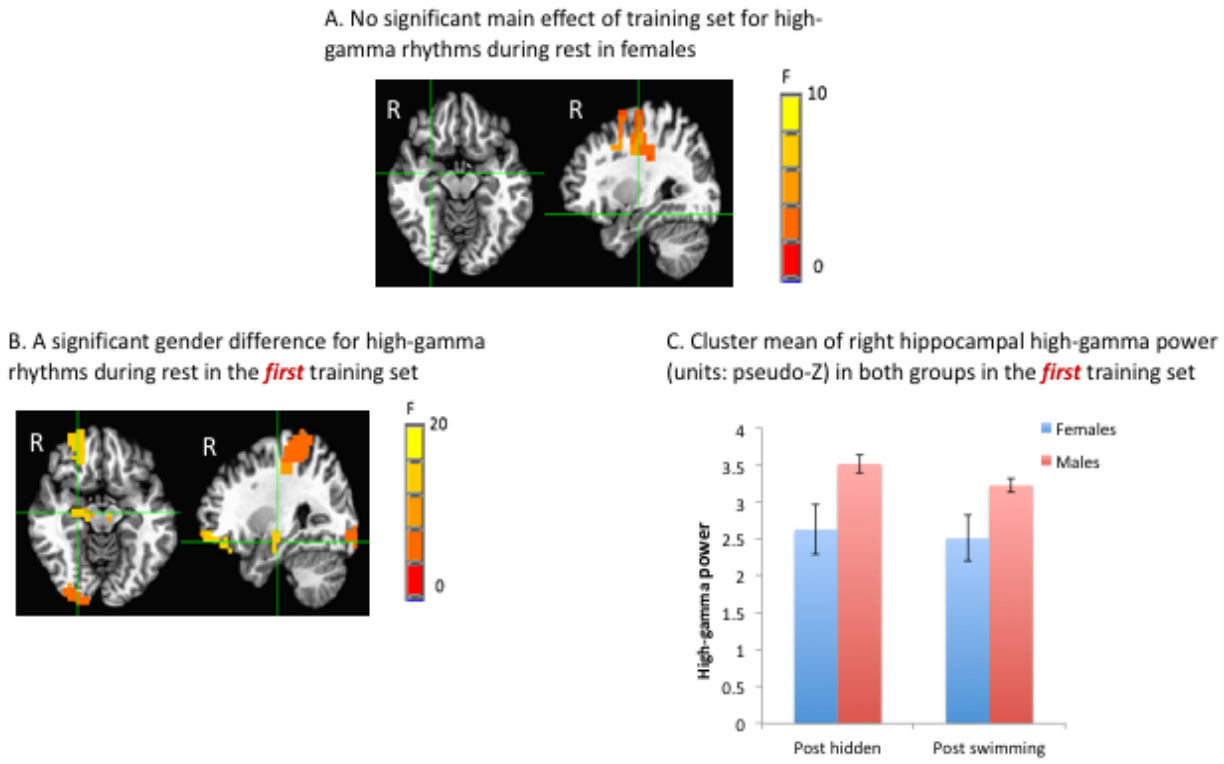

Figure 5. A. Females showed no main effect of training set in the hippocampus for high-gamma oscillations during inter-trial rest period. **B.** Main effect of gender in the right hippocampus (peak voxel: x = 22, y = -17, z = -12) for the first training set for high-gamma oscillations. **C.** The cluster mean of high-gamma power during inter-trial rest period in the right hippocampal region showing gender difference in each condition in males and females in the first training set.

Right hippocampal high-gamma during rest. We performed a two (gender: females vs. males) × two (conditions: hidden platform condition vs. random swimming condition) mixed design ANOVA for each voxel across the voxels of the whole brain for training set one and two respectively. ANOVA showed a significant main effect of

group in the right hippocampus ($p < 0.05$, corrected, peak voxel at right hippocampus: Talairach coordinate x = 22 y = -17 z = -12. Fig. 5B & 5C) in the first training set, with the resting high-gamma activation strength of males being significantly higher than that of females. No other significant effects were found for this training set. As for the second training set, no significant effect was found. TFRs (Fig. 6) also confirmed that in the first training set, when the environment was new, males showed more high-gamma bursts than females during the inter-trial rest period. These results suggest that females may have weaker automatic consolidation processing after spatial leaning, which might be a reason why they required continuing encoding of the environment and persistently high theta power in the second training set when male's theta power had significantly declined from the first training set.

New environment

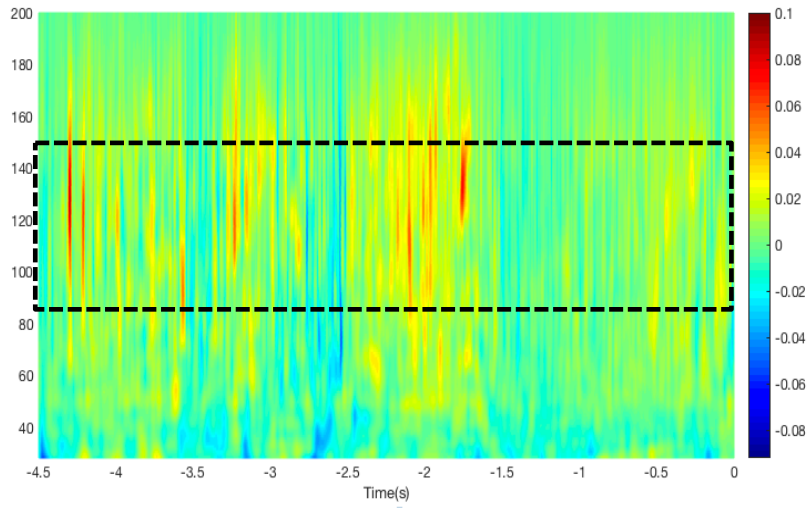

Familiar environment

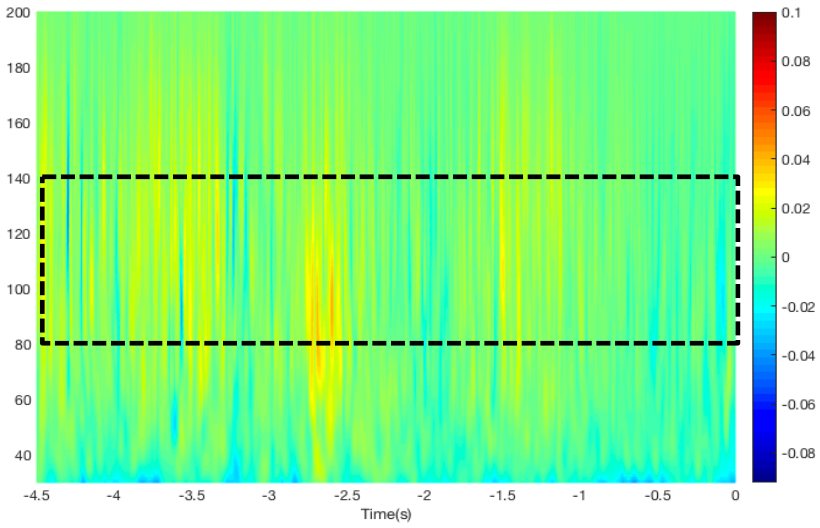

Figure 6. Time frequency representations (units: pseudo-Z) of right hippocampal high-gamma difference between males and females (males minus females) during inter-trial rest period in training set one (new environment) and training set two (familiar environment). The black rectangular shows the time window and frequency range (80 – 140 Hz) used in

SAM beamformer analysis for group comparison.

Correlation between theta and high-gamma with navigation performance.

To investigate whether theta power change during navigation relative to navigation and high-gamma power change during ITI relative to navigation were related to navigation performance across participants, we collapsed males and females together and correlated theta power change during navigation and high-gamma power change during IIT in the first training set where the learning requirement was the maximum across the two genders with navigation performances, because we reasoned if hippocampal theta and high-gamma have an important functional property in spatial learning in humans, they should correlate navigation performance across genders. We found right hippocampal theta power change in the first training set during navigation in the hidden platform condition relative to ITI was negatively correlated with path lengths in both training sets in hidden platform condition (Fig. 7) and right hippocampal high-gamma power change in the first training set during ITI after hidden platform condition relative to navigation was positively correlated to learning rate in the second training set in the hidden platform condition (Fig. 8). No significant group difference was found between the correlation coefficients of the two genders ($z = -0.34$, $p = 0.73$; $z = -0.52$, $p = 0.60$ for the comparison between the correlation coefficients from the correlation between hippocampal theta in the first training set and path lengths in the first and second training set respectively and $z = 0.94$, $p = 0.35$ for the comparison of the correlation coefficients from the correlation between

high-gamma power and learning rate).

These results suggested the more the right hippocampal theta power increase during navigation was, the shorter the path lengths were in both training sets, in line with previous results that stronger right hippocampal activity during navigation corresponded to shorter path lengths (Cornwell et al., 2010). The results also suggested that the more the high-gamma power increase during ITI was, the larger the learning rate would be in the subsequent learning, in agreement of previous reports that higher high-gamma power during rest/sleep after learning associated with better subsequent memory performance (Axmacher et al., 2008; Cornwell et al., 2014).

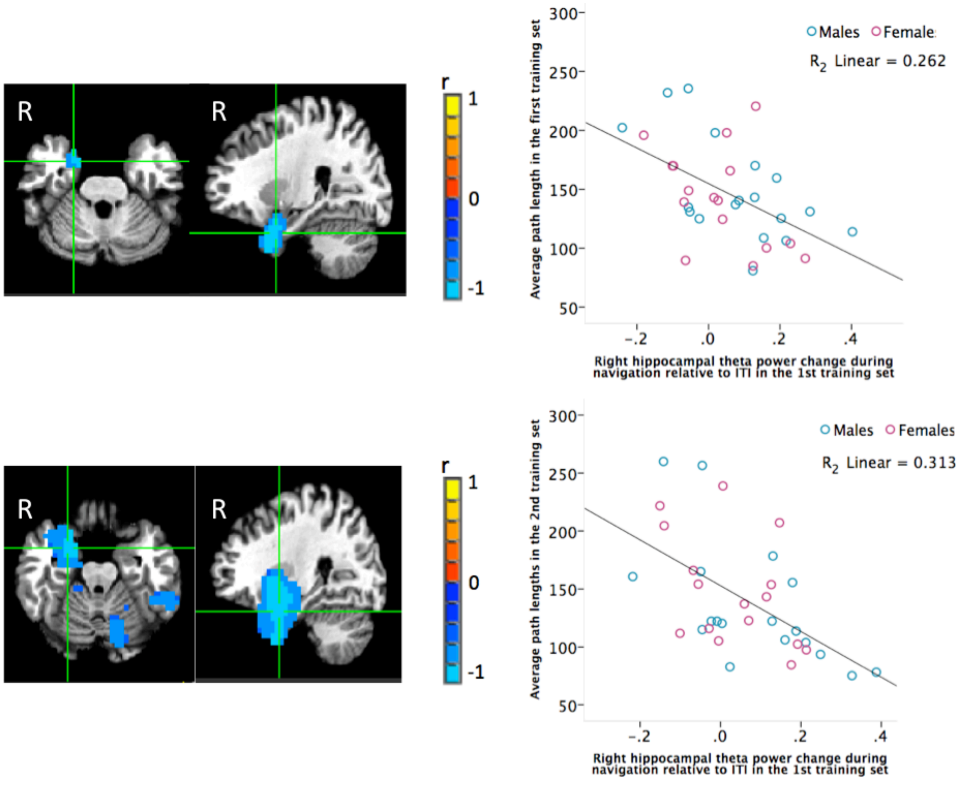

Figure 7. Correlation between hippocampal theta power change during navigation relative to ITI baseline in the first training set and path lengths in both training sets across genders. The

left figures of upper panel whole brain images which exhibit more theta power increase during navigation in the first training set in the hidden platform condition corresponded to shorter path length in the first training set. The right figure of upper panel is the scatter plot of right hippocampal theta power change during navigation in the first training set plotted against the path lengths in the first training set in the hidden platform condition. The left figures of lower panel shows whole brain images which show more theta power increase during navigation in the first training set in the hidden platform condition corresponded to shorter path length in the second training set. The right figure of lower panel is the scatter plot of right hippocampal theta power change during navigation in the first training set plotted against the path lengths in the second training set in the hidden platform condition.

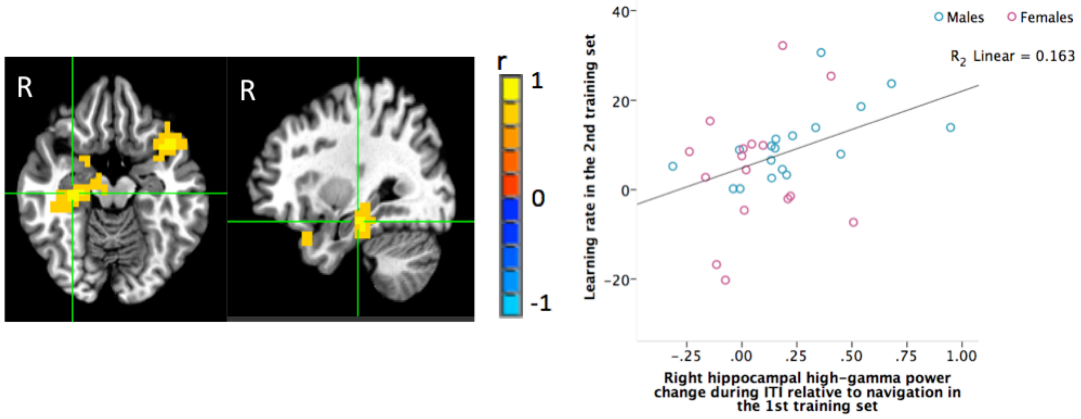

Figure 8. Correlation between high-gamma power change during ITI relative to navigation in the first training set in the hidden platform condition with learning rate in the second training set in the hidden platform condition. The left brain images show the more hippocampal-high gamma power increase during ITI in the first training set was, the quicker the participants would learn in the subsequent training set two. The scatter plot on the right side is the right hippocampal high-gamma power change during ITI plotted against the learning rate in the

second training set in the hidden platform condition.

Correlation between high-gamma power change during ITI in the first training set with theta power change during navigation in the second training set.

To further investigate whether the right hippocampal high-gamma power change during ITI in the first training set was related to theta power change during ITI in the second training set, because in the group comparison above, we saw decreased right hippocampal theta power in males but not in females in the second training set, while increased high-gamma power during ITI in the first training set in males but not in females, we extracted right hippocampal theta power change during the second training set in the two genders and correlated that with their high-gamma power change during ITI in the first training set. As expected, we found a negative correlation between high-gamma power change during ITI in the first training set with theta power change in the second training set during navigation (Fig. 9). No significant difference was found between the correlation coeffiencies of the two groups ($z = 0.65$, $p = 0.52$).

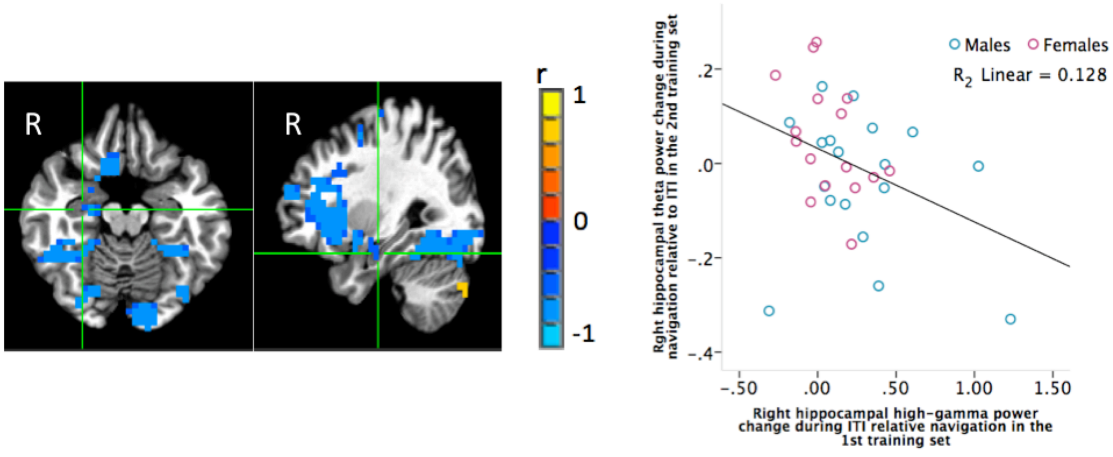

Figure 9. Correlation between high-gamma power change during ITI relative to navigation in the first training set and theta-power change during navigation during navigation relative to ITI in the second training set. The brain images on the left side show the more high-gamma power increase is in the first training set, the less the navigation related theta power is in the second training set. The scatter plot on the right side shows a scatter plot of right hippocampal high-gamma power change during ITI in the first training set plotted against the right hippocampal theta power change in the second training set.

Discussion

In this study, we investigated whether gender differences in navigation performance are associated with gender differences in hippocampal theta during navigation and high-gamma activities during rest period using a whole-head MEG with a virtual Morris water maze task. The behavioral results were consistent with previous behavioral studies: males had a significantly better sense of direction and were able to find the hidden platform faster than females; in the second training set, males took less time to find the hidden platform than that in the first training set, but females did not show any improvement. MEG results revealed that (1) in both groups, navigation elicited left hippocampal and parahippocampal theta, with comparable magnitudes; (2) there were gender differences in right hippocampal theta and high-gamma activity. From the first to the second training set during navigation period, males showed decreased right hippocampal theta power, while females did not;

during inter-trial rest periods, males showed significantly higher right hippocampal high-gamma power in the first training set than females; (3) the more the right high-gamma power during ITI in the first training was, the less the right hippocampal theta power during navigation was; (4) both theta power during navigation and high-gamma power during ITI were associated with better navigation performance across genders.

The behavioral data agree with previous studies (e.g., Astur et al., 1998; Mueller et al., 2008) showing that males were faster than females to find the hidden platform in a virtual Morris water maze task. We further showed that males, but not females, significantly improved performance from the new (training set one) to familiar (training set two) environment. These results support the conclusion that there are gender differences in environment learning, in line with previous findings (e.g., Mueller et al., 2008; Sandstrom et al., 1998; Saucier et al., 2002; Woolley et al., 2010) showing gender differences in environmental processing. The group differences are not attributable to differences in the interaction with the computer programme between the two groups for the following reasons. First, males outperformance of females in spatial navigation is consistent with previous studies (e.g., Astur et al., 1998; Astur et al., 2004) and with the significantly higher scores on the Santa Barbara sense of direction scale (SBSOD); second, there was no significant group difference in the control condition (visible platform condition), indicating that motivational, motor, or sensory aspects of interacting with the computer program were not

significantly different between the two groups (Astur et al., 1998).

In both groups during navigation, left hippocampal and parahippocampal theta oscillations showed greater power in the hidden platform relative to the random swimming condition, and no gender difference was found in left hippocampal and parahippocampal theta. Left hippocampal theta has been proposed to be functionally involved in binding the platform to its spatial location (Cornwell et al., 2008), and the left hippocampus has been conceputalised as a binding device (Chalfonte et al., 1996; Kessels et al., 2004; Mitchell et al., 2000). Our MEG results are consistent with previous behavioural studies which found that females and males performed equally well in object-to-position binding processing (Postma et al., 1998; Postma et al., 2004); and a meta-analysis (Voyer et al., 2007), showing no gender difference in remembering the location of a gender-neutral object. The similarity of the functional activation of the left hippocampus in both groups is further corroborated by a recent MRI study (Joel et al., 2015), which reported that there was a significant overlap between males and females in the volume of the left hippocampus.

Our results do provide evidence for a gender difference in right hippocampus in environmental encoding during spatial navigation. From the first to second training set, males showed decreased theta power in the right hippocampus. In contrast, females' right hippocampal theta power showed no change (was equally high) in both training sets. Previous studies demonstrated that the right hippocampus showed a

time-dependent decrease of activity during spatial learning as performance achieved ceiling (Igloi, 2010; Wolbers & Buchel, 2005). Thus, decreased right hippocampal theta power in the second training set in males might indicate reduced environmental learning requirements from training set one to two, while environmental learning requirements did not decrease in females as the magnitude of right hippocampal theta was equally high in both training sets.

In males, we observed that during inter-trial rest period, right hippocampal high-gamma power mirrored the right hippocampal theta power change during navigation, with right hippocampal high-gamma power being higher in the first training set than that in the second one to replay and consolidate the newly learned environment); in contrast, females showed no evidence of such a high-gamma replay effect. Group comparison showed that in the first training set, where the environment was new, right hippocampal high-gamma power of males was significantly higher than that of females. These findings suggest that replay of newly learned spatial knowledge of females is significantly less than that of their male counterparts. This idea was supported by the correlation results that the more the right high-gamma power was during ITI, the less the right hippocampal theta power was during navigation. Thus, a weaker consolidation mechanism in females might explain why right hippocampal theta activation in the second training set was as high as that in the first one in this group, because they might still need to encode the environment, which has already been familiar for males. That explains why males, but not females,

showed improved navigation performance over the first to second training sets, while females did not. The gender difference in the (replay-related) high-gamma effect during the rest period is corroborated by previous findings (Wang & Fu, 2009) that the effect of daytime sleep on declarative memory for pictures is different for males and females. For instance, after sleep, there was an increased familiarity with the previously learned pictures in males relative to that before sleep after learning, while the familiarity with previously learned pictures in females was not influenced by daytime sleep.

Collapsing across genders, we found stronger right hippocampal theta power during navigation and right hippocampal high-gamma power during ITI in the first training set where learning requirement was the strongest, corresponded to better navigation performance across genders. These correlations with behavioral performance across genders are in agreement with previous reports that stronger navigation related theta and high-gamma power during rest/sleep period are associated with better memory performance (Cornwell et al., 2010, 2014; Kaplan et al., 2012; Axmacher et al., 2008) and further reinforce the functional importance and behavioral relevance of hippocampal theta and high-gamma rhythms in spatial learning in humans.

Our MEG results are in agreement with the fMRI results of Gron et al. (2000), showing no gender difference in right hippocampal activation strength in a new

environment. However, our results do show a gender difference in right hippocampal activation in a familiar environment. In contrast with Gron et al. (2000), which showed left hippocampal activation was specific to males, the present study revealed that females also activated left hippocampus during navigation. The discrepancy may be due to the fact that the task in Gron et al. (2000) involved both allocentric and egocentric navigation. Previous behavioral studies (e.g., Dabbs, 1998; Sandstrom et al., 1998) showed there was a gender difference in preferred usage of egocentric and allocentric navigation strategies. Thus, the difference in left hippocampal activation found in Gron et al. (2000) may reflect a different usage of allocentric and egocentric navigation strategies between males and females. In the present study, the virtual Morris water maze task restricted the type of navigation strategy that can be used or at least makes an allocentric strategy more efficient than other approach (Mueller et al., 2008), and we found that if both groups used external cues to remember the goal location, left hippocampus would be activated in both groups with the same strength.

While the results of the present study strongly implicate the hippocampal function as a crucial neural substrate for known gender differences in navigation ability, further studies are needed to systematically investigate the precise nature of these differences in hippocampal rhythms. Many factors could be involved, including sex hormones (e.g., Driscoll et al., 2005), genetic factors (e.g. Ruiz-Opazo & Tonkiss, 2006), and navigation experiences (e.g. Waller, 2000).

In sum, we found that gender differences in navigation performance were reflected in the differences in both environmental encoding-related right hippocampal theta activities during navigation and environmental replay-related right hippocampal high-gamma activates during rest period. Left hippocampal theta activities, which was used to bind the hidden platform to its location using external landmarks during navigation were similar between the two genders. The similarities and differences between males and females reinforce the functional importance of hippocampal rhythms in different stages of spatial learning and also further our understanding of the neural substrates underlying spatial navigation of the two groups.

Acknowledgements: This work was supported by Australian Research Council Grants CE110001021, DP1096160. Thanks also go to the China Scholarship Council and Macquarie University for financial support of the author. I would also like to thank Dr. Zhiguo Wang, Dr. Xiangzhen Kong and Dr. Jie Yang for discussion of the results.

References

Arai, M., Brandt, V., & Dabaghian, Y. (2014). The effects of theta precession on spatial learning and simplicial complex dynamics in a topological model of the hippocampal spatial map. *PLoS Comput Biol, 10*(6), e1003651. doi:10.1371/journal.pcbi.1003651

Astur, R. S., Ortiz M. L., & J., S. R. (1998). A characterization of performance by men and women in a virtual Morris water task: A large and reliable sex difference. *Behav Brain Res, 93*(1998), 185-190.

Astur, R. S., Tropp, J., Sava, S., Constable, R. T., & Markus, E. J. (2004). Sex differences and correlations in a virtual Morris water task, a virtual radial arm maze, and mental rotation. *Behav Brain Res, 151*(1-2), 103-115. doi:10.1016/j.bbr.2003.08.024

Axmacher, N., Elger, C. E., & Fell, J. (2008). Ripples in the medial temporal lobe are relevant for human memory consolidation. *Brain, 131*(Pt 7), 1806-1817. doi:10.1093/brain/awn103

Backus, A. R., Schoffelen, J. M., Szebenyi, S., Hanslmayr, S., & Doeller, C. F. (2016). Hippocampal-Prefrontal Theta Oscillations Support Memory Integration. *Curr Biol, 26*(4), 450-457. doi:10.1016/j.cub.2015.12.048

Blanch, R. J., Brennan, D., Condon, B., Santosh, C., & Hadley, D. (2004). Are there gender-specific neural substrates of route learning from different perspectives? *Cereb Cortex, 14*(11), 1207-1213. doi:10.1093/cercor/bhh081

Blokland, A., Rutten, K., & Prickaerts, J. (2006). Analysis of spatial orientation

strategies of male and female Wistar rats in a Morris water escape task. *Behav Brain Res, 171*(2), 216-224. doi:10.1016/j.bbr.2006.03.033

Buzsaki, G. (1989). Two-stage model of memory trace formation: a role for "noisy" brain states *Neuroscience, 31*(3), 551-570.

Buzsaki, G. (2002). Theta oscillations in the hippocampus. *Neuron, 33*, 325-340.

Buzsaki, G. (2015). Hippocampal sharp wave-ripple: A cognitive biomarker for episodic memory and planning. *Hippocampus, 25*(10), 1073-1188. doi:10.1002/hipo.22488

Buzsaki, G., & Lopes da Silva, F. H. (2012). High frequency oscillations in the intact brain. *Prog Neurobiol, 98*(3), 241-249. doi:10.1016/j.pneurobio.2012.02.004

Buzsaki, G., & Moser, E. I. (2013). Memory, navigation and theta rhythm in the hippocampal-entorhinal system. *Nat Neurosci, 16*(2), 130-138. doi:10.1038/nn.3304

Carr, M. F., Jadhav, S. P., & Frank, L. M. (2011). Hippocampal replay in the awake state: a potential substrate for memory consolidation and retrieval. *Nat Neurosci, 14*(2), 147-153. doi:10.1038/nn.2732

Chai, X. J., & Jacobs, L. F. (2009). Sex differences in directional cue use in a virtual landscape. *Behav Neurosci, 2*, 276-283. doi:10.1037/a0014722.supp

Chalfonte, B. L., Verfaellie, M., Johnson, M. K., & Reiss, L. (1996). Spatial location memory in amnesia: binding item and location information under incidental and intentional encoding conditions. *Memory, 4*(6), 591-614. doi:10.1080/741940998

Cohen, J., & Cohen, P. (1983). *Applied multiple regression/correlation analysis for the behavioral sciences*: Hillsdale, NJ: Eribaum.

Cornwell, B. R., Johnson, L. L., Holroyd, T., Carver, F. W., & Grillon, C. (2008). Human hippocampal and parahippocampal theta during goal-directed spatial navigation predicts performance on a virtual Morris water maze. *J Neurosci, 28*(23), 5983-5990. doi:10.1523/JNEUROSCI.5001-07.2008

Cornwell, B. R., Overstreet, C., & Grillon, C. (2014). Spontaneous fast gamma activity in the septal hippocampal region correlates with spatial learning in humans. *Behav Brain Res, 261*, 258-264. doi:10.1016/j.bbr.2013.12.031

Cornwell, B. R., Salvadore, G., Colon-Rosario, V., Latov, D. R., Holroyd, T., Carver, F. W., . . . Grillon, C. (2010). Abnormal hippocampal functioning and impaired spatial navigation in depressed individuals: evidence from whole-head magnetoencephalography. *Am J Psychiatry, 167*(7), 836-844. doi:10.1176/appi.ajp.2009.09050614

Cox, R. W. (1996). AFNI: software for analysis and visualization of functional magnetic resonance neuroimages. *Comput Biomed Res, 29*, 162-173. doi:10.1006/cbmr.1996.0014

Dabbs, J. M., Chang, E. L., Strong, R. A., Milun, R. (1998). Spatial ability, navigation strategy, and geographic knowledge among men and women. *Evol Hum Behav, 19*, 89-98.

Driscoll, I., Hamilton, D. A., Yeo, R. A., Brooks, W. M., & Sutherland, R. J. (2005). Virtual navigation in humans: the impact of age, sex, and hormones on place

learning. *Horm Behav, 47*(3), 326-335. doi:10.1016/j.yhbeh.2004.11.013

Dymond, S., Lawrence, N. S., Dunkley, B. T., Yuen, K. S., Hinton, E. C., Dixon, M. R., . . . Singh, K. D. (2014). Almost winning: induced MEG theta power in insula and orbitofrontal cortex increases during gambling near-misses and is associated with BOLD signal and gambling severity. *Neuroimage, 91*, 210-219. doi:10.1016/j.neuroimage.2014.01.019

Foster, B. L., Kaveh, A., Dastjerdi, M., Miller, K. J., & Parvizi, J. (2013). Human retrosplenial cortex displays transient theta phase locking with medial temporal cortex prior to activation during autobiographical memory retrieval. *J Neurosci, 33*(25), 10439-10446. doi:10.1523/JNEUROSCI.0513-13.2013

Gron, G., Wunderlich, A. P., Spitzer, M., Tomczak, R., & Riepe, M. W. (2000). Brain activation during human navigation gender-different neural networks as substrate of performance. *Nat Neurosci, 3*(4), 404-408.

Hao, X., Huang, Y., Li, X., Song, Y., Kong, X., Wang, X., . . . Liu, J. (2016). Structural and functional neural correlates of spatial navigation: a combined voxel-based morphometry and functional connectivity study. *Brain Behav, 6*(12), e00572. doi:10.1002/brb3.572

Hegarty, M., Montello, D. R., Richardson, A. E., Ishikawa, T., & Lovelace, K. (2006). Spatial abilities at different scales: Individual differences in aptitude-test performance and spatial-layout learning. *Intelligence, 34*(2), 151-176. doi:10.1016/j.intell.2005.09.005

Hegarty, M., Richardson, A. e., Montello, D. R., Lovelace, K., & Subbiah, I. (2002).

Development of a self-report measure of enviornmental sparial ability. *Intelligence, 30*(2002), 425-447.

Hillebrand, A., Singh, K. D., Holliday, I. E., Furlong, P. L., & Barnes, G. R. (2005). A new approach to neuroimaging with magnetoencephalography. *Hum Brain Mapp, 25*(2), 199-211. doi:10.1002/hbm.20102

Iachini, T., Sergi, I., Ruggiero, G., & Gnisci, A. (2005). Gender differences in object location memory in a real three-dimensional environment. *Brain Cogn, 59*(1), 52-59. doi:10.1016/j.bandc.2005.04.004

Igloi, K., Doeller, C. F., Berthoz, A., Rondi-Reig, L., Burguess, N. (2010). Lateralized human hippocampal activity predicts navigation based on sequence or place memory. *Proc Natl Acad Sci U S A, 107*(32), 14466-14471.

Isabella, S., Ferrari, P., Jobst, C., Cheyne, J. A., & Cheyne, D. (2015). Complementary roles of cortical oscillations in automatic and controlled processing during rapid serial tasks. *Neuroimage, 118*, 268-281. doi:10.1016/j.neuroimage.2015.05.081

Joel, D., Berman, Z., Tavor, I., Wexler, N., Gaber, O., Stein, Y., . . . Assaf, Y. (2015). Sex beyond the genitalia: The human brain mosaic. *Proc Natl Acad Sci U S A*. doi:10.1073/pnas.1509654112

Jones, C. M., Braithwaite, V. A., & Healy, S. D. (2003). The evolution of sex differences in spatial ability. *Behavioral Neuroscience, 117*(3), 403-411. doi:10.1037/0735-7044.117.3.403

Kado, H., Higuchi, M., Shimogawara, M., Haruta, Y., Adachi, Y., Kawai, J., &

Uehara, G. (1999). Magnetoencephalogram systems developed at KIT. *IEEE Trans. Appl. Supercond, 9*, 4057-4062. doi:doi:10.1109/77.783918

Kaplan, R., Doeller, C. F., Barnes, G. R., Litvak, V., Duzel, E., Bandettini, P. A., & Burgess, N. (2012). Movement-related theta rhythm in humans: coordinating self-directed hippocampal learning. *PLoS Biol, 10*(2), e1001267. doi:10.1371/journal.pbio.1001267

Kelemen, E., Moron, I., & Fenton, A. A. (2005). Is the hippocampal theta rhythm related to cognition in a non-locomotor place recognition task? *Hippocampus, 15*(4), 472-479. doi:10.1002/hipo.20071

Kessels, R. P. C., Hendriks, M. P. H., Schouten, J., Asselen, M. V., & Postma, A. (2004). Spatial memory deficits in patients after unilateral selective amygdalohippocampectomy. *J Int Neuropsychol Soc, 10*, 907-912. doi:DOI: 10.10170S1355617704106140

Konishi, K., Etchamendy, N., Roy, S., Marighetto, A., Rajah, N., & Bohbot, V. D. (2013). Decreased functional magnetic resonance imaging activity in the hippocampus in favor of the caudate nucleus in older adults tested in a virtual navigation task. *Hippocampus, 23*(11), 1005-1014. doi:10.1002/hipo.22181

Lalancette, M., Quraan, M., & Cheyne, D. (2011). Evaluation of multiple-sphere head models for MEG source localization. *Phys Med Biol, 56*(17), 5621-5635. doi:10.1088/0031-9155/56/17/010

Lawton, C. A. (1994). Gender differences in way-finding strategies—relationship to spatial ability and spatial anxiety. *Sex Roles, 30*, 765-779.

Maguire, E. A., Burgess, N., & O'Keefe, J. (1999). Human spatial navigation: cognitive maps, sexual dimorphism, and neural substrates. *Curr Opin Neurobiol, 9*, 171-177.

Meyer, S. S., Rossiter, H., Brookes, M. J., Woolrich, M. W., Bestmann, S., & Barnes, G. R. (2017). Using generative models to make probabilistic statements about hippocampal engagement in MEG. *Neuroimage*. doi:10.1016/j.neuroimage.2017.01.029

Mitchell, K. J., Johnson, M. K., Raye, C. L., & D'Esposito, M. (2000). fMRI evidence of age-related hippocampal dysfunction in feature binding in working memory. *Brain Res Cogn Brain Res, 10*(2000), 197-206.

Moffat, S. D., Hampson, E., & Hatzipantelis, M. (1998). Navigation in a "virtual" maze: Sex differences and correlation with psychometric measures of spatial ability in humans. *Evol Hum Behav, 19*, 73-87.

Morris, R. (1984). Development of a water-maze procedure for studying spatial learning in the rat. *J Neurosci Methods, 11*, 47-60.

Mueller, S. C., Jackson, C. P., & Skelton, R. W. (2008). Sex differences in a virtual water maze: an eye tracking and pupillometry study. *Behav Brain Res, 193*(2), 209-215. doi:10.1016/j.bbr.2008.05.017

Newhouse, P., Newhouse, C., & Astur, R. S. (2007). Sex differences in visual-spatial learning using a virtual water maze in pre-pubertal children. *Behav Brain Res, 183*(1), 1-7. doi:10.1016/j.bbr.2007.05.011

O'Keefe, J., & Nadel, L. (1978). The hippocampus as a cognitive map. *Hippocampus,*

9, 352-364.

Olvera-Cortes, M. E., Garcia-Alcantar, I., Gutierrez-Guzman, B., Hernandez-Perez, J. J., Lopez-Vazquez, M. A., & Cervantes, M. (2012). Differential learning-related changes in theta activity during place learning in young and old rats. *Behav Brain Res, 226*(2), 555-562. doi:10.1016/j.bbr.2011.10.019

Postma, A., Izendoorn, R., & De Haan, E. H. F. (1998). Sex differences in object location memory. *Brain Cogn, 36*, 334-354.

Postma, A., Jager, G., Kessels, R. P. C., Koppeschaar, H. P. F., & van Honk, J. (2004). Sex differences for selective forms of spatial memory. *Brain Cogn, 54*(1), 24-34. doi:10.1016/s0278-2626(03)00238-0

Quraan, M. A., Moses, S. N., Hung, Y., Mills, T., & Taylor, M. J. (2011). Detection and localization of hippocampal activity using beamformers with MEG: a detailed investigation using simulations and empirical data. *Hum Brain Mapp, 32*(5), 812-827. doi:10.1002/hbm.21068

Riggs, L., Moses, S. N., Bardouille, T., Herdman, A. T., Ross, B., & Ryan, J. D. (2009). A complementary analytic approach to examining medial temporal lobe sources using magnetoencephalography. *Neuroimage, 45*(2), 627-642. doi:10.1016/j.neuroimage.2008.11.018

Robinson, S. E., & Vrba, J. (1999). *Functional neuroimaging by synthetic aperture magnetometry (SAM)*

(T. Yoshimoto, M. Kotani, S. Kuriki, H. Karibe, & N. Nakasato Eds.). Sendai, Japan: Tohoku UP.

Ross, S. P., Skelton, R. W., & Mueller, S. C. (2006). Gender differences in spatial navigation in virtual space: implications when using virtual environments in instruction and assessment. *Virtual Reality*. doi:DOI 10.1007/s10055-006-0041-7

Ruiz-Opazo, N., & Tonkiss, J. (2006). Genome-wide scan for quantitative trait loci influencing spatial navigation and social recognition memory in Dahl rats. *Physiol Genomics, 26*(2), 145-151. doi:10.1152/physiolgenomics.00019.2006

Sandstrom, N. J., Kaufman, J., & Huettel, S. A. (1998). Males and females use different distal cues in a virtual environment navigation task. *Brain Res Cogn Brain Res, 6*(1998), 351-360.

Sarvas, J. (1987). Basic mathmatical and electromagnetic concepts of the biomagnetic inverse problem. *Phys Med Biol, 32*, 11-22.

Saucier, D. M., Green, S. M., Leason, J., MacFadden, A., Bell, S., & Elias, L. J. (2002). Are sex differences in navigation caused by sexually dimorphic strategies or by differences in the ability to use the strategies? *Behavioral Neuroscience, 116*(3), 403-410. doi:10.1037//0735-7044.116.3.403

Smith, S. M. (2002). Fast robust automated brain extraction. *Hum Brain Mapp, 17*(3), 143-155. doi:10.1002/hbm.10062

Stephen, J. M., Ranken, D. M., Aine, C. J., Weisend, M. P., & Shih, J. J. (2005). Differentiability of simulated MEG hippocampal, medial temporal and neocortical temporal

epileptic spike activity. *J Clin Neurophysiol, 22*, 388-401.

doi:10.1097/01.WNP.0000172141.26081.78

Tallon-Baudry, C., Bertrand, O., Delpuech, C., & Pernier, J. (1996). Oscillatory g-band (30–70 Hz) activity induced by a visual search task in humans. *J Neurosci, 17*(2), 722-734.

Uehara, G., Adachi, Y., Kawai, J., Shimogawara, M., Higuchi, M., Haruta, Y., & Kado, H. (2003). Multi-channel SQUID systems for biomagnetic measurement. *IEICE Trans Electron, E86c*(43–54).

Voyer, D., Postma, A., Brake, B., & Imperato-McGinley, J. (2007). Gender differences in object location memory: A meta-analysis. *Psychon Bull Rev, 14*(1), 23-38.

Vul, E., Harris, C., Winkielman, P., & Pashler, H. (2009). Puzzlingly high correlations in fMRI studies of emotion, ersonality, and social cognition. *Perspect Psychol Sci, 4*(3), 274-290.

Waller, D. (2000). Individual differences in spatial learning from computer-simulated environments. *Journal of Experimental Psychology: Applied, 6*(4), 307-321. doi:10.1037//1076-898x.6.4.307

Wang, B., & Fu, X. L. (2009). Gender difference in the effect of daytime sleep on declarative memory for pictures. *J Zhejiang Univ Sci B, 10*(7), 536-546. doi:10.1631/jzus.B0820384

Wegman, J., Fonteijn, H. M., van Ekert, J., Tyborowska, A., Jansen, C., & Janzen, G. (2014). Gray and white matter correlates of navigational ability in humans. *Hum Brain Mapp, 35*(6), 2561-2572. doi:10.1002/hbm.22349

Wegman, J., & Janzen, G. (2011). Neural encoding of objects relevant for navigation and resting state correlations with navigational ability. *J Cogn Neurosci, 23*(12), 3841-3854.

Wolbers, T., & Buchel, C. (2005). Dissociable retrosplenial and hippocampal contributions to successful formation of survey representations. *J Neurosci, 25*(13), 3333-3340. doi:10.1523/JNEUROSCI.4705-04.2005

Wolbers, T., & Hegarty, M. (2010). What determines our navigational abilities? *Trends Cogn Sci, 14*(3), 138-146. doi:10.1016/j.tics.2010.01.001

Woolley, D. G., Vermaercke, B., Op de Beeck, H., Wagemans, J., Gantois, I., D'Hooge, R., . . . Wenderoth, N. (2010). Sex differences in human virtual water maze performance: novel measures reveal the relative contribution of directional responding and spatial knowledge. *Behav Brain Res, 208*(2), 408-414. doi:10.1016/j.bbr.2009.12.019

Wyble, B. P., Hyman, J. M., Rossi, C. A., & Hasselmo, M. E. (2004). Analysis of theta power in hippocampal EEG during bar pressing and running behavior in rats during distinct behavioral contexts. *Hippocampus, 14*(5), 662-674. doi:10.1002/hipo.20012

Chapter six

General discussion

In this concluding chapter, the main research findings of the current thesis will be outlined, followed by discussion of how these findings relate to our understanding of the functional role of human hippocampal theta and high-gamma oscillations in different stages of spatial learning. The results support the conclusion that memory formation in the human brain proceeds through two consecutive stages accompanied by low and high frequency band oscillations respectively for encoding and consolidation as shown in animal models. Implications of these findings for future investigations will then be considered. Finally, I will highlight the validity and value of using magnetoencephalography (MEG) to study neuronal oscillations from the human hippocampus by routine experimentation.

Overview of the thesis

The present thesis systematically investigated the functional properties of low frequency theta oscillations and high frequency gamma oscillations during spatial encoding and consolidation in healthy humans, using non-invasive MEG recordings while participants performed a highly translational virtual Morris water maze task. The broad aim was to assess whether the two-stage model of memory formation -- derived from animal models -- (Buzsaki, 1989, 2015) can be translated to the human hippocampus.

Chapter two made the case that MEG is able to reliably detect the signals from

the human hippocampus. The main lines of evidence are reviewed: 1) the principle neurons in the hippocampus are neatly aligned with the dendrites facing one direction and the soma another, such that the magnetic fields generated by this type of neurons can be detected by MEG sensors (Lorente de No, 1947; Murakami & Okada, 2006); 2) despite of the folded geometry of the hippocampus, signal cancelation is partial and only occurs when all the hippocampal subfields and dentate gyrus are activated together simultaneously (Stephen et al., 2005); 3) simulation studies have demonstrated that magnetic fields emanating from the hippocampus are strong enough to be detected by MEG sensors and can be reliably localized to the hippocampus; 4) a body of empirical MEG studies have reported hippocampal activity using a variety of experimental paradigms and validated by independent measurements by iEEG or fMRI.

In **Chapter three**, I had two aims. The first was to replicate and confirm the MEG measurements of hippocampal theta reported by Cornwell et al. (2008) using a different MEG system (KIT MEG; Cornwell et al. used a CTF MEG system). The second aim was to examine the functional role of hippocampal theta rhythms in environmental encoding and the relationship between theta oscillations and performance. Two training sets of a virtual Morris water maze (vMWM) task were administered to 18 male participants with the environmental layout of the two training sets being constant to measure the environmental encoding. Each training set contained a hidden platform condition, in which the participants needed to find a

hidden goal platform in a fixed location by using visual cues attached on the pool walls and a random swimming condition, in which participants swam randomly in a pool without visual cues. It was found that **1)** in agreement with (Cornwell et al., 2008), left hippocampal/parahippocampal theta power was significantly stronger in the hidden platform condition than in the random swimming condition. I further found that left hippocampal theta power was not modulated by environmental novelty; **2)** right hippocampal theta activation was significantly stronger in the first training set than that in the second one; **3)** the magnitude of right hippocampal theta in the first training set was significantly correlated with navigation performance in both training sets. These results confirm that that MEG can reliably detect and localize human hippocampal theta and that this rhythm is significantly related to navigation performance. I interpreted these results to suggest that, as in rodents, human hippocampal theta oscillations function in spatial encoding during navigation, with right hippocampal theta oscillations being responsible for environmental encoding and left hippocampal theta oscillations for goal-oriented spatial navigation.

Chapter four examined high frequency gamma oscillations (80 – 140 Hz) during the inter-trial rest periods of the dataset from chapter three. This analysis was motivated by animal studies showing that the hippocampal cell ensembles used for encoding during navigation accompanied by theta oscillations would be reactivated during rest, accompanied by high frequency oscillations (termed as ripple oscillations in animal studies), to replay the newly learned spatial knowledge for consolidation. I

found that **1)** right hippocampal high-gamma power during the inter-trial rest period showed the same power change pattern of right hippocampal theta oscillations during navigation, with the power being significantly higher during rest period in the new environment relative to the familiar one; **2)** right hippocampal high-gamma power during the rest period was positively correlated with right hippocampal theta power during navigation in the new environment and also predicted navigation performance in the familiar environment. No significant effect was found for left hippocampal high-gamma oscillations. These findings support the interpretation that human hippocampal high-gamma oscillations play an important role in replay of newly learned spatial knowledge as demonstrated in animal models. Since high-gamma power during ITI was proportional to theta power during navigation and was predictive of subsequent navigation performance, it argues strongly that human hippocampal high-gamma during rest period after spatial learning is involved in memory consolidation. Notably, only right hippocampal showed the high-gamma 'replay' effect. Left hippocampus did not show this effect, although left hippocampal theta was significantly stronger during goal-directed navigation to encode the hidden platform location. This might suggest that replay mechanism accompanied by high-gamma oscillations is selective, such that not every aspect of learning is replayed (Deuker et al., 2013). The detailed mechanisms underlying the selection are still unclear.

In **Chapter five**, I examined hippocampal theta and high-gamma oscillations in a

group of female participants; and contrasted these with the patterns of responses in the male participants described in the previous two chapters. Previous behavioural studies in animals and humans have shown significant gender differences in spatial abilities and navigation performance (e.g., Astur et al., 1998; Astur et al., 2004; Blokland et al., 2006). To the extent that MEG-measured theta and high-gamma oscillations are functionally involved in spatial navigation, I reasoned that they should reflect such gender differences in performance. On this logic, MEG scans were obtained from 18 healthy female participants while they performed the virtual Morris water maze task. **At the behavioral level**, there was a clear gender difference: males scored significantly higher on the Santa-Barbara-Sense-of-Direction Scale and were significantly faster to find the hidden platform in the water maze task. Notably, in the familiar environment, males showed improved navigation performance compared to the new environment, while females did not show any improvement. **At the brain level**, during navigation, the two groups showed comparable left hippocampal theta (associated with remembering the hidden goal location). But there were gender differences in right hippocampal theta oscillations. From the first to second training set, in males, right hippocampal theta power decreased, but was equally high in both training sets in females. During the inter-trial rest period in the new environment, right hippocampal high-gamma power of males was significantly greater than that of females. These findings suggest that gender differences in environmental learning in the water maze task are associated with both (environmental encoding-related) right hippocampal theta during navigation and (environmental replay-related) right

hippocampal high-gamma oscillations during the rest period, in agreement with previous studies that males and females differ in environmental processing (Chai & Jacobs, 2009; Iachini et al., 2005; Mueller et al., 2008). The lack of a gender difference for left hippocampal theta oscillations during navigation can be interpreted with respect to previous behavioral studies (Postma et al., 1998; Postma et al., 2004), showing that no gender differences were found in the task which needs to bind the object to the location and the left hippocampus is thought to be responsible for this binding (Kessels et al., 2004). The finding that gender differences in theta and high-gamma rhythms are associated with differences in behavioral performance strongly reinforces the functional importance of human hippocampal theta and high-gamma rhythms in spatial learning.

Contributions of the thesis and implications for future studies

Empirically, the results demonstrated that as reported in rodent studies, human hippocampal theta and high-gamma were modulated by environmental novelty during navigation and rest period and correlated with navigation performance. Direct correlations with navigation performance strengthen the functional interpretation of these oscillations. The results show distinct functional roles of human hippocampal theta and high-gamma oscillations in the encoding and consolidation stages of spatial learning, and establish a clear linkage between human and animal hippocampal functioning. The functional interpretation of human theta and gamma is further

reinforced by the finding that gender differences in navigation performance are reflected in these rhythms.

Theoretically, these results contribute to our understanding of the neurophysiological mechanisms of memory formation in the human hippocampus, and indicate that the two-stage model of memory formation put forward based on animal models (Buzsaki, 2015) can be translated to the human brain. That is, during the initial encoding phase, hippocampal regions are activated accompanied by low frequency theta oscillations to encode the new information from the environment. However, spatial memory needs to be reinforced to form a more stable representation in the brain. Thus, during the offline period, when the brain has little interaction with the environment, the hippocampal region used for encoding the new information is reactivated accompanied by high frequency oscillations to 'replay' the newly formed memory to consolidate the otherwise labile memory traces.

There are several implications for future investigations. First, the thesis provides a framework for systematically investigating memory formation in humans. Previously, researchers have mainly investigated the active navigation component of spatial memory in isolation and the inter-trial rest period after each learning trial has been largely ignored. The present thesis showed that 1) during navigation, low frequency theta oscillations are the dominant neuromagnetic signals from the hippocampus; 2) high frequency oscillations become prominent during the inter-trial

rest period; 3) gamma magnitude during rest is proportional to theta magnitude during navigation and both rhythms are relevant to navigation performance. Thus, in the future, researchers should analyze both types of oscillations to reveal a fuller picture of the dynamics of brain during learning. This perspective may also help uncover more meaningful information when comparing groups, including patient groups (such as people with Alzheimer's disease) with pathologies of the hippocampus, and hippocampal theta during encoding and hippocampal high-gamma during rest might be used as potential neurophysiological biomarkers for these group comparisons.

Second, it would be interesting to investigate what determines individual differences in the strength of hippocampal low frequency oscillations during navigation and hippocampal high frequency oscillations during the offline state. For instance, what are the structural and genetic bases of the strength the hippocampal rhythms? The findings of the thesis also indicate that deep brain stimulation studies could probe both navigation states and offline states using stimulation in different frequency bands. Further, since a complex cognitive process needs a network of brain regions, it is important to study how the hippocampus interacts with other brain regions during memory encoding and consolidation. Thus, it would be of interest to apply phase-phase coupling or phase-amplitude coupling analyses to study regional interaction during encoding and consolidation. Dynamical causal modeling or Granger causality can also be applied to investigate the direction of information flow between hippocampus and cortex. Graph theory can be employed to determine the

networks supporting memory encoding and consolidation, with the help of leakage correction algorithms (Colclough et al., 2015) to alleviate cross-talk problems at the source space.

Using MEG to study human hippocampal functions and future directions

The hippocampus plays an important role in a range of cognitive processes, such as spatial navigation (Buzsaki & Moser, 2013), memory (Horner & Doeller, 2017), violation detection (Garrido et al., 2015) and online language processing (Piai et al., 2016). Pathologies in this region may result in many brain diseases/dysfunctions, such as Alzheimer's diseases, depression, anxiety, epilepsy, and schizophrenia. Accurate characterization of the functions of the hippocampus and its interactions with other brain regions is key to the treatment of these diseases/dysfunctions and a deeper understanding of the nature of memory. In the last two decades, fMRI has been the most commonly used neuroimaging technique to study the hippocampus and it indeed has provided many insights (e.g., Backus et al., 2016; Doeller et al., 2008; Igloi, 2010) and enhanced our understanding of hippocampal functions. With the advent and proliferation of high-field (7-Tesla) MRI, researchers have further unveiled different functions of hippocampal subfields (e.g., Deuker et al., 2014; Duncan et al., 2014; Suthana et al., 2015). However, due to the low temporal resolution of fMRI (on the order of seconds, Buckner & Logan, 2001), fast rhythmic neuronal activities cannot be resolved with this technique. Thus, neurophysiological mechanisms revealed by

animal studies, including the theta and faster rhythms that are the topics of this thesis, are not directly accessible to fMRI. iEEG has both excellent temporal and spatial resolution, and can record not only local field potentials of synchronized neurons but also activities of individual neurons, which can exhibit a full picture of the dynamics of the hippocampal activities (Buzsaki et al., 2012). However, it depends on very limited opportunities for recordings from pre-surgery epileptic patients, who may also have pathologies that alter the functioning of the hippocampus.

Due to its high temporal resolution, non-invasive nature, and the fact that the skull, skin and other brain tissues and fluid do not distort the magnetic fields emanating from the activation of the neurons of the brain regions, using MEG to record and localize the rhythmic neuronal activities of the hippocampus by routine experimentation becomes a valuable method to study the hippocampal functions in the healthy and disease. As has been shown in the literature review and the empirical studies of this thesis, MEG is capable of reliably detecting the signals from the hippocampus and revealing the dynamics of this region in different stages of learning as shown in animal models. Thus, MEG provides important advantages for bridging the gap between human data and animal and computational models of electrophysiology (Baillet, 2017) and permitting routine experimental exploration of the function of healthy and pathological human hippocampi.

However, it is still challenging to study hippocampal function using MEG at the

individual level. Studying the hippocampus on an individual basis is important for studying individual differences and clinical implications. As shown in the simulation study of Meyer, Rossiter, et al. (2017), at the individual level, if the co-registration error was greater than 3 mm, model comparison could not choose the correct model. This problem can be compensated with subject-specific headcasts using 3D printing recently introduced to the MEG community (Meyer, Bonaiuto, et al., 2017). Greater use of individual headcasts may significantly improve the sensitivity of MEG to hippocampal signals. Moreover, accurately detecting the hippocampal signal also depends on accurate forward modeling, although it still needs to validate the realistic model based on individual MRI segmentations (Dalal et al., 2013). However, not every MEG toolbox has implemented realistic head modeling and it is still computationally consuming to construct a realistic forward model. In the near future, more studies need to be done to validate the realistic modeling first and then implement it in more toolboxes to reach more cognitive neuroscientists. More efficient computational approaches in realistic forward models are also important for future advances. New/improved source localization methods are needed to further improve the spatial resolution of the source space in order to investigate the functions of hippocampal subfields.

It should be noted that new types of MEG sensors are currently under development and are likely to significantly improve MEG performance over that achieved with conventional SQUID sensors. For example, optically pumped

magnetometers (OPMs; Boto et al., 2017) can be placed directly on the scalp, about 2-3 cm closer to the brain than conventional SQUID-based sensors. OPMs can detect both evoked and induced changes with signals as much as four times larger than equivalent SQUID measurements. The current thesis confirms that conventional SQUID MEG systems are capable of interrogating human hippocampal function; these deep source capabilities would be dramatically enhanced with OPM systems that significantly reduce the distance between the hippocampus and sensors with dramatic increases in signal to noise ratios.

References

Astur, R. S., Ortiz M. L., & J., S. R. (1998). A characterization of performance by men and women in a virtual Morris water task: A large and reliable sex difference. *Behav Brain Res, 93*(1998), 185-190.

Astur, R. S., Tropp, J., Sava, S., Constable, R. T., & Markus, E. J. (2004). Sex differences and correlations in a virtual Morris water task, a virtual radial arm maze, and mental rotation. *Behav Brain Res, 151*(1-2), 103-115. doi:10.1016/j.bbr.2003.08.024

Backus, A. R., Bosch, S. E., Ekman, M., Grabovetsky, A. V., & Doeller, C. F. (2016). Mnemonic convergence in the human hippocampus. *Nat Commun, 7*, 11991. doi:10.1038/ncomms11991

Baillet, S. (2017). Magnetoencephalography for brain electrophysiology and imaging. *Nat Neurosci, 20*(3), 327-339. doi:10.1038/nn.4504

Blokland, A., Rutten, K., & Prickaerts, J. (2006). Analysis of spatial orientation strategies of male and female Wistar rats in a Morris water escape task. *Behav Brain Res, 171*(2), 216-224. doi:10.1016/j.bbr.2006.03.033

Boto, E., Meyer, S. S., Shah, V., Alem, O., Knappe, S., Kruger, P., . . . Brookes, M. J. (2017). A New Generation of Magnetoencephalography: Room Temperature Measurements using Optically-Pumped Magnetometers. *Neuroimage*. doi:10.1016/j.neuroimage.2017.01.034

Buckner, R. L., & Logan, J. M. (2001). Functional Neuroimaging Methods: PET and fMRI. In R. Cabeza & A. Kinstone (Eds.), *Handbook of Functional*

Neuroimaging of Cognition. Cambridge, MA: The MIT Press.

Buzsaki, G. (1989). Two-stage model of memory trace formation: a role for "noisy" brain states. *Neuroscience, 31*(3), 551-570.

Buzsaki, G. (2015). Hippocampal sharp wave-ripple: A cognitive biomarker for episodic memory and planning. *Hippocampus, 25*(10), 1073-1188. doi:10.1002/hipo.22488

Buzsaki, G., Anastassiou, C. A., & Koch, C. (2012). The origin of extracellular fields and currents--EEG, ECoG, LFP and spikes. *Nat Rev Neurosci, 13*(6), 407-420. doi:10.1038/nrn3241

Buzsaki, G., & Moser, E. I. (2013). Memory, navigation and theta rhythm in the hippocampal-entorhinal system. *Nat Neurosci, 16*(2), 130-138. doi:10.1038/nn.3304

Chai, X. J., & Jacobs, L. F. (2009). Sex differences in directional cue use in a virtual landscape. *Behav Neurosci, 2*, 276-283. doi:10.1037/a0014722.supp

Colclough, G. L., Brookes, M. J., Smith, S. M., & Woolrich, M. W. (2015). A symmetric multivariate leakage correction for MEG connectomes. *Neuroimage, 117*, 439-448. doi:10.1016/j.neuroimage.2015.03.071

Cornwell, B. R., Johnson, L. L., Holroyd, T., Carver, F. W., & Grillon, C. (2008). Human hippocampal and parahippocampal theta during goal-directed spatial navigation predicts performance on a virtual Morris water maze. *J Neurosci, 28*(23), 5983-5990. doi:10.1523/JNEUROSCI.5001-07.2008

Dalal, S., Jerbi, K., Bertrand, O., Adam, C., Ducorps, A., Schwarts, D., . . . Lachaux, J.

(2013). Simultaneous MEG-intracranial EEG: New insights into the ability of MEG to capture oscillatory modulations in the neocortex and the hippocampus. *Epilepsy Behav, 28*, 310-311. doi:10.1016/j.yebeh.2013.03.012

Deuker, L., Doeller, C. F., Fell, J., & Axmacher, N. (2014). Human neuroimaging studies on the hippocampal CA3 region - integrating evidence for pattern separation and completion. *Front Cell Neurosci, 8*, 64. doi:10.3389/fncel.2014.00064

Deuker, L., Olligs, J., Fell, J., Kranz, T. A., Mormann, F., Montag, C., . . . Axmacher, N. (2013). Memory consolidation by replay of stimulus-specific neural activity. *J Neurosci, 33*(49), 19373-19383. doi:10.1523/JNEUROSCI.0414-13.2013

Doeller, C. F., King, J. A., & Burgess, N. (2008). Parallel striatal and hippocampal systems for landmarks and boundaries in spatial memory. *Proc Natl Acad Sci U S A, 105*(15), 5915-5920. doi:10.1073/pnas.0801489105

Duncan, K., Tompary, A., & Davachi, L. (2014). Associative encoding and retrieval are predicted by functional connectivity in distinct hippocampal area CA1 pathways. *J Neurosci, 34*(34), 11188-11198. doi:10.1523/JNEUROSCI.0521-14.2014

Garrido, M. I., Barnes, G. R., Kumaran, D., Maguire, E. A., & Dolan, R. J. (2015). Ventromedial prefrontal cortex drives hippocampal theta oscillations induced by mismatch computations. *Neuroimage, 120*, 362-370. doi:10.1016/j.neuroimage.2015.07.016

Horner, A., & Doeller, C. F. (2017). Plasticity of hippocampal memories in humans. *Curr Opin Neurobiol, 43*, 102-109. doi:10.1016/j.conb.2017.02.004

Iachini, T., Sergi, I., Ruggiero, G., & Gnisci, A. (2005). Gender differences in object location memory in a real three-dimensional environment. *Brain Cogn, 59*(1), 52-59. doi:10.1016/j.bandc.2005.04.004

Igloi, K., Doeller, C. F., Berthoz, A., Rondi-Reig, L., Burguess, N. (2010). Lateralized human hippocampal activity predicts navigation based on sequence or place memory. *Proc Natl Acad Sci U S A, 107*(32), 14466-14471.

Jacobs, J., Miller, J., Lee, S. A., Coffey, T., Watrous, A. J., Sperling, M. R., . . . Rizzuto, D. S. (2016). Direct Electrical Stimulation of the Human Entorhinal Region and Hippocampus Impairs Memory. *Neuron, 92*(5), 983-990. doi:10.1016/j.neuron.2016.10.062

Kessels, R. P. C., Hendriks, M. P. H., Schouten, J., Asselen, M. V., & Postma, A. (2004). Spatial memory deficits in patients after unilateral selective amygdalohippocampectomy. *J Int Neuropsychol Soc, 10*, 907-912. doi:DOI: 10.10170S1355617704106140

Lorente de No, R. (1947). Action potential of the motoneurons in the hypoglossus nucleus. *J Cell Comp Physiol, 29*, 207-287.

Meyer, S. S., Bonaiuto, J., Lim, M., Rossiter, H., Waters, S., Bradbury, D., . . . Barnes, G. R. (2017). Flexible head-casts for high spatial precision MEG. *J Neurosci Methods, 276*, 38-45. doi:10.1016/j.jneumeth.2016.11.009

Meyer, S. S., Rossiter, H., Brookes, M. J., Woolrich, M. W., Bestmann, S., & Barnes,

G. R. (2017). Using generative models to make probabilistic statements about hippocampal engagement in MEG. *Neuroimage*. doi:10.1016/j.neuroimage.2017.01.029

Mueller, S. C., Jackson, C. P., & Skelton, R. W. (2008). Sex differences in a virtual water maze: an eye tracking and pupillometry study. *Behav Brain Res, 193*(2), 209-215. doi:10.1016/j.bbr.2008.05.017

Murakami, S., & Okada, Y. (2006). Contributions of principal neocortical neurons to magnetoencephalography and electroencephalography signals. *J Physiol, 575*(Pt 3), 925-936. doi:10.1113/jphysiol.2006.105379

Piai, V., Anderson, K. L., Lin, J. J., Dewar, C., Parvizi, J., Dronkers, N. F., & Knight, R. T. (2016). Direct brain recordings reveal hippocampal rhythm underpinnings of language processing. *Proc Natl Acad Sci U S A, 113*(40), 11366-11371. doi:10.1073/pnas.1603312113

Postma, A., Izendoorn, R., & De Haan, E. H. F. (1998). Sex differences in object location memory. *Brain Cogn, 36*, 334-354.

Postma, A., Jager, G., Kessels, R. P. C., Koppeschaar, H. P. F., & van Honk, J. (2004). Sex differences for selective forms of spatial memory. *Brain Cogn, 54*(1), 24-34. doi:10.1016/s0278-2626(03)00238-0

Stephen, J. M., Ranken, D. M., Aine, C. J., Weisend, M. P., & Shih, J. J. (2005). Differentiability of simulated MEG hippocampal, medial temporal and neocortical temporal epileptic spike activity. *J Clin Neurophysiol, 22*, 388-401. doi:10.1097/01.WNP.0000172141.26081.78

Suthana, N. A., Donix, M., Wozny, D. R., Bazih, A., Jones, M., Heidemann, R. M., . . . Bookheimer, S. Y. (2015). High-resolution 7T fMRI of Human Hippocampal Subfields during Associative Learning. *J Cogn Neurosci, 27*(6), 1194-1206. doi:10.1162/jocn_a_00772

Ethics approval

Appendix (Ethics Approval) of this thesis has been removed as it may contain sensitive/confidential content